The Thesis Committee for Gulcan Koparal
Certifies that this is the approved version of the following Thesis:

Surfactant Retention Analysis in Berea Sandstones

APPROVED BY

SUPERVISING COMMITTEE:

Kishore K. Mohanty, Supervisor

Gary A. Pope

Krishna K. Panthi

Surfactant Retention Analysis in Berea Sandstones

by

Gulcan Koparal

Thesis

Presented to the Faculty of the Graduate School of

The University of Texas at Austin

in Partial Fulfillment

of the Requirements

for the Degree of

Master of Science in Engineering

The University of Texas at Austin

May 2019

Dedication

To mom

Acknowledgements

First and foremost, I would like to express my very great appreciation to my supervisor Dr. Kishore Mohanty, who has been a tremendous mentor for me. Whenever I had a question or ran into a trouble with my research, his door was always open throughout my two years at the University of Texas at Austin. Also, I would like to extend my sincerest thanks to my thesis committee member Dr. Gary Pope for his valuable inputs for my research work. My special thanks to Krishna Panthi for being on my thesis committee and always offering his patient guidance for my research.

I am also extremely thankful and indebted to the experienced research staff, Jith Liyanage, Himanshu Sharma and Nadeeka Upamali for sharing expertise, sincere and valuable guidance. Without their assistance, this work would not be accomplished. I would also like to extend my sincere thanks to the research stuff in the lab Pinaki Ghosh, Chammi Miller, Jaebum Park, and Haofeng Song. My colleagues from Ultimate EOR Services Chris Britton, Jonathan Driver, Amir Alizadeh and Pearson Suniga have also offered their patient guidance and valuable inputs have made this thesis better. My undergraduate research assistants Xavier and Joey, great thanks for all the help and contribution to this research.

Additionally, I would like to show my gratitude to faculty members, Dr. Gary Pope, Dr. Kamy Sepehrnoori, Dr. Paul Bommer, and Dr. Hugh C. Daigle, who have facilitated my learning in petroleum engineering at The University of Texas at Austin.

Speacial thanks to departmental staff at the University of Texas at Austin: Amy Stewart, Barbara Messmore, Glen Baum, John Cassibry and Gary Miscoe for their technical and administrative support.

Furthermore, a very special thanks to my family, in particular my mother and my twin sisters Mehtap and Mujde and also to all my friends for their love, support and encouragement.

Finally, I place on record, my sense of gratitude to one and all, who directly or indirectly, have lent their hand in this venture.

Abstract

Surfactant Retention Analysis in Berea Sandstones

Gulcan Koparal, M.S.E.

The University of Texas at Austin, 2018

Supervisor: Kishore K. Mohanty

With the diminishing amount of oil has been produced through primary and secondary oil production methods, the need of chemical EOR techniques has become more important. The objective of Chemical EOR is mobilizing the residual oil by using chemicals such as surfactants, polymers, alkalis, co- solvents. The main obstacle with Chemical EOR is the cost efficiency of the chemicals that profoundly depends on the amount of surfactants absorbed onto the rock surface and trapped in the porous medium of the rock matrix. In this research, decreasing the anionic surfactant retention was targeted without using alkalis in the presence/absence of oil. In Berea outcrop sandstones, anionic surfactants were used to reduce the IFT between oil and water, which results in the mobilization of residual oil. High molecular water-soluble polymers were used to mitigate the reservoir heterogeneity and provide the sweep efficiency. Advancements in CEOR have enabled cost effective usage of surfactants and polymers with the consistency of alkalis in both sandstones and carbonate rocks. However, in the existence of gypsum and anhydrite, the usage of alkalies can be even detrimental. Thus, alternative methods are necessary to the robustness of the CEOR processes. In this research, to obtain an ultra-low interfacial tension (IFT) between oil and aqueous phase, chemical formulations were developed with conventional and novel surfactants as combination of internal olefin sulfonate (IOS) co-surfactants and co-solvents. Prior to the

corefloods, the performance of the formulations were tested systematically through phase behavior and aqueous stability tests with different combinations of surfactants and co-surfactants with different ratios and with several kinds of co-solvents such as IBA, phenol and TEGBE.

Formulations with good phase behaviors were investigated further with corefloods with and without oil. For the experiments with low surfactant retention, the same formulations were tested by adding sodium polyacrylate (NaPA) to decrease the surfactant retention. With the formulations with high solubilization ratio, high residual oil recovery and low surfactant retention were obtained and with a small amount of NaPA, a favorable economic to the surfactant-polymer applications was gained in Berea sandstones at 40°C.

Table of Contents

List of Tables

List of Figures

Chapter 1: Introduction

This chapter presents the main objectives and the outline of this work.

1.1 Research objectives

Globally increasing energy demand and decreasing energy supply require additional methods to enhance the oil production. Chemical EOR method is defined as the injection of chemical components into reservoirs to enhance oil recovery. It is often applied as a tertiary technique, i.e., after water flooding. The technique comprises of injecting surfactant, polymer, alkali, and co-solvent as the main chemicals. The purpose is to improve oil production with the lowest amount of chemicals. Thus, retention, which is the amount of chemicals lost to the rock matrix, of surfactant and polymer, and the durability and stability of the chemical mixtures in reservoir conditions are main concerns in chemical EOR applications. By selecting good surfactant formulations and having good mobility control, it is possible to leave less than 10% of oil behind in both outcrops and reservoir rocks (Yang et al., 2010). When surfactant slug is injected into the core and followed by polymer drive, the chemical process is called surfactant-polymer (SP); in the presence of alkali in surfactant formulation, it is called alkali-surfactant-polymer (ASP). Alkali changes surface charges from positive to negative by increasing the pH, causing the anionic surfactants to be repelled from the rock surface; therefore, reduces the surfactant adsorption. In the last decade, Hirasaki and his colleagues (2008) conducted a meticulous review of recent advances in chemical EOR with the focus of ASP flooding. The effects of alkali broadly have been analyzed in both sandstones and carbonate rocks and it is well established that using alkali decreases the adsorption and retention of surfactants.

The main purpose of this study is to determine the retention of some new and some conventional surfactants on Berea Sandstone without using alkali. For this purpose, several

surfactants were screened by phase behavior tests for a given light dead oil. Then their mixtures with co-solvents and co-surfactants were also examined at the same conditions with the same oil. Additionally, the concentrations of ingredients were optimized. The best formulations were selected in terms of equilibration time, salt concentration and phase behavior, and examined for surfactant retention in single phase floods (without oil) and core floods (with oil).

1.2 Description of Chapters

This study is composed of five chapters. Chapter 2 introduces the background information about chemical EOR and its components. Chapter 3 discusses the methodology applied in this study and introduces the equipment and a quick summary of calculations. Chapter 4 represents the experimental results of surfactant-polymer floods in the presence and absence of oil. The last chapter, discusses the conclusions made from the experimental results and suggestions for the future work.

Chapter 2: Literature Review

This chapter discussed the research background and the literature review in the area of surfactant EOR processes.

2.1. Chemicals

In order to improve the efficacy of the formulation for a given oil at the reservoir temperature, pressure, and salinity, it is very important to choose the best chemical composition. The work analyses and tests were designed based on the screening test results of chemicals. This section comprises screening criteria of used chemicals based on the literature.

2.1.1. Surfactants

Surface active agents (surfactants) have been used for many years for enhanced oil recovery processes. These chemicals act in the oil water interface (between the oil phase and aqueous phase) in the reservoir, which in turn improve the displacement efficiency by reducing the interfacial tension (IFT) (Lake et al., 2014, Sharma et al., 2016). According to Stegemeier (1976), it is very essential to reduce the IFT to ultralow values ($<10^{-2}$ mN/m) in order to obtain high capillary number ($>10^{-5}$) and to produce additional oil.

Surfactants are composed of a hydrophobic tail which does not like water but likes oil and hydrophilic head which likes water. Due to this amphiphilic structure, surfactants aggregate at interfaces. Interfacial tension decreases with the adsorption of surfactant to the interface. Surfactants can be classified into four categories: anionic (negatively charged surfactants), cationic (positively charged surfactants), non-ionic (surfactants with no charge) and zwitterionic (surfactants have both negative and positive charges in the same molecule) based on their head group charge. The retention of surfactants is strongly associated with the surface charge of the rock and the head group charge of the surfactant used. For this study, anionic

surfactants were used with Berea sandstone. The surface charges on rocks are very dependent on the brine composition and pH (Churcher et al., 1991).

The structure of surfactants plays an important role in estimating their function and use (Yang et al., 2010). Structural properties of surfactants depend on the number of propylene oxide (PO) and ethylene oxide (EO) and also branching of hydrophobe (Yang et al., 2010). Branching prevents gel like formations, reduces equilibration time, and reduces microemulsion viscosity (Levitt et al., 2009, Hirasaki et al., 2011). The number of PO and EO groups changes the optimum salinity and oil solubilization. For example, Guerbet alcohol-(PO)m-$(EO)_n$-sulfate surfactants are very useful because they enable a varying number of PO and EO groups which can be used to find the best formulation for given conditions and oil (Adkins et al., 2012, Lu et al., 2014, Yan et al., 2017, Pinnawala et al., 2018). Increasing the number of PO makes formulations more hydrophobic and leads to decrease in optimum salinity; increasing the number of EO creates the reverse effect (Bourrel & Schechter, 1998).

Internal olefin sulfonates (IOS) such as C_{19-23}IOS and C_{20-24}IOS perform better than surfactants with short hydrophobes such as CH_3O xPO yEO groups due to their high carbon numbers (Flaaten et al., 2009, Levitt et al., 2009, Yang et al., 2010, Zhao et al., 2008).

The best formulation should be selected not only by considering the structure of surfactant, the type of oil and reservoir conditions, but also by considering the compatibility between surfactant, polymer and electrolytes. Surfactant retention, aqueous and thermal stability and trapping are considered as well (Levitt, 2009).

2.1.2. Co-solvents

By definition, co-solvents are small carbon-carbon chain alcohols (up to C-8), one of the most important additives in chemical EOR. The needed amount of co-solvent is case dependent and even the usage of a small amount of co-solvents brings about many benefits (Nelson et al., 1984), despite the fact that using co-solvents is an additional cost and it also

decreases the solubilization ratio (Sahni et al., 2010). For instance, they improve the aqueous stability of surfactant which results in lower retention in rock matrix, decreases equilibration time and prevents formation of viscous gels and macroemulsions. Additionally, they improve the oil recovery, decrease the microemulsion viscosity (Tagavifar et al., 2016, Zhao et al., 2008) and improve the sweep efficiency by giving a better consistency between surfactant and polymer (Sahni et al., 2010). Flaaten et al., (2008) analyzed both sec-butanol (SBA) and iso-butanol (IBA), but preferred to use relatively cheaper co-solvent IBA for high salinity, low temperature and light oil conditions. Levitt and his colleagues (2006), examined the isopropanol (IPA) and SBA in the presence of light oil, they found SBA performance superior than IPA. Zhao et al., (2008) developed high performance chemical solutions for difficult oils (meaning high viscosity or having high wax content) by using co-solvents such as ethylene glycol monobutyl ether (EGBE), diethylene glycol monobutyl ether (DGBE) and triethylene glycol monobutyl ether (TGBE). Walker et al. (2012) developed a successful SP formulation with 1% of co-solvent triethylene glycol monobutyl ether (TEGBE) for a viscous oil system.

2.1.3. Polymers

Water soluble polymers, which are large molecules composed of many monomers, increase the viscosity of aqueous solutions and provide a better sweep by decreasing the mobility of the displacing fluid. Polymers are very important components of chemical floods. Especially, in case of viscous oils, polymer rheology is one of the critical parameters to obtain a good mobility control (Yang et al., 2010). In order to have an economically beneficial tertiary recovery by increasing the sweep efficiency, chemical flood should be designed based on the viscosities of an oil and microemulsion. To have a stable displacement of oil bank after water flood, displacing fluid (chemical mixture) should have a higher viscosity than oil viscosity and microemulsion viscosity. When oil comes in contact with surfactant, the interaction between

them causes the low IFT, resulting in an increased mobility. At that point, polymers are required to counter balance this effect and attain stable displacement.

Hydrolyzed Polyacrylamides (HPAM) is the most commonly used polymers (Sorbie, 1991) to increase the viscosity of the solution. HPAM polymers are very sensitive to salinity due to the negatively charged carboxyl groups into the polymer chains of HPAM. At low salinities, these negative groups repel each other and stretch the polymer structure, causing low mobility while high salinity environments prevent repulsive forces by a double layer of electrolytes and brings about a higher mobility. HPAM is subject to free radical degradation depending on the temperature and oxygen concentration in the water; high temperature and/or high pH can cause the additional hydrolysis of polyacrylamide polymers which may then cause precipitation in the presence of high concentrations of divalent cations (Levitt et al., 2008).

Polymers are one of shear thinning fluids and the dependence of viscosity on the deformation rate, shear rate, can be represented by the Carreau Model. When viscosity is plotted as a function of the shear rate in a log scale, the decreasing function will be observed for non-Newtonian fluids. This negative slope of viscosity is the signature of shear thinning behavior. For many fluids, at very low shear rates (or slow flows), the viscosity is approximately constant and fluid behaves like a Newtonian fluid. When shear rate increases beyond a critical shear rate, the shear thinning behavior occurs. In this regime, the relationship between the viscosity and the shear rate is a power-law function and viscosity can be expressed as:

$$\eta(\hat{y}) = K\,\hat{y}^{n-1} \qquad (2.1)$$

where n is the power-law index (for Newtonian fluids n=1), n-1 is the slope of power-law model and the intercept is log (K), the transition from constant viscosity plateau to the shear thinning curve occurs where $\hat{y}^*\lambda = 1$.

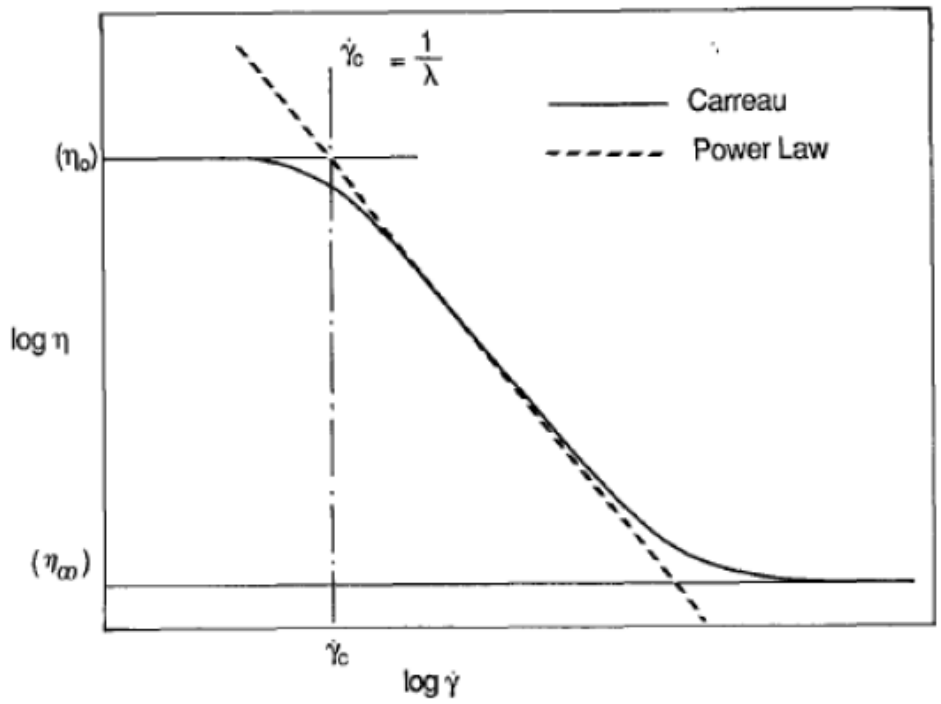

Figure 2. 1 Carreau and Power Law Model (Sorbie, 1991)

When different batches of polymers are compared to each other, power-law index is very useful to quantify the similarity between materials.

2.1.4. Alkali

Alkalis such as sodium carbonate and sodium metaborate react in situ with napthenic acids of active oils, resulting in soap generation and contribution to ultra-low IFT over a wide range of salinity. Furthermore, the ratio of soap/surfactant affects the optimum salinity and the lowest IFT (Hirasaki et al., 2011). Considering this relationship, it is easier to increase the oil production by using low amount of surfactant and also having the polymer in the same solution without any phase separation (Hirasaki et al. 2011). The use of alkalis increases the pH and turns the surface charge of the rock negative, thus creates a repulsive force between rock surface and anionic surfactants. Therefore, alkalis decrease the anionic surfactant retention on the rock matrix (ShamsiJazeyi et al., 2014; Sharma et al., 2016). Since 1930s, a wide variety of alkalis have been used in chemical EOR processes. In 1980s, addition of alkali in the presence of

surfactant resulted in dramatically reduced surfactant retention. Additionally, in the last decade it has been proven that alkali helps decreasing the adsorption of anionic surfactants even in calcite and dolomite rock minerals, causing the process useful for carbonate rock matrix (Wang et al., 2019).

On the other hand, using alkali in the presence of anhydrite ($CaSO_4$), which is a slightly soluble calcium sulfate present in rocks, is not effective due to the reactivity of carbonate with anhydrite especially in dolomites (ShamsiJazeyi et al., 2014 (See Equation 2.2). Additionally, in the field applications alkalis are not easy to handle due to their corrosive properties. Thus, alternative alkalis have been studied such as ammonia (Sharma et al., 2016) and sodium metaborate (Sharma et al., 2015; Panthi et al., 2016). Therefore, lately the interest of Surfactant EOR extended to surfactant-polymer applications (without alkali). In high temperature and high salinity reservoirs, it is hard to develop ultra-low IFT and aqueous stability for SP applications (Wang et al., 2008). However, Han and his colleagues (2013) developed successful SP formulations with amphoteric surfactants for Middle East carbonate reservoirs. Additionally, Ghosh and Mohanty (2019) and Abalkhail et al. (2019) developed SP/ASP formulations for high temperature and high salinity carbonate reservoirs with carboxylate surfactants, including high number of EO groups (>30EO). They were able to produce 77-92% of residual oil with 0.2-0.32 mg/g-rock surfactant retention.

$$CaSO_4 + Na_2CO_3 = Na_2SO_4 + CaCO_3\downarrow \qquad (2.2)$$

As an alternative to alkali, a negatively charged polyelectrolyte can also decrease the surfactant retention by irreversibly adsorbed on the surface. As a sacrificial adsorbent agent, the usage of sodium polyacrylate (NaPA) decreases the surfactant adsorption, so that causing significantly lower surfactant retention due to sodium polyacrylate's desorption and high surface coverage (ShamsiJazeyi et al., 2013). ShamsiJazeyi et al. (2013) stated that the other polyelectrolytes such as pectin and alginate are not as effective as sodium polyacrylate.

2.2. Phase Behavior

One of the key aspects of chemical EOR is microemulsion phase behavior (Huh, 1983). The surfactant/oil/water behavior determines the success of the chemical flood in tertiary recoveries (Levitt et al., 2006; Flaaten et al., 2008). The surfactant/ oil/ water phase behavior was studied by Winsor (1948). In 1954, Winsor predicted three types of surfactant/ oil/ water microemulsions, which are Type I, presence of microemulsion with an excess phase of oil, Type II, presence of microemulsion with an excess phase of water and Type III, presence of microemulsion with both excess phases of oil and water. Healy et al., (1976) improved the understanding of equilibrium microemulsion phase behaviors (Type I, Type II and Type III) in terms of phase behavior differences at different salinities, changes of IFT based on salinity for anionic surfactants and oil and water solubilization ratios. Nelson and Pope (1978) studied the screening of surfactants for enhanced oil recovery applications by phase behaviors.

Phase behavior observations are a good method of screening chemical composition of surfactant formulation in a series of laboratory tests. At a certain temperature, surfactant formulation is mixed with different salinity/hardness of water and given oil by using pipettes. Keeping the formulation same, different phase behavior mixtures are prepared with different salinity of water, resulting in a transition in phase behavior from Winsor Type I to Type III to Type II as salinity increases. A visual example of different phase behavior at different salt concentrations is presented in Figure 2.2. In order to capture all three types of behavior, salinity scan is done over a wide range of salinities and phase behavior of the surfactant formulation were observed (Adkins et al., 2012).

Phase behavior tests enable researchers to analyze the performance of a chemical composition before it is injection into the core or reservoirs. By doing phase behavior tests prior to corefloods, chemical solutions can be designed in an easier and faster way than going directly to the coreflood and observing the oil production results to screen the chemical formulation. Phase behavior visually shows both the interaction between oil and surfactant rich phase and

water, and surfactant rich phase (Arachchilage et al., 2018). Based on those interactions adding of new chemicals or changing the concentration of ingredients can be applied. When the best formulation is obtained that would be used to perform core flood experiments. Thereby, phase behavior tests increase the efficacy of chemical floods in EOR applications.

Additionally, optimizing surfactant formulations by lowering IFT to ultra-low values, lowering microemulsion viscosity and lowering equilibration time (Levitt et al., 2006; Tagavifar et al. 2016) at different temperatures with different formulations can be conducted via phase behavior analysis.

Historically, phase behavior tests were performed at lower temperature (below 70^{o}C); however, recently, the interest is extended to higher temperatures (up to 120^{o}C). Adkins et al., (2012) and Lu et al., (2012) conducted aqueous stability and phase behavior analyses at 120^{o}C. Gayani et al., (2008) represented a new method to derive the accurate results for higher temperature than 120^{o}C by using the experimental results of phase behaviors and aqueous stability at temperature below 100^{o}C. Arachchilage et al., (2018) studied the aqueous stability and optimum salinity changes with temperature above 100^{o}C.

Conducting phase behavior experiments at temperatures above 80^{o}C requires special safety precautions in order to reduce health and safety risks. Borosilicate phase behavior tubes were designed to be durable up to 110^{o}C (Arachchilage et al., 2018). Therefore, in this study, surfactants formulations were developed and analyzed at 40^{o}C.

After preparing phase behavior solutions, they were mixed for the next few days and sometimes weeks to observe equilibrated solutions. After equilibration, the aqueous level changes were noted and solubilization ratio plots were obtained and solubilization ratios were recorded.

Interfacial tension as a function of the solubilization ratio was derived by Huh (1979) as follows.

$$\gamma = \frac{C}{\sigma^2} \tag{2.3}$$

The solubilization ratio of oil (σ_o) is the ratio of volume of oil to the volume of surfactant in the microemulsion; the solubilization ratio of the water (σ_w) is the volume of water to the volume of surfactant in the microemulsion. The optimal salinity is the salinity at which oil and water solubilization ratios are equal, which corresponds to the Type III region.

In the formula, C is a constant and σ is the solubilization ratio. With a good formulation, a solubilization ratio >10 gives an IFT of <0.003 dynes/cm assuming C is equal to 0.3 dynes/cm (typical value) and this IFT can be considered as ultra-low IFT.

Dilution tests are another visual analysis showing the behavior of surfactant at optimum salinity mixed with water flood brine and oil and polymer drive brine. Since water flood was applied prior to surfactant slug which was followed by polymer drive, different salinities from each step can dramatically affect the behavior of surfactant. Ideally, polymer drive, should approach Type I conditions to avoid middle phase microemulsion trapping and viscous microemulsion should not be formed between slug and oil (Veedu et al., 2015). Precipitation and high IFT with dilutions of slug is undesirable. If dilution tests do not show the needed behavior, addition of co-solvents or change in co-solvent type or concentration are applied.

Additionally, in the presence of alkali and active crude oil, in situ soap formation occurs. Soap has a different hydrophilic-lipophilic balance (HLB) than the synthetic surfactants, resulting in a shift in type III region. Sometimes, co-solvents and hardness may cause the same effect as well. Activity diagrams are formed at different volume fraction of oil to demonstrate the shift in Type III region. To adjust the formulation, co-solvents can be added.

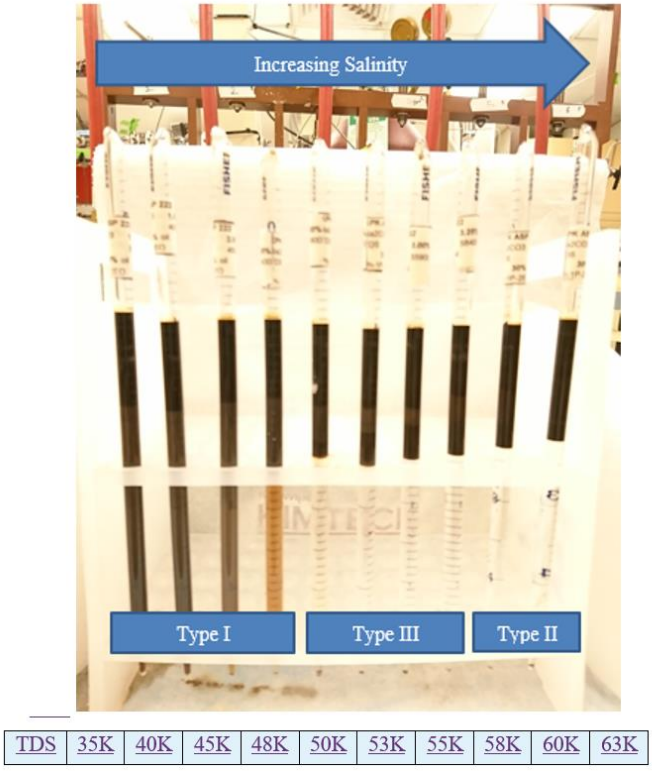

Figure 2. 2 An Example of Classical Phase Behavior

2.3. Aqueous Stability

Aqueous stability is described as the total solubility of the chemical in brine which has no opacity and no phase separation. One of the most important criteria to achieve the highest recovery with lowest surfactant retention is clarity and stability of the injected surfactant slug (Dwarakanath et al., 2008; Levitt et al 2006) under low pressure gradient (Dwarakanath et al., 2008, Yang et al., 2010). For the success of chemical flood, clarity is an essential factor for both surfactant slug and chase liquids (Flaaten et al., 2009, Arachchilage et al., 2018, Levitt et al., 2009). The surfactant solution in brine is not necessarily always clear at optimum salinity (Miller et al., 1986) and also sometimes adding polymer might cause the formation of cloudy mixtures which might cause plugging in the permeable medium due to large anisotropic micelles (Hirasaki et al., 2008). In this case, co-surfactants and/ or co-solvents may be added to obtain a better phase behavior (Sahni et al., 2010).

Aqueous stability depends on temperature, salt concentration and chemical components of the formulation. For a developed composition of chemical formulation and for a given temperature, aqueous stability can be tested by a salinity scan. Typically, formulations that optimum salinity is equal or lower than the aqueous stability. Due to its aqueous stability when the formulation injected into the core at optimum salinity, it shows a better behavior in porous medium and results in lower surfactant retention.

2.4. Microemulsion Viscosity

Microemulsion viscosity is one of the key parameters to design a chemical flood. In the presence of light oil, microemulsion is more viscous and less mobile than the oil itself (Tagavifar et al., 2016). Non-Newtonian microemulsion shows shear thinning behavior. Unlike core floods, the flow in real reservoirs is not at a constant shear rate. With distance from injection well, shear rate decreases with the decrease in fluid velocity and results in more viscous microemulsion. If there is no Newtonian plateau, sweep efficiency is reduced and thus surfactant retention is increased. Co-solvent may be added to make microemulsion viscosity Newtonian (Tagavifar et al., 2016).

2.5. Mobility Control

In the design of a chemical flood, one of the most important parameters is mobility control. Mobility control can be obtained by using polymers as was stated before. Choosing polymer and designing the viscosity is a very delicate process and it should be well estimated. Adding too much polymer with too high viscosity can slow the oil recovery rate. On the other hand, adding too little polymer decreases sweep efficiency. By definition, relative mobility of each phase equals to relative permeability of the phase divided by the viscosity and the total mobility of the oil bank is the sum of the relative mobility of water and oil:

$$\lambda_j = \frac{k_{rj}}{\mu_j} \tag{2.4}$$

$$\lambda_{total} = \lambda_{oil} + \lambda_{water} \tag{2.5}$$

The apparent viscosity of oil bank can be calculated as below:

$$\mu_{oil\,bank} = \frac{1}{\frac{k_{ro}}{\mu_o} + \frac{k_{rw}}{\mu_w}} \tag{2.6}$$

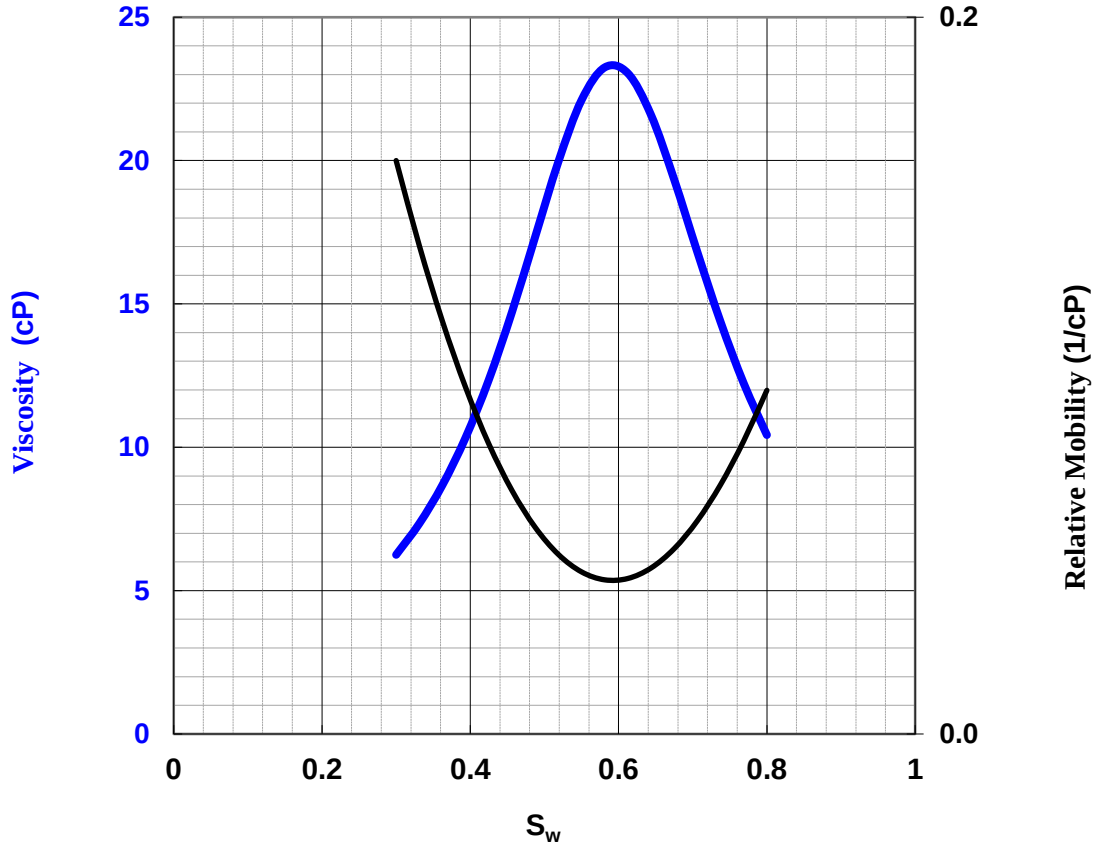

Figure 2. 3 Effective Viscosity and Total Relative Mobility Curves

Figure 2.3 is a plot of total relative mobility by using the relative permeability and viscosity data. The maximum of viscosity curve is typically equal to the apparent viscosity of the oil bank which is used to determine the required viscosity of chemical slug. Chemical slug viscosity is designed to be equal or higher than the oil bank viscosity for a stable sweep.

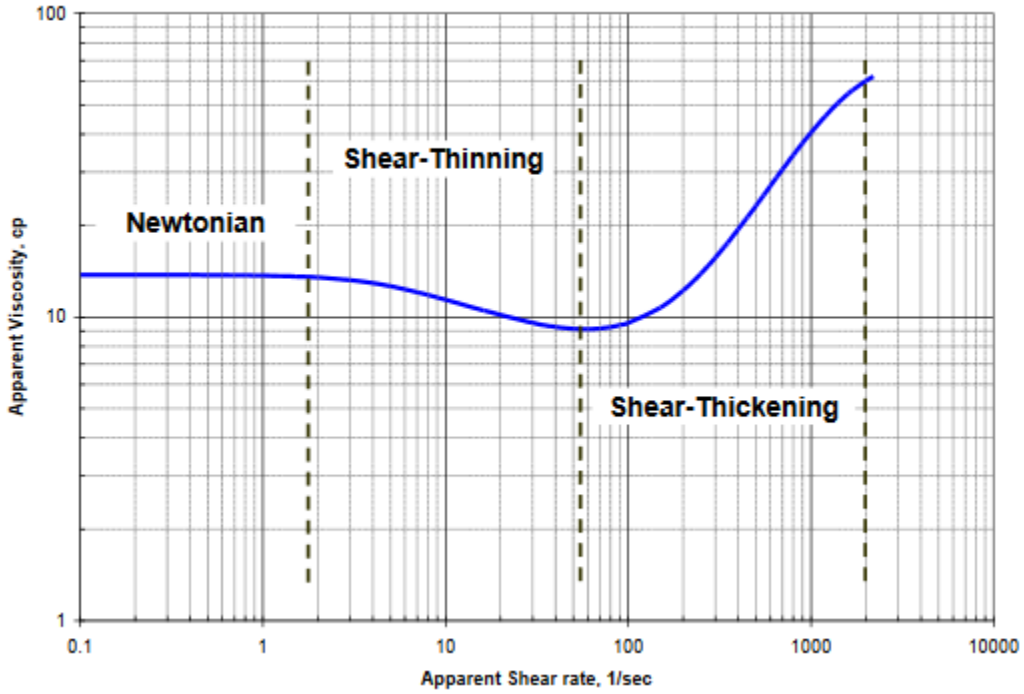

Figure 2. 4 Shear Thinning and Shear Thickening Behavior of Polymers

As stated previously, polymers show non-Newtonian behavior at higher shear rates which is described by (Koh et al. 2016). Calculation of shear rate in a porous media is essential before starting a chemical flood to determine the viscosity as a function of shear rate. As modeled by Cannella et al. (1988), the following equation can be used to describe the flow of a power-law fluid in a permeable medium for the apparent shear rate:

$$\gamma_{app} = C\left(\frac{3n+1}{4n}\right)^{\frac{n}{n-1}} \frac{u}{\sqrt{k_w S_w \phi}} \quad (2.7)$$

where γ_{app} is apparent viscosity, C is a shear rate correction factor, n is power-law exponent, k_w is water permeability, S_w is water saturation, u is Darcy velocity (u=Q/A) and $\emptyset$ is porosity.

Mobility control in low permeability media with high molecular weight polymers is challenging and requires specialized methods to prepare the chemical solutions prior to the coreflood for a robust transportation. Recently, Ghosh et al. (2018) developed a method to improve the polymer transportation in tight carbonate reservoirs. By shearing 1wt% well-hydrated polymer stock for 5 minutes before chemical solutions preparation and filtering the solutions through 0.4µm, 0.2 µm, 0.1 µm, 0.2 µm and 0.4 µm filter papers, they were able to efficiently transport the chemicals through very low permeability (15-20) carbonate outcrop cores. In this study, for the very low permeability reservoir sandstone, chemicals were prepared in the same way.

2.6. Salinity Gradient

Salinity gradient is another design concept. As discussed in Green and Willhite (1998), the best displacement can be obtained at the optimal salinity. Ideally, a negative salinity gradient is used to increase the robustness and efficiency of a chemical flood. Water flood or a preflood have salinity higher than chemical slug salinity which is followed by a lower salinity polymer drive. The chemical slug is injected at the optimum salinity to obtain the lowest possible IFT and based on that salinity, water flood and polymer drive salinities can be designed. In real reservoirs, uncertainties (such as oil composition and dilution effects) can cause shifts in optimum salinity (Green and Willhite, 2018). Based on the salinity differences from water flood to polymer drive, a positive slope is undesirable (Yang et al., 2010). A slightly negative salinity

slope, where Type II water flood salinity followed by Type III chemical slug followed by Type I polymer drive salinity, is defined as the most robust salinity design.

On the other hand, a steep negative salinity slope is unfavorable because the dramatic variations in salinity will lead to a very narrow region of optimum conditions (Yang et al., 2010).

2.7. Surfactant retention

Surfactant retention can be described as the amount of surfactant left in a reservoir/core during a surfactant flood. The amount of surfactant retained in the rock directly affects the economics of the project because high surfactant retention requires higher amount of surfactant to be injected to obtain a satisfactory oil production. Surfactant retention comprises the amount of surfactant adsorbed onto the rock and the surfactant loss to phase trapping. Shear-thinning behavior of chemical slugs in EOR results in more phase trapping, which contributes to retention. Entrapment of immiscible microemulsions can be limited by using co-solvents and a negative salinity gradient (Pope et al., 1979; Jang et al. 2016; Upamali et al., 2016) to decrease the overall retention.

Surfactant loss in a core/reservoir due to adsorption in porous media represents the largest consumption of chemicals in a flood; thus minimizing the surfactant adsorption is very essential for economic viability of chemical floods (Grigg and Bai 2005, Lv et al., 2011). The adsorption of surfactants at the interface is controlled by the properties of both solution and solid substrates (Lu et al., 2011). Depending on the rock mineralogy, oil composition, pH, salinity, hardness, temperature, microemulsion viscosity, surfactant structure and mobility, surfactants perform different and exhibit different amount of adsorption onto the rock surface (Lu et al., 20011; Solairaj et al., 2012). One of the main mechanisms of adsorption on sandstones or carbonates is the ionic attraction between positive surface charge of the rock matrix and anionic surfactants.

In contact with an aqueous medium, the solid surfaces are either negatively or positively charged because of ionization of surface groups or by the adsorption of ion from solution. At low concentration of surfactants, the charge on the electrical double layer of solid surfaces controls the amount of surfactant to be adsorbed. For high concentration of surfactants other factors such as surfactant aggregation at the surface play important role (Somasundaran and Krishnakumar 1997).

Somasundaran and Krishnakumar (1997) describe the typical adsorption isotherm of a negatively charged surfactant on a positively charged solid surface (See Figure 2.5). The isotherm is characterized in four regions; with the lowest surfactant concentration region I represents the existence of electrostatic interactions between the ionic surfactant and oppositely charged surface. In region II, the prominent increase in adsorption with the increase in surfactant concentration was attributed to the initiation of surfactant aggregation. In this region, both lateral and electrostatic interaction forces contributes to the adsorption. As surfactant concentration increases, because of the adsorption of charged species onto the rock surface, the reversal interfacial charge occurs and remarkably decreases the adsorption in Region III. In the last region, the plateau occurs after the micelle formation, demonstrating no further increase in adsorption with the increase in surfactant concentration.

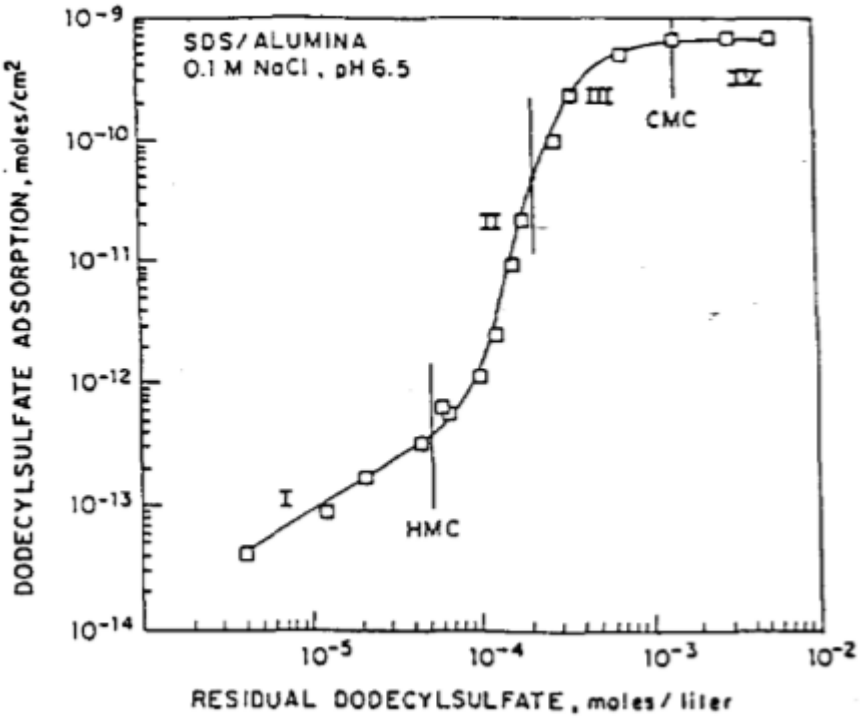

Figure 2.5 Adsorption isotherm of negatively charged sodium dodecylsulfate (SDS) on positively charged alumina at pH=6.5 (Somasundaran and Krishnakumar 1997).

For carbonates, surfactant retention and adsorption are typically higher than for sandstones, mainly due to divalent ions and positive charged surface rock matrix. In carbonates, surfactant adsorption was calculated over a wide range of pH and surfactant to solid ratios by Tagavifar et al. (2017) and it is stated that anionic surfactant retention decreases almost linearly with pH values above 9. Thus, sodium carbonate or sodium hydroxide at higher pH values can be used to reverse the positive edge charge of clays to negative and decrease the retention dramatically.

At reservoir conditions, silica has a negative charge; thus, for silica dominated media such as sandstones, formulations are developed by using anionic surfactants to decrease surfactant adsorption (Hirasaki et al., 2008). In sandstone reservoirs, for formulations composed of anionic surfactants, adsorption mostly occurs on clay surfaces. At neutral pH, clays have a negative surface charge on plates with positive charges on edges which are expected to reverse

their charge at higher pH values. Hirasaki et al., (2011) stated that isoelectric point for clays occurs at pH of 9. Surfactant retention in alkali surfactant polymer (ASP) floods in sandstones with a high clay content of 8.8wt% was decreased to values of 0.061 mg/g-rock and in some cases almost zero retention within experimental error with high solubilization ratio and low viscosity microemulsion and in the presence of co-solvents (Jang et al. 2016. However, using alkali adds cost to chemical floods and its dynamics in the reservoirs is complex. In this study, the surfactant retention was examined in the absence of alkali.

Chapter 3: Materials and Procedure

This chapter discusses the methods and procedure as well as the experimental setup used for this study.

3.1. MATERIALS

3.1.1. Oil

Two different dead crude oils, one is a crude oil with API° 29 and 5cP viscosity and the other one is API° 27 and 21cP viscosity 40℃, were used for all coreflood experiments in this study. Before their usage, oils was filtered through 0.45μm membrane cellulose filters at 40℃.

3.1.2. Surfactants, Co-surfactants, Co-solvents

Surfactants used in this research were Tridecyl alcohol (TDA) propoxy (xPO) sulfates and internal olefin sulfonates (IOS) with varying carbon numbers. The TDA-xPO surfactants were synthesized in collaboration with Harcos Chemicals (Kansas, USA) (Sharma et al., 2018). The IOS surfactants were obtained from Shell Chemical Company and Stepan Chemical Company. The surfactants were diluted to 10% activity and used after pH adjusted to 8. As a co-solvent, triethylene glycol monobutyl ether (TEGBE) samples were obtained from Huntsman and Sigma-Aldrich Corporations and used at 70% activity level. Also IBA xPO yEO and Phenol xPO yEO were obtained from Harcros Chemicals and used in this research to optimize the phase behavior.

Surfactant formulations consisted of both a single component and combinations of surfactants. Among the best formulations, five different surfactants (two conventional and three new) formulations were chosen for further analyses. Four of these formulations were designed with the same concentrations of $C_{19\text{-}23}$ IOS and TEGBE and in the same oil. The

fifth formulation was used with a different oil with co-surfactant C_{15-18} IOS. By using both conventional and new surfactants, the retention of each system and plausible reasons for their retentions were examined.

3.1.3. Polymers and Brines

The polymer used in this study was Flopaam 3330S, which is a co-polymer of acrylamide and acrylic acid, PAM, supplied by SNF Floerger (Cedex, France) in a powder form. In this study, brines were prepared by mixing laboratory grade salts with deionized water at pH of 7. Sodium chloride (NaCl) was purchased from Fisher Scientific with the purity above 99%.

3.1.4. Cores

Mostly the outcrop Berea sandstone cores, were used in this study, which were purchased from Kocurek Industries, Texas. The XRD (X-ray diffraction) analysis conducted by KT-Geoservices Inc. on Berea sandstone cores indicated that their clay content is about 12 wt%, as shown in the Table 3.1. Also see Table 3.2 for the mineralogical composition of the reservoir core which was obtained from Ultimate EOR Services.

Table 3. 1 Mineralogy of Berea Sandstones by XRD

Whole Rock Mineralogy (Weight Percent)	**Sample #1**	**Sample #2**	**Sample #3**	**Sample #4**	**Sample #5**
Quartz	79.8	82.9	78.5	79.5	78.9
K-Feldspar	3.5	3	4.6	4.2	4.7
Plagioclase	3.1	2.5	1.8	2.2	1.9
Calcite	0.6	0.2	0.4	0.3	0.7
Fe-Dolomite	0.4	0.6	0.5	1.1	0.9
Siderite	0.5	0.2	0.3	0.3	0.4
Pyrite	0.2	0	0.2	0	0.2
Total Phyllosilicates	11.9	10.6	13.7	12.4	12.3
Total	100	100	100	100	100
Phyllosilicate Mineralogy (Relative Abundance)					
R3 M-L I/S (15%S)*	8.4	7.5	7.3	4.8	10.6
Illite&Mica	35.3	29.2	29.9	29	30.9
Kaolinite	51.3	52.9	57	54.1	53.6
Chlorite	5	10.4	5.8	12.1	4.9
Total	100	100	100	100	100
Summary Mineralogy (Weight Percent)					
Quartz	79.8	82.9	78.5	79.5	78.9
K-Feldspar	3.5	3	4.6	4.2	4.7
Plagioclase	3.1	2.5	1.8	2.2	1.9
Calcite	0.6	0.2	0.4	0.3	0.7

Table 3.1 Continued 1

Fe-Dolomite	0.4	0.6	0.5	1.1	0.9
Siderite	0.5	0.2	0.3	0.3	0.4
Pyrite	0.2	0	0.2	0	0.2
R3 M-L I/S (15%S)*	1	0.8	1	0.6	1.3
Illite&Mica	4.2	3.1	4.1	3.6	3.8
Kaolinite	6.1	5.6	7.8	6.7	6.6
Chlorite	0.6	1.1	0.8	1.5	0.6
Total	100	100	100	100	100
*R3 M-L I/S (15%S) - R3 Ordered Mixed-Layer Illite/Smectite with 15% Smectite Layers					

In this research, the successful formulation was also tested on a reservoir core, which is a very low permeability sandstone, to compare the results with that of high permeability Berea outcrop. See Table 3.2 for the mineralogy of the reservoir sandstone.

Table 3. 2 Mineralogy of Reservoir Sandstone by XRD

XRD Results (Weight %)	
Sample ID	GBWS
Quartz	92.9
K-Feldspar	1
Plagioclase	1.3
Calcite	0
Dolomite	0
Siderite	0
Pyrite	0.2
Heulandite/Clinoptilolite	0
Halite	0.4
R0 M-L I/S (90%S)*	0
R3 M-L I/S (15%S)**	0.6
Illite&Mica	1
Kaolinite	2
Chlorite	0.6
TOTAL	100

3.2. Procedure

This section discusses the procedures, preparation criteria and related equipment used in this research.

3.2.1. Polymer Hydration

Polymer solutions were prepared by dissolving the FP3330S polymer powder in DI water to make a 1wt% stock solution. While DI water was stirred with a 5.5 cm magnetic stirrer, the polymer powder was slowly added to ensure that no agglomerates were formed and then the mixture was allowed to mix at 250 rpm for a day to homogenize. The solution was then stored safely with a lid. 500 ml stock solutions were prepared prior to each core flood and single-phase flood.

3.2.2. Surfactant Slug and Polymer Drive Solutions

Surfactant slug mixtures (including surfactants, co-solvents, polymer, and brine at certain concentrations) were prepared by mixing stock polymer solutions with other chemicals. Surfactant stock solutions consisting co-surfactant and co-solvent were prepared in 4X and then diluted to required concentrations for surfactant slug. Needed amount of polymer solutions were diluted from previously prepared 1wt% polymer stock solution for both surfactant slug and polymer drive. Prepared solutions were allowed to mix by using 5.5cm magnetic stirrers at room temperature for one hour or until the solutions were homogeneous. After mixing, the solutions were filtered through 1.2μm filters at a constant pressure of 15 psi under argon. The filtering was followed by the calculation of filtration ratio (F.R.) which is:

$$F.R. = \frac{(t_{200ml} - t_{180ml})}{(t_{80ml} - t_{60ml})} \tag{3.1}$$

where t is the time of the filtration that takes to reach the volume indicated. The filtration ratio is required to be between 1 and 1.2 to avoid plugging in core floods. For values above 1.2, there is a high probability of plugging in porous media. Thus, for filtration ratio above 1.2, the chemical solutions were prepared again and mixed longer for a better homogeneity. After filtering, argon is bubbled through the chemical mixtures for a couple of hours in a round-bottom flask while stirring and then the mixture is transferred to previously vacuumed and leak-tested glass columns or sometimes, transferred to vacuumed stainless steel accumulators or columns.

3.2.3. Oil Filtration

Crude oils were filtered through a 0.45μm Nitrocellulose Esters Membrane filter by air pressure of 60psi above reservoir temperature 40℃.

3.2.4. Surfactant Screening and Materials

The procedure of screening surfactants and other chemicals including co-solvents is explained in this section.

3.2.4.1. Pipettes and tubes

Borosilicate pipettes with 5ml volume was used for phase behaviors and dilution tests. Additionally, borosilicate 15ml-20ml tubes with screw caps were used for aqueous stability tests.

3.2.4.2. Pipette Repeater

All pipettes and tubes were filled by using an Eppendorf Repeater Plus with various volume tips in order to minimize the preparation errors. Tips were changed for each different ingredient to obtain the accurate required volume from each sample without any contamination.

3.2.4.3. Aqueous Stability

Aqueous phase solutions were prepared to determine the maximum salinity for an aqueous stable surfactant mixture at 40℃. 15ml glass tubes were used for the convenience of visual examination. Tubes were prepared with the target surfactant mixture concentration in each tube with different salinities. The aqueous solutions were observed for any haziness or phase separation after at least one day of equilibration at 40℃. The highest salinity for the clear aqueous solution's salinity was noted as the aqueous stability for each formulation. Ideally, aqueous stability should be higher than the optimum salinity.

3.2.4.4. Phase Behavior

Surfactant mixtures were diluted from 4X surfactant stock to desired values and in the presence of oil, diluted surfactant mixture was scanned at different salinity of brine to observe the microemulsion behavior. After adding the mixture into 5ml borosilicate pipets, the pipettes were sealed using a flame torch. The solutions were mixed regularly and left to equilibrate at

40℃. In all phase behavior tests, 2.8ml of aqueous phase and 1.2ml of oil was used. Since alkali was not used in this study, only one oil volume fraction was used. Aqueous phase levels were noted before adding the oil into the pipets in order to determine the solubilization ratios based on the level differences after equilibration. Microemulsion viscosity was observed qualitatively. Optimum salinity was determined as the salinity where the solubilization ratio curves crossed each other.

3.2.4.5. Dilution Tests

The phase behaviors obtained from the mixing of the oil bank with the polymer drive and the mixing of the oil bank with waterflood brine were determined via dilution tests. Different concentrations of surfactant solution and waterflood brine and polymer drive brine salinities were tested in the presence of oil with and without co-solvent. The idea was to mimic the surfactant behavior as it was injected after waterflooding the cores and followed by polymer drive. Usually, ±60 or 70 % difference from surfactant slug salinity was preferred. Having the highest salinity in the waterflood and the lowest salinity in the polymer drive led to a negative salinity gradient.

3.2.5. Coreflooding

Berea cores were heated in an 80℃ oven for 2 days prior to any coreflood to evaporate any water vapor trapped in the core. Afterwards the core was set aside for couple of hours until it cooled down and then a heat shrink wrap was used to protect the core from contamination by mineral oil in case of confining pressure leak. Subsequently, the core was placed into the core holder including a rubber sleeve with O-rings and metal end caps on both sides. A mineral oil was used for the confining pressure. In the case of using core holders with old sleeves, tap water was used for confining pressure, to prevent mineral oil contamination of the core in case of oil leak due to high confining pressure. For the corefloods in the presence of oil, core holders with

pressure taps along the length of the core were chosen to observe the sectional pressure drops by connecting these taps and inlet and outlet of the core to pressure transducers.

Once the core was loaded inside the core holder, an overburden pressure of 600-800 psi was applied using either mineral oil or tap water. Then a vacuum is applied to the core. Then carbon dioxide was injected into the core from the top to replace the air inside the core. The main idea of carbon dioxide injection is the ability of carbon dioxide molecules to dissolve in brine, so that the core can be saturated with only brine. At the beginning of the carbon dioxide injection, the bottom valve to the core was kept open for 5-10mins. Afterwards, the bottom valve was shut and the pressure inside the core was increased up to 50 psi and then vacuumed from the bottom of the core holder. That injection and vacuuming cycle was repeated a couple of times and then core was vacuumed at least 3 hours. The core was then leak tested by using a pressure gauge to observe the vacuum pressure change. Once the core was vacuumed successfully, a brine solution was injected from the bottom of the core holder at constant pressure of 200 psi while the outlet valve was closed and then flow rate of the pump was observed. When pump flow rate was zero, meaning the core holder was fully saturated at the pressure, the outlet valve was opened and first flush of the brine was collected in a 15ml centrifuge tubes, which was typically around 1-2ml. By using the volume of the pump at zero psi and 200 psi and the amount of leak volume, the saturation pore volume was calculated. The same brine solution was then injected at various flow rates to determine the brine permeability by observing the pressure drop. Afterwards, tracer test was conducted by using a different salinity brine to determine the heterogeneity of the core and verify the pore volume.

For oil recovery experiments, the core was oil flooded with the backpressure regulator set at ~50 psi. The core was oil flooded for more than 2 pore volumes or until the water cut was less than 1%. The oil saturation was determined based on the amount of brine displaced by oil,

determining by the volume of brine collected into the 100cc burets. The end point relative oil and water permeabilities were determined once the pressure drop reached the steady state.

Oil flood was followed by waterflood with brine injection until the oil cut was less than 1%. Based on the volume of oil displaced by brine, the residual oil saturation to waterflood was determined by a volume balance. When the pressure drop reached a steady state, the endpoint water relative permeability was determined. The final step was to inject chemical solutions, comprising surfactant slug and polymer drive. The chemical flood oil recovery results were recorded and chemical residual oil saturation was determined. Effluents were analyzed for surfactant retention, polymer degradation, salinity and pH properties of samples.

For single phase flood experiments, after the brine saturation and the tracer test, the core was flooded with optimum salinity if the tracer brine was not the optimum salinity and then surfactant slug was injected and followed by the polymer drive (of the oil recovery experiments). At the end of the flood, effluent samples were analyzed in the same way as the oil production experiment effluents.

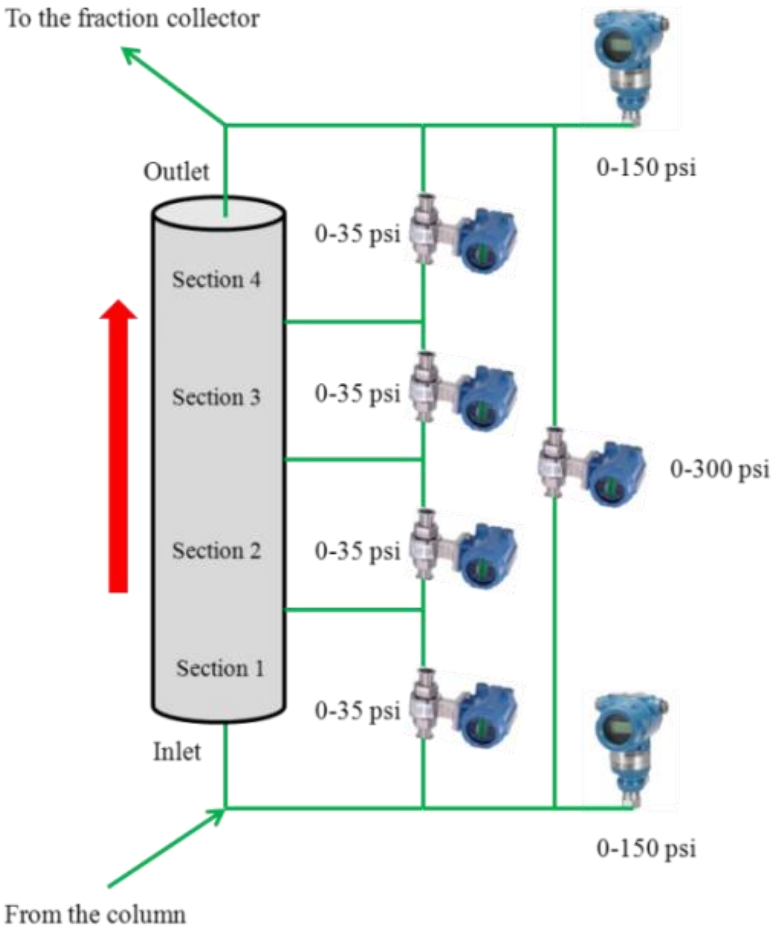

Figure 3. 1 The coreflood set up with pressure transducers

3.2.5.1. Effluent Analysis

Effluent samples were examined for oil production, surfactant, pH, salinity and viscosity. For some of the floods, ion concentration measurements were conducted as well. In case of oil recovery experiments, effluent samples were centrifuged at 2000rpm for 10 minutes and then oil cut was determined in each tube. Surfactant concentration in each tube is determined by HPLC analysis. Salinity was determined by using a refractometer. The pH of samples was measured using a pH meter. Viscosity was measured using either AR-G2 or proRheo LS300 rheometers.

3.2.5.2. Pumps

Teledyne ISCO 500ml capacity syringe pumps were used to apply and maintain confining pressure as well as injecting mineral oil at required pressure or flow rate into the columns or accumulators to displace the injection fluid towards core.

3.2.5.3. Pressure Transducers

Rosemount 3051T versatile gauge and absolute pressure transmitters were used to determine the pressure drop through core holder during injection by converting the applied pressure into an electrical signal. Each gauge has two valves (high and low) connecting the core holder based on liquid injection direction and the pressure difference between these lines was obtained as the pressure drop. Nylon tubing was used to maintain the connection between core holder and pressure transducers and the data was received and graphed by using NI Labview™ software.

3.2.5.4. Fraction Collector

ISCO Retriever II was used to collect effluents in 15 ml plastic/glass centrifuge tubes at ambient conditions. Based on the desired liquid volume in each tube, the collector was set to shift from one tube to another.

3.2.5.5. Refractometer

Fisher Scientific brand refractometers were used to measure the salinity based on the index of refraction. Refractometers used in this research were calibrated to NaCl brine, so measurements had to be correlated for other chemical solutions.

3.2.5.6. PH Measurement

2cc plastic pH tubes, having 1cc of effluents, were used to determine the pH for each sample. Effluent samples were analyzed at ambient conditions, by using a pH probe and giving enough time until the reading was stabilized. Since the experimental temperature was 40°C, the

stated pH values in this research is expected to be a little higher than that of in experimental conditions.

3.2.5.7. High Performance Liquid Chromatography (HPLC)

Thermo Scientific Dionex Ultimate 3000 HPLC with an evaporative light scattering detector (ELSD) was used to determine the surfactant concentration in the effluent samples and estimate the surfactant retention. For HPLC analysis, effluents were prepared in two different ways.

For oil recovery experiments, effluents were heated up in a 55℃ oven for 10-15mins to homogenize the samples and then samples were diluted 3-fold with the mixture of 1% bleach (sodium hypochlorite) and 10% co-solvent (TEGBE). Afterwards, diluted samples were left in 78℃ oven to degrade the polymer with the bleach mixture and high temperature. The samples were mixed every ten minutes for an hour or until the solutions were water alike.

For single phase dynamic experiments, effluents were diluted 4-fold with the mixture of 1% bleach and 10% TEGBE and left in 40℃ oven for couple of hours until the polymer degraded. Unlike oil recovery experiments, to degrade the polymer, high temperature oven was not necessary due to lower concentration of polymers used for single phase flood experiments.

Surfactant concentration in each sample was then determined by HPLC analysis. With the information of injected amount of surfactant, total rock mass and the produced amount of surfactant and thereby surfactant retention for gram-rock was calculated.

$$Surfactant\ Retention = \frac{(m_{injected\ \ surfactant} - m_{produced\ surfactant})}{m_{rock}} \tag{3.2}$$

3.2.5.8. Rheometer

A proRheo LS-300 rheometer and TA DHR-3 was used to measure effluent and solution viscosities. A parallel plate geometry was used and measurements were conducted at the room temperature or 40°C.

3.3. Calculations

A brief description of equations and calculations are presented in this section.

3.3.1. Solubilization Ratio Plots

Solubilization ratio plots were used to estimate the optimum salinity for classical phase behaviors, which show three types of Winsor phase behavior Type I, III and II, at a specific temperature for specific oil and aqueous phases. By definition, solubilization ratio is the volume of either water or oil solubilized per volume of surfactant. The equations used to determine the solubilization ratios of oil (σ_o) and water (σ_w) were:

$$\sigma_w = {V_{water}}/{V_{surfactant}} \tag{3.3}$$

$$\sigma_o = {V_{oil}}/{V_{surfactant}} \tag{3.4}$$

Solubilization ratios are an indication of Winsor Types. For example, only the oil solubilization ratio shows Type I phase behavior, while both oil and water solubilization ratios indicate the Type III and only water solubilization ratio shows Type II phase behavior. Figure 3.2 shows an example of a solubilization ratio plot.

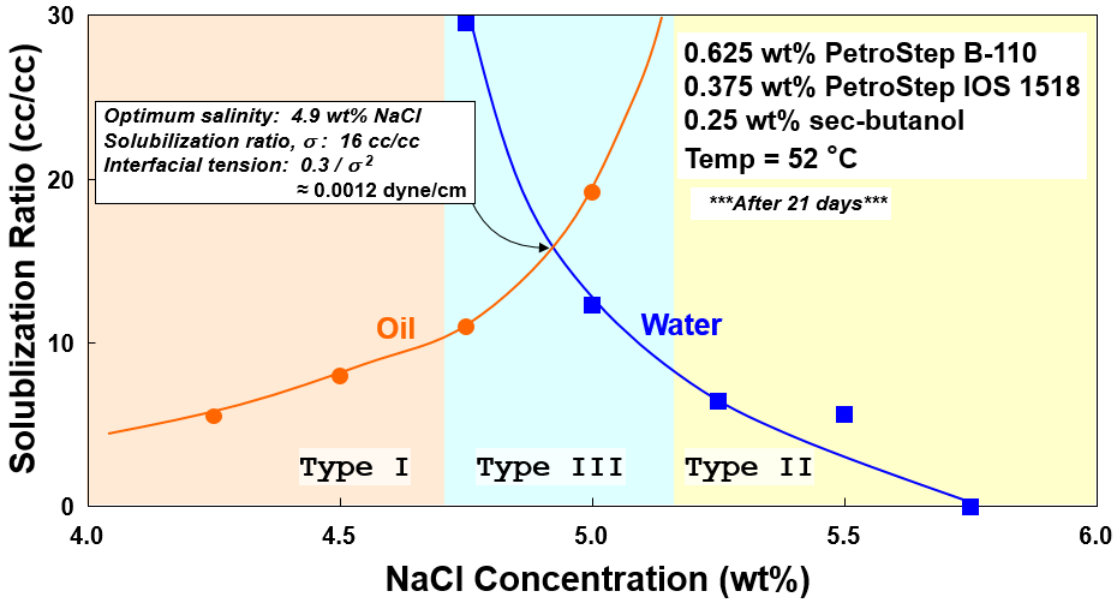

Figure 3. 2 An example of classical microemulsion phase behavior with light crude oil (Flaaten 2012)

3.3.1. Pore Volume and Porosity

In addition to brine saturation pore volume, a tracer test was conducted to determine the pore volume of each core. Tracer test is also a good indication of the cores' heterogeneity. Early breakthrough is an indication of heterogeneity. If the heterogeneity is extreme, then the core should be replaced with a better one for a trustable estimation of oil production and surfactant adsorption. As stated, a tracer test was conducted by injecting a different salinity brine than the resident salinity and the dispersion of tracer brine effluent samples. By using a fraction collector, the effluent samples were collected in 6ml plastic graded tubes with 2ml/min flow rate. After about 2 PV (estimated PV) of injection, the effluents were analyzed for the collected volume of brine and the salinity via refractometer. By transferring the salinity to normalized values, normalized salinity vs. collected volume of brine plots were obtained, as can be seen in Figure 3.3.

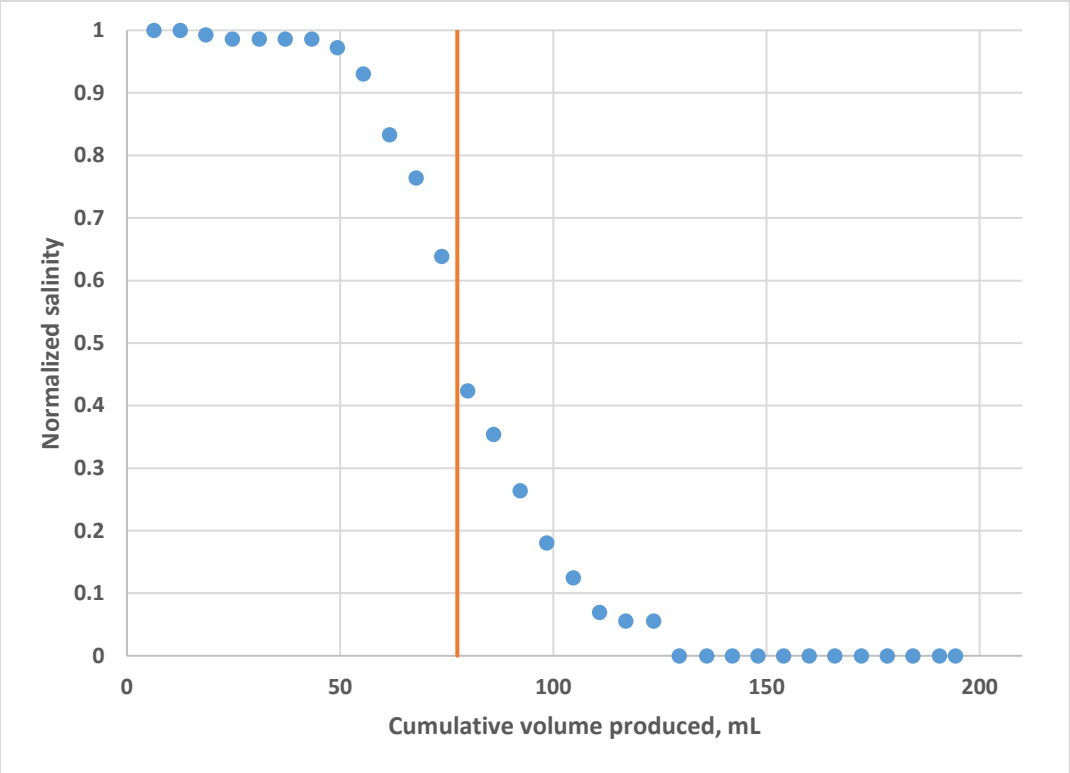

Figure 3. 3 An example of a Tracer Test

Once pore volume was determined, by knowing the size of the core, the porosity was calculated based on the pore volume of rock matrix divided by the bulk volume of the core.

3.3.1. Phase Saturation

Based on mass balance, the initial oil saturation (S_{oi}) after oil flood, the residual oil saturation to waterflood (S_{orw}) and the residual oil saturation to chemical flood (S_{orc}) were calculated. Volume adjustment from thermal expansion was neglected since the reservoir temperature was not too high.

$$\text{Soi} = {V_{produced\ water}}\Big/{V_{pore}} \tag{3.3}$$

$$\text{Sorw} = \frac{(\text{V}_{\text{oil produced after waterflood}})}{V_{pore}} \tag{3.4}$$

$$S_{orc} = \frac{(V_{oil\ produced\ after\ chemical\ flood})}{V_{pore}} \quad (3.5)$$

3.3.2. Effective and End Point Permeability

By using the steady state pressure drop data as well as the core properties permeability was obtained via the Darcy's equation.

$$k = \frac{q\mu L}{A\Delta P} \quad (3.6)$$

Where permeability is k, flow rate is q, viscosity is μ, length of the core is L, pressure drop across the core is ΔP, cross-sectional area is A.

End point oil and water permeability values can be calculated via equations indicated below:

$$k^*_{rw} = \frac{k^*_{water}}{k_{brine}} \quad (3.7)$$

$$k^*_{ro} = \frac{k^*_{oil}}{k_{brine}} \quad (3.8)$$

Where k^*_{rw} is the water relative permeability and k^*_{ro} is the oil relative permeability and k_{brine} is the brine salinity at S_w=1.

Chapter 4: Experimental Results

4.1. Phase Behavior Results

As stated in Literature Review, every crude oil is unique based on its composition due to the contribution of chemical, environmental and geological effects. Thus, the interaction of surfactant solution with oil is different for every oil. In this research, combinations of alkoxy-carboxylate (or alkoxy-sulfate) surfactants and internal olefin sulfonate (IOS) surfactants were tested in the presence and absence of co-solvents via phase behavior tests to tailor the surfactant mixtures to the oil. The types of surfactants and co-solvents used for the phase behavior tests are listed in Table 4.1.1.a and Table 4.1.1.b summarizes the phase behavior tests.

Table 4.1.1. a Surfactants and Co-solvents used for Phase Behavior Tests

Surfactant	**Co-Solvent**
CH3O 21PO 10 EO SO4-	TEGBE
CH3O 40PO 30EO COO-	IBA 3EO
CH3O 60PO 30EO COO-	IBA 5EO
CH3O 60PO 30EO COO-	IBA 7EO
CH3O 70PO 100EO COO-	IBA 1PO 5EO
CH3O 70PO 100EO COO-	IBA 1PO 7EO
CH3O 70PO 30 EO COO-	Phenol 2EO
CH3O 80PO 100EO COO-	Phenol 5EO
2EH 7PO SO4-	Phenol 1PO 2EO
TDA 7PO SO4-	Phenol 1PO 5EO
TDA 13PO SO4-	
TDA 35PO 10EO SO4-	
TDA 35PO 20EO SO4-	
TDA 35PO 30EO SO4-	
TDA 35PO 45EO COO-	
TDA 45PO 10EO SO4-	
C18 7PO SO4-	
Oleyl 25PO 45EO COO-	
C28 35PO 30EO COO-	
C28 35PO 50EO COO-	
C28 25PO 45EO COO-	
TSP 35PO 40EO COO-	
TSP 35PO 45EO COO-	
TSP 35PO 65EO COO-	
TSP 35PO 40EO COO-	
C15-18 IOS	
C19-23 IOS	
C19-28 IOS	
C20-24 IOS	

Table 4.1.1. b Phase Behavior Tests

Exp. #	**Surfactant**		**Co-Surfactant 1**		**Co-Surfactant 2**		**Co-Solvent**		**Oil Type**
	Name	**wt%**	**Name**	**wt%**	**Name**	**wt%**	**Name**	**wt%**	
PB-1	**CH_3O 21PO 10 EO SO_4**	**0.5**	**C_{19-23} IOS**	**0.5**			**TEGBE**	**1**	**O-1**
PB-2	CH_3O 40PO 30EO COO^-	1							O-1
PB-3	CH_3O 60PO 30EO COO-	1							O-1
PB-4	CH_3O 60PO 30EO COO-	0.5	C_{20-24} IOS	0.5					O-1
PB-5	CH_3O 70PO 100EO COO-	1							O-1
PB-6	CH_3O 70PO 100EO COO-	0.5	C_{20-24} IOS	0.5					O-1
PB-7	CH_3O 70PO 30 EO COO-	1							O-1
PB-8	CH_3O 80PO 100EO COO-	1							O-1
PB-9	TDA 35PO 10EO SO_4	1							O-1
PB-10	TDA 35PO 20EO SO_4	1							O-1
PB-11	TDA 35PO 45EO COO-	1							O-1
PB-12	**TDA 13PO** SO_4	**0.5**	**C_{19-23} IOS**	**0.5**			**TEGBE**	**1**	**O-1**
PB-13	**TDA 7PO** SO_4	**0.5**	**C_{19-23} IOS**	**0.5**			**TEGBE**	**1**	**O-1**
PB-14	C_{28} 35PO 30EO COO-	1							O-1
PB-15	C_{28} 35PO 50EO COO-	1							O-1
PB-16	C_{28} 25PO 45EO COO-	1							O-1
PB-17	TSP 35PO 40EO COO-	1							O-1
PB-18	TSP 35PO 45EO COO-	1							O-1
PB-19	TSP 35PO 65EO COO-	1							O-1
PB-20	TSP 35PO 40EO COO-	0.5	C_{20-24} IOS	0.5					O-1

Table 4.1.1.b Continued 1

PB-21	Oleyl 25PO 45EO COO-	1							O-1
PB-22	**2EH 7PO** SO_4	**0.5**	**C_{19-23}IOS**	**0.5**			**TEGBE**	**1**	**O-1**
PB-23	TDA 13PO SO_4	0.6	C_{15-18} IOS	0.3			TEGBE	0.5	O-2
PB-24	TDA 13PO SO_4	0.5	C_{15-18} IOS	0.5			TEGBE	1	O-2
PB-25	TDA 13PO SO_4	0.6	C_{15-18} IOS	0.3			Phenol 2EO	0.5	O-2
PB-26	TDA 13PO SO_4	0.6	C_{15-18} IOS	0.3			IBA 5EO	0.5	O-2
PB-27	TDA 13PO SO_4	0.6	C_{15-18} IOS	0.4			Phenol 1PO 2EO	0.5	O-2
PB-28	TDA 13PO SO_4	0.6	C_{15-18} IOS	0.4			TEGBE	0.5	O-2
PB-29	**TDA 13PO** SO_4	**0.6**	**C_{15-18} IOS**	**0.3**			**TEGBE**	**0.25**	**O-2**
PB-30	TDA 13PO SO_4	0.6	C_{15-18} IOS	0.4			TEGBE	0.75	O-2
PB-31	TDA 13PO SO_4	0.5	C_{15-18} IOS	0.2	C_{19-23} IOS	0.3	IBA 3EO	0.5	O-2
PB-32	TDA 13PO SO_4	0.5	C_{15-18} IOS	0.3	C_{19-23} IOS	0.2	IBA 5EO	0.5	O-2
PB-33	TDA 13PO SO_4	0.6	C_{15-18} IOS	0.2	C_{19-23} IOS	0.2	IBA 3EO	0.5	O-2
PB-34	TDA 13PO SO_4	0.6	C_{15-18} IOS	0.2	C_{19-23} IOS	0.3	TEGBE	1	O-2
PB-35	TDA 13PO SO_4	0.6	C_{15-18} IOS	0.3			IBA 3EO	0.25	O-2
PB-36	TDA 13PO SO_4	0.6	C_{15-18} IOS	0.3			Phenol 5EO	0.25	O-2
PB-37	TDA 13PO SO_4	0.6	C_{15-18} IOS	0.3			Phenol 1PO 2EO	0.25	O-2
PB-38	TDA 13PO SO_4	0.6	C_{15-18} IOS	0.3			IBA 3EO	0.25	O-2
PB-39	TDA 13PO SO_4	0.6	C_{15-18} IOS	0.4			IBA 3EO	0.25	O-2
PB-40	TDA 13PO SO_4	0.6	C_{15-18} IOS	0.25	C_{19-23} IOS	0.25	TEGBE	1	O-2
PB-41	TDA 13PO SO_4	0.6	C_{15-18} IOS	0.25	C_{19-23} IOS	0.25	IBA 5EO	1	O-2

Table 4.1.1.b Continued 2

PB-42	TDA 13PO SO_4	0.6	C_{15-18} IOS	0.25	C_{19-28} IOS	0.25	IBA 5EO	1	O-2
PB-43	TDA 13PO SO_4	0.6	C_{15-18} IOS	0.25	C_{19-28} IOS	0.25	IBA 1PO 5EO	1	O-2
PB-44	TDA 13PO SO_4	0.6	C_{15-18} IOS	0.25	C_{19-23} IOS	0.25	IBA 1PO 7EO	1	O-2
PB-45	TDA 13PO SO_4	0.6	C_{15-18} IOS	0.3			-	-	O-2
PB-46	TDA 13PO SO_4	0.6	C_{15-18} IOS	0.45			IBA 5EO	0.5	O-2
PB-47	TDA 13PO SO_4	0.6	C_{15-18} IOS	0.4			TEGBE	0.25	O-2
PB-48	TDA 13PO SO_4	0.3	C_{15-18} IOS	0.2			TEGBE	0.25	O-2
PB-49	TDA 13PO SO_4	0.4	C_{15-18} IOS	0.2			TEGBE	0.25	O-2
PB-50	TDA 13PO SO_4	0.3	C_{15-18} IOS	0.2	C_{19-23} IOS	0.1	TEGBE	0.25	O-2
PB-51	TDA 13PO SO_4	0.3	C_{15-18} IOS	0.2	C_{19-23} IOS	0.1	TEGBE	0.25	O-2
PB-52	TDA 13PO SO_4	0.3	C_{15-18} IOS	0.2			TEGBE	0.25	O-2
PB-53	TDA 13PO SO_4	0.3	C_{15-18} IOS	0.2			IBA 3EO	0.25	O-2
PB-54	TDA 13PO SO_4	0.3	C_{15-18} IOS	0.2			IBA 5EO	0.25	O-2
PB-55	TDA 13PO SO_4	0.3	C_{15-18} IOS	0.2			IBA 1PO 5EO	0.25	O-2
PB-56	TDA 13PO SO_4	0.3	C_{15-18} IOS	0.2			TEGBE	0.5	O-2
PB-57	TDA 13PO SO_4	0.3	C_{15-18} IOS	0.2			TEGBE	0.75	O-2
PB-58	TDA 35PO 20EO SO_4	0.5	C_{15-18} IOS	0.5					O-2
PB-59	TDA 35PO 20EO SO_4	0.5	C_{15-18} IOS	0.2	$C_{19-23}C_{19-23}$ IOS	0.3	IBA 3EO	0.5	O-2
PB-60	TDA 35PO 30EO SO_4	0.5			$C_{19-23}C_{19-23}$ IOS	0.5	IBA 3EO	0.5	O-2
PB-61	TDA 35PO 10EO SO_4	0.5	C_{15-18} IOS	0.2	C_{19-23} IOS	0.3	Phenol 1PO 2EO	0.5	O-2

Table 4.1.1.b Continued 3

PB-62	TDA 45PO 10EO SO_4	0.5	C_{15-18} IOS	0.15	C_{19-23} IOS	0.35	Phenol 1PO 5EO	1	O-2
PB-63	C18 7PO SO_4	0.6	C_{15-18} IOS	0.4					O-2
PB-64	C18 7PO SO_4	0.5	C_{15-18} IOS	0.2	C_{19-23} IOS	0.3			O-2
PB-65	TDA 35PO 10EO SO_4	0.5			C_{19-23} IOS	0.5			O-2
PB-66	TDA 35PO 10EO SO_4	0.5			C_{19-23} IOS	0.5	IBA 5EO	0.5	O-2
PB-67	TDA 35PO 10EO SO_4	0.5	C_{15-18} IOS	0.1	C_{19-23} IOS	0.4	IBA 5EO	0.5	O-2
PB-68	TDA 35PO 10EO SO_4	0.5	C_{15-18} IOS	0.1	C_{19-23} IOS	0.4	IBA 7EO	0.5	O-2
PB-69	TDA 35PO 10EO SO_4	0.5	C_{15-18} IOS	0.1	C_{19-23} IOS	0.4	IBA 5EO	0.25	O-2
PB-70	TDA 35PO 10EO SO_4	0.5	C_{15-18} IOS	0.1	C_{19-23} IOS	0.4	IBA 5EO	0.75	O-2
PB-71	TDA 7PO SO_4	0.6	C_{15-18} IOS	0.3	C_{19-23} IOS	0.5			O-2
PB-72	TDA 7PO SO_4	0.6	C_{15-18} IOS	0.4	C_{19-23} IOS	0.5			O-2
PB-73	TDA 7PO SO_4	0.3	C_{15-18} IOS	0.2	C_{19-23} IOS	0.5			O-2
PB-74	TDA 7PO SO_4	0.4	C_{15-18} IOS	0.2	C_{19-23} IOS	0.25			O-2

The phase behavior samples were equilibrated in pipettes at 40℃ after mixing them properly for two days. After equilibration, the formulations were tested qualitatively and four different formulations for oil O-1 and one formulation for oil O-2 were chosen to be analyzed further. These formulations are written in bold in Table 4.1.1. As seen from Figure 4.1.2, F1, F2, F3 and F4 composed of the same co-surfactant and co-solvent with one different surfactant in each formulation. The objective of these chosen formulations were to determine the effect of different types of surfactant (conventional and novel) with different hydrophobicity (ultra-short hydrophobe and medium hydrophobe) with different structures (different EO and PO numbers) on surfactant adsorption and retention in Berea sands and sandstones. Formulation F5 was formulated with a different oil O-2. For oil O-2, the formulation with similar composition to

previously chosen formulations showing ultra-low IFT was selected to observe the effect of a different oil on Berea sandstone.

Table 4.1.2. Chosen Formulations after Phase Behavior Tests

Experiment	Formulation	Surfactant		Co-Surfactant		Co-Solvent		Oil Type
		Name	wt%	Name	wt%	Name	wt%	
PB-1	**F1**	CH3O 21PO 10 EO SO4	0.5	C19-23IOS	0.5	TEGBE	1	O-1
PB-11	**F2**	TDA 13PO SO4	0.5	C19-23IOS	0.5	TEGBE	1	O-1
PB-12	**F3**	TDA 7PO SO4	0.5	C19-23IOS	0.5	TEGBE	1	O-1
PB-22	**F4**	2EH 7PO SO4	0.5	C19-23IOS	0.5	TEGBE	1	O-1
PB-29	**F5**	TDA 13PO SO4	0.6	C15-18 IOS	0.3	TEGBE	0.25	O-2

For oil O-2, the effect of the concentration and the type of surfactants on phase behavior and aqueous stability of the formulations was tested at the same temperature. With oil O-2, even a change of 0.25wt% in concentration of co-solvents resulted in a considerable change in optimum salinity and aqueous stability. The impact of co-solvents IBA-3EO, IBA-5EO, TEGBE and Phenol-2EO on phase behavior was determined to be similar. However, in some phase behavior, it was observed that IBA-3EO was enhancing the equilibration more than others. On the other hand, TEGBE was observed to prevent gel formation better than others. Co-solvents with 1 PO group decreased the optimum salinity and aqueous stability limit significantly due to their hydrophobicity.

Another important parameter for phase behavior and aqueous stability is optimizing the co-surfactants and concentrations. As a hydrophilic surfactant, $C_{15\text{-}18}$ IOS was used to increase

aqueous stability while C_{19-23} IOS, a hydrophobic surfactant, was used to lower IFT. The mixture of these two IOS surfactants at various concentrations were used in some formulations in order to utilize the synergy and reduce IFT further. However, surfactants without EO groups like TDA-13PO-SO_4 brought about low aqueous stability due to their hydrophobicity. See Figure 4.1.1-4.1.5 for the solubilization ratios of the chosen formulations.

Phase behavior samples with 30% oil were equilibrated at 40°C for 2 weeks and then visually investigated for oil/water solubilization ratios. With the aqueous stability limit of 45,000ppm TDS, the ultra-low IFT range for formulation F1 is 40,000-50,000 ppm TDS and the optimum salinity is ~40,000ppm TDS. See Figure 4.1.1 for the solubilization ratios.

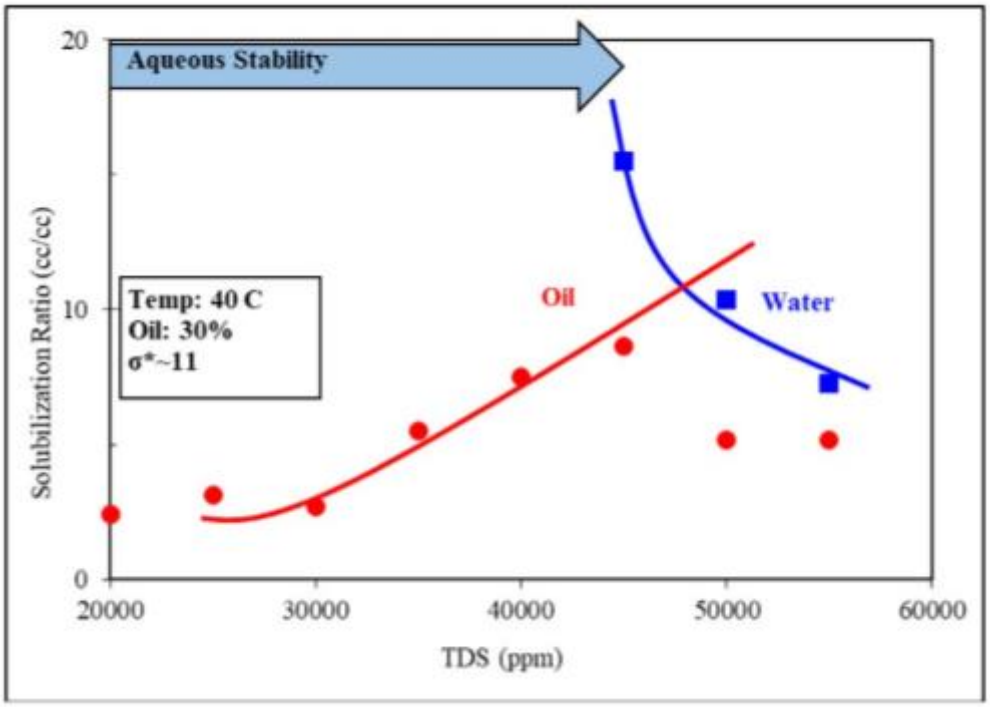

Figure 4.1. 1 Solubilization Ratios for Formulation F1 (Sharma et al., 2018)

Phase behavior samples with 30% oil were equilibrated at 40°C for 2 weeks and then visually investigated for oil/water solubilization ratios. With the aqueous stability limit of

35,000ppm TDS, the ultra-low IFT range for formulation F2 is 30,000-40,000 ppm TDS and the optimum salinity is ~35,000ppm TDS. See Figure 4.1.2 for the solubilization ratios.

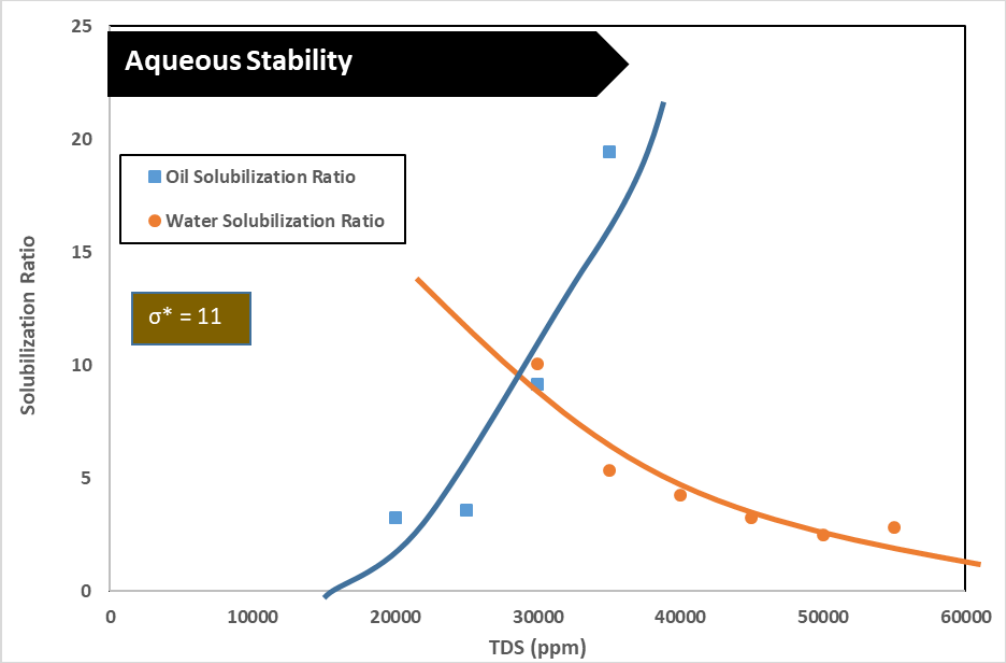

Figure 4.1. 2 Solubilization Ratios for Formulation F2

Phase behavior samples with 30% oil were equilibrated at 40°C for 2 weeks and then visually investigated for oil/water solubilization ratios. With the aqueous stability limit of 45,000ppm TDS, the ultra-low IFT range for formulation F3 is 40,000-45,000 ppm TDS and the optimum salinity is ~45,000ppm TDS. Since TDA 7PO SO_4 is less hydrophobic then TDA 13PO SO_4, the optimum salinity shifted to higher salinity. See Figure 4.1.3 for the solubilization ratios.

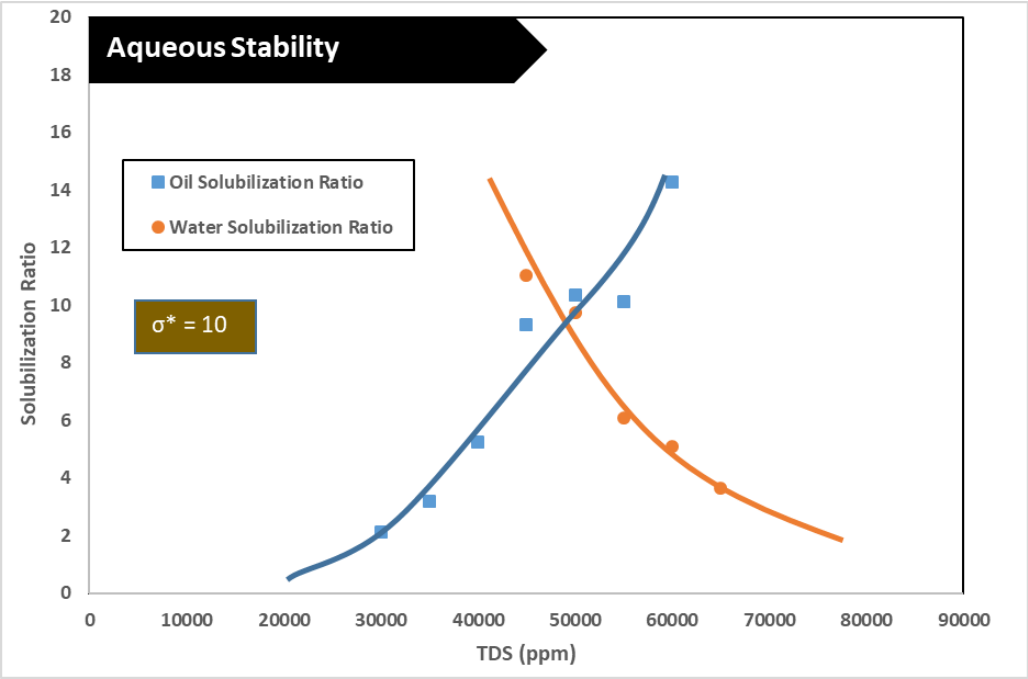

Figure 4.1. 3 Solubilization Ratios for Formulation F3

Phase behavior samples with 30% oil were equilibrated at 40°C for 2 weeks and then visually investigated for oil/water solubilization ratios. With the aqueous stability limit of 52,500ppm TDS, the ultra-low IFT range for formulation F4 is 50,000-55,000 ppm TDS and the optimum salinity is ~50,000ppm TDS. See Figure 4.1.4 for the solubilization ratios.

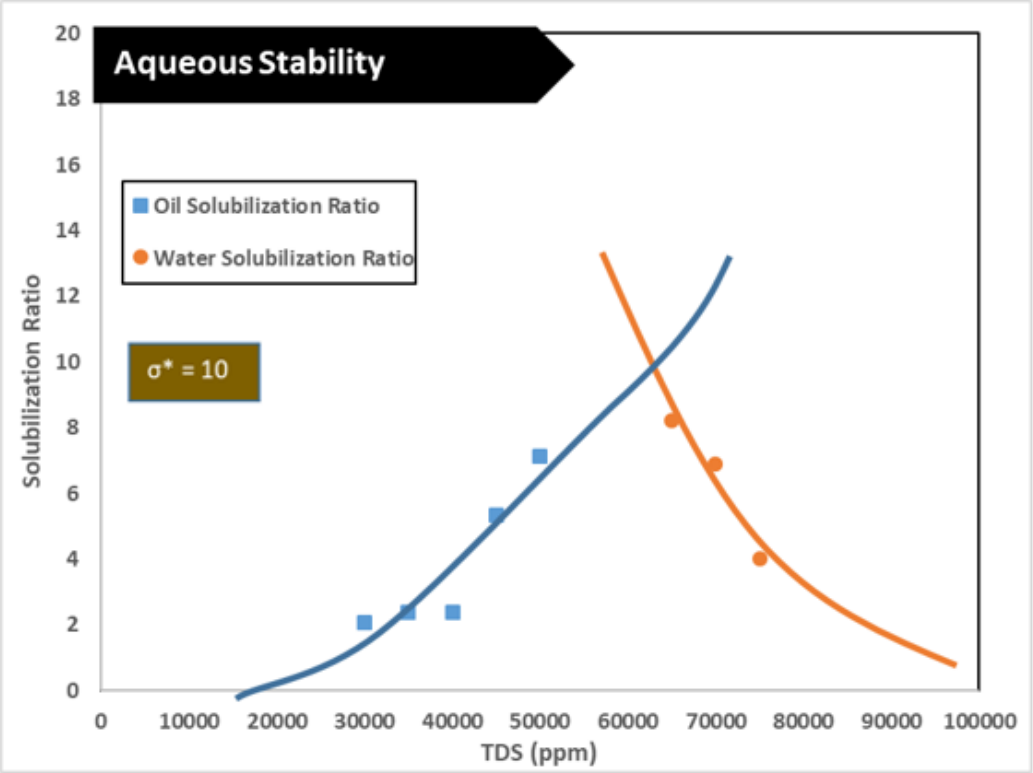

Figure 4.1. 4 Solubilization Ratios for Formulation F4

Phase behavior samples with 30% oil were equilibrated at 40℃ for a month and then visually investigated for oil/water solubilization ratios. With the aqueous stability limit of 55,000ppm TDS, the ultra-low IFT range for formulation F5 is 52,500-60,000 ppm TDS and the optimum salinity is ~53,000ppm TDS. See Figure 4.1.5 for the solubilization ratios.

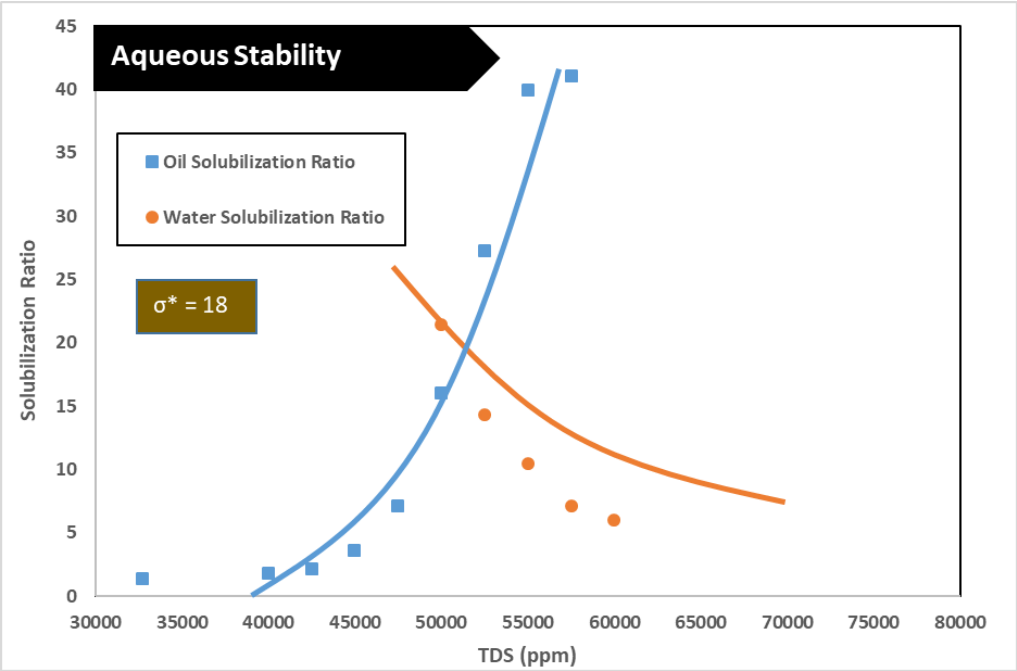

Figure 4.1. 5 Solubilization Ratios for Formulation F5

4.2. Static Adsorption Experiments

Static surfactant adsorption experiments were conducted to measure the surfactant adsorption on crushed Berea sandstone at neutral pH (7.0-7.5). Berea sandstone was crushed and sieved through 90 microns and 313 microns sieves to eliminate the very fine and coarse grains. Since, surfactant adsorption is a function of surface area, 2 g of 90-313µm size Berea sands were analyzed for the average surface area of the Berea rock sands. Brunauer–Emmett–Teller (BET) analysis was conducted with liquefied nitrogen and surface areas of samples were determined to be 1.0123 ± 0.0145 m^2/g. Adsorption also depends on the temperature and salinity. For these experiments, the chosen formulations were prepared at their optimum salinity and mixed with two grams of crushed Berea samples and then mixed properly for two days and kept at 40°C to equilibrate. Afterwards, samples were centrifuged at 2000 rpm for 10 minutes, and 1ml of supernatant was extracted. These samples were properly diluted and the surfactant concentration was measured by HPLC. The static adsorption was calculated by following equation:

$$Surfactant\ adsorption\left(\frac{mg}{g\ rock}\right) = \frac{10(Co(wt\%) - C(wt\%))M_{liq}\ (g)}{M_{rock}\ (g)} \quad (4.2.1)$$

where C_o initial surfactant concentration, C is final surfactant concentration, M_{liq} is mass of the aqueous phase and M_{rock} is the amount of rock sample. See Figure 4.2.1-Figure 4.2.5 for the results of total surfactant adsorption values for each formulation.

Static adsorption for formulation F1 increases with the increasing surfactant concentration up to 2000ppm. Above this concentration, the increase in surfactant adsorption is negligible. For formulation F1, the static total surfactant adsorption is 0.67mg/g-rock (See Figure 4.2.1).

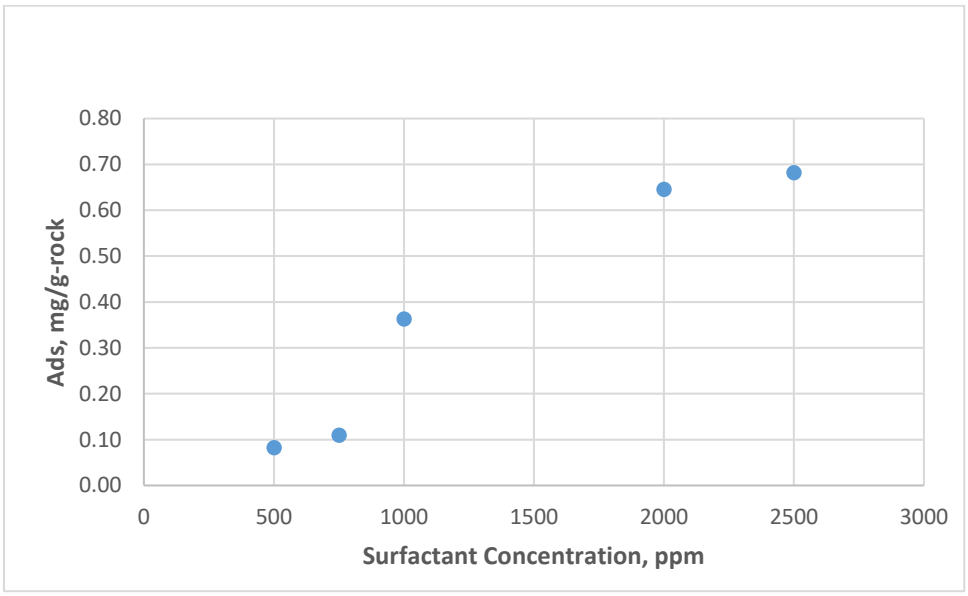

Figure 4.2. 1 Static Adsorption on crushed Berea for Formulation F1

Static adsorption for formulation F2 increases with the increasing surfactant concentration up to 2500ppm. Above this concentration, the change in surfactant adsorption is

negligible. For formulation F2, the static total surfactant adsorption is 0.5 mg/g-rock (See Figure 4.2.2).

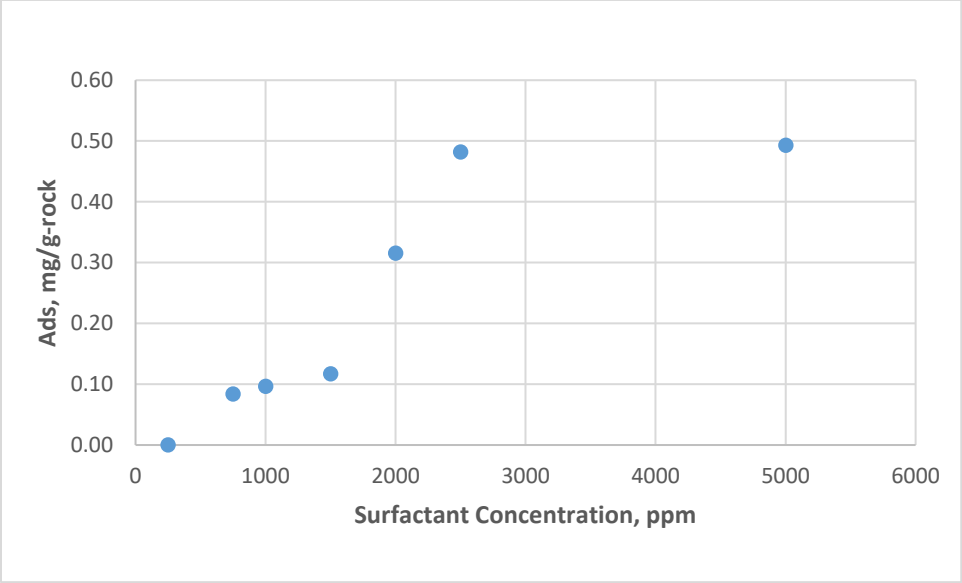

Figure 4.2. 2 Static Adsorption on crushed Berea for Formulation F2

Static adsorption for formulation F3 increases with the increasing surfactant concentration up to 1500ppm. Above this concentration, the change in surfactant adsorption is negligible. For formulation F3, the static total surfactant adsorption is 0.42 mg/g-rock (See Figure 4.2.3).

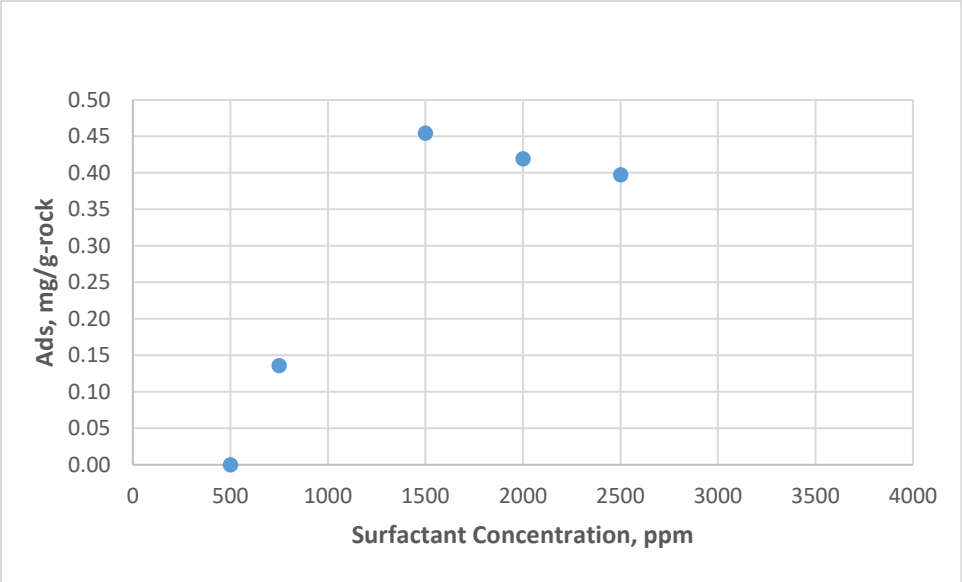

Figure 4.2. 3 Static Adsorption on crushed Berea for Formulation F3

Static adsorption for formulation F4 increases with the increasing surfactant concentration up to 2000ppm. Above this concentration, the change in surfactant adsorption is negligible. For formulation F4, the static total surfactant adsorption is 0.60 mg/g-rock (See Figure 4.2.4).

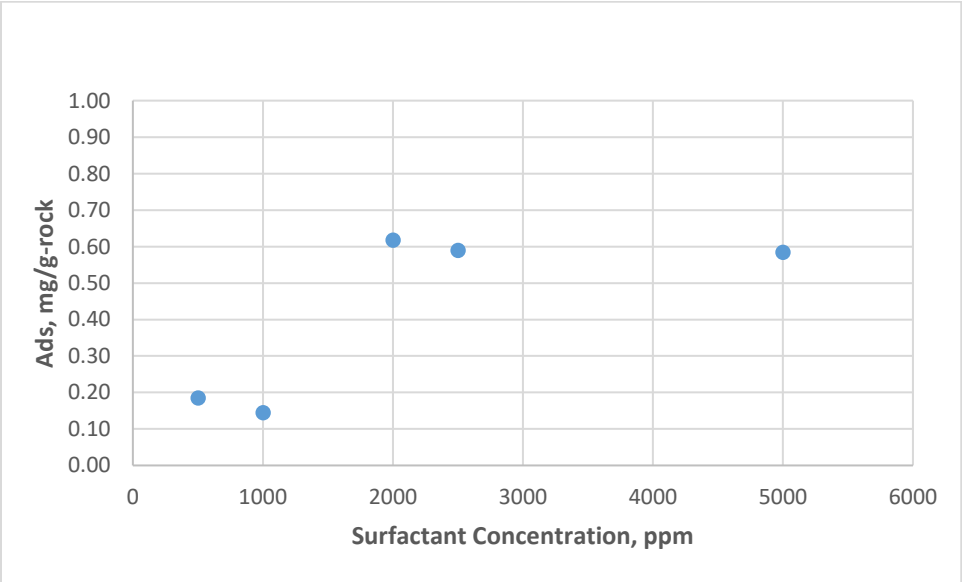

Figure 4.2. 4 Static Adsorption on crushed Berea for Formulation F4

Static adsorption for formulation F5 increases with the increasing surfactant concentration up to 2500ppm. Above this concentration, the change in surfactant adsorption is negligible. For formulation F5, the static total surfactant adsorption is 0.74 mg/g-rock (See Figure 4.2.5).

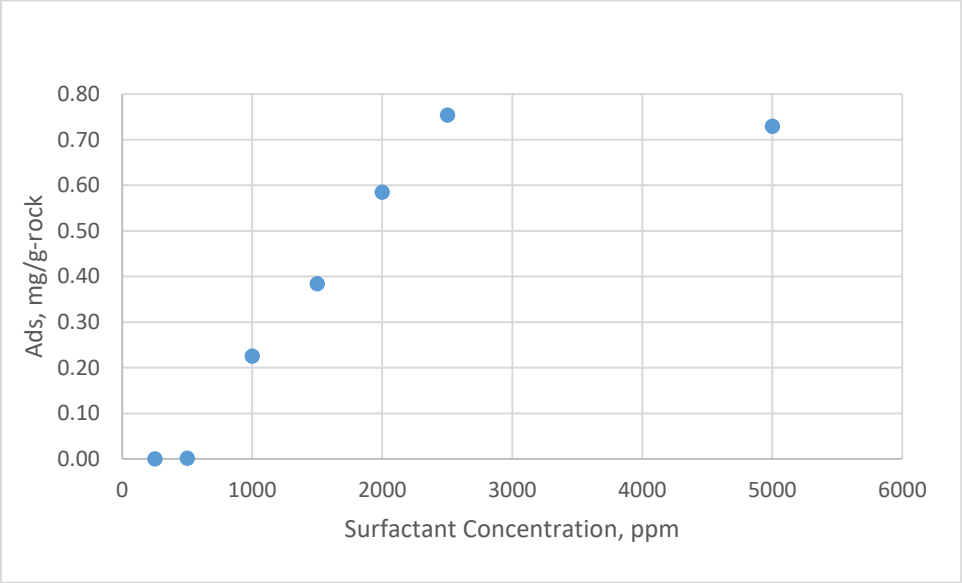

Figure 4.2. 5 Static Adsorption on crushed Berea for Formulation F5

Static Adsorption of each formulation at optimum salinity and at neutral pH (7.0-7.6) with 1% NaPA was estimated after equilibrating the samples for a week at 40°C (See Figure 4.2.6).

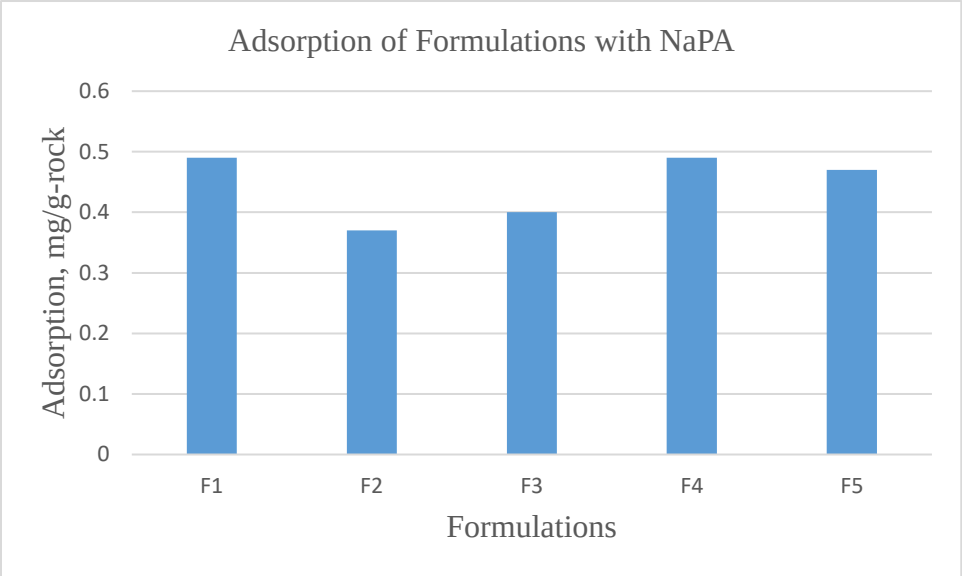

Figure 4.2. 6 Static Adsorption of the Formulations in the Presence of NaPA

As seen from the figures, adsorption of surfactant mixtures is between 0.5mg/g-rock and 0.72mg/g-rock for each formulation. By adding 1wt% of NaPA, the surfactant adsorption was reduced about 30-35wt% for each sample. For detailed information see Table 4.2.1 and Figure 4.2.7.

Table 4.2. 1 The Summary of the Static Adsorption Experiment with and without NaPA

Formulations	**Optimum Salinity, ppm**	**Without NaPA**	**With 1wt% NaPA**
		Ads, mg/g-rock	**Ads, mg/g-rock**
F1	40,000	0.67	0.49
F2	35,000	0.5	0.37
F3	45,000	0.42	0.40
F4	50,000	0.6	0.49
F5	53,000	0.74	0.47

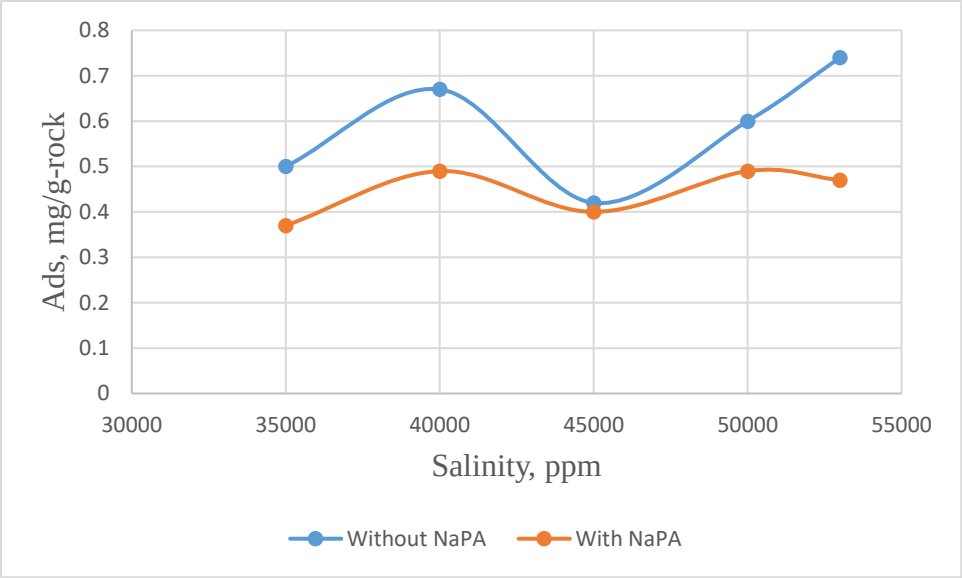

Figure 4.2. 7 Static Adsorption of Formulations at Optimum Salinity in the Presence and Absence of NaPA

4.3. Single Phase Dynamic Adsorption Experiments

Single phase flood (S) experiments were conducted using the chosen formulations to determine surfactant adsorption in corefloods in the absence of oil. The experiments were conducted at the 40°C. 0.5-0.6 PV of surfactant slugs were injected in each case. Low concentration, i.e., low viscosity of FP33330S polymer was used due to high permeability rock matrix. Once effluents were collected in fractions, polymers were degraded by TEGBE and bleach mixture and samples were analyzed with HPLC for surfactant concentration. Surfactant retention values for each experiment were determined and then some of the formulations were chosen to be analyzed further with NaPA to measure the effect of NaPA on surfactant retention.

4.3.1. Single Phase Flood Dynamic Experiments without NaPA

4.3.1.1. Single Phase Flood Experiment S-1

The purpose of experiment S-1 was to determine the surfactant retention of formulation F1 on a Berea Sandstone. The core properties are given in the Table 4.3.1. This experiment was

conducted without oil and without co-solvent in the polymer drive. The core used in this experiment was a new outcrop core (never was a subject of any flood). After the core was dried in an 80℃ oven for two days, the core was cooled down and dimensions of the core was measured. Afterward, the core was prepared as described in Chapter III and saturated with 4 wt% NaCl.

Table 4.3. 1 Core Properties for Experiment S-1

Rock Type	Berea Sandstone	
Temperature	40.00	°C
Diameter	3.76	cm
Length	29.90	cm
Mass	716.25	g
Area X	11.13	cm^2
Pore Volume	64.00	ml
Bulk Volume	332.76	cm^3
Porosity	0.19	
Brine Viscosity @40°C	0.70	cP
Brine Permeability	86.47	mD

Brine Flood and Pore Volume Calculation

4 wt% NaCl brine was used to determine the pore volume and brine permeability. After injecting carbon dioxide and vacuuming the core, the injection line was pressurized up to 200 psi using a syringe pump. While keeping the outlet valve shut, the inlet valve to the core was opened until the core was fully saturated with brine and the pump flow rate was zero. When the flow rate was zero, the pump was stopped and the outlet was opened to equilibrate the pressure. The liquid produced was collected in a graded plastic centrifuge tube and the volume which was 1.2 ml was noted as the leak volume. By knowing the liquid volume before pressurizing the system, and knowing the dead-end volume of the system which was 2.1ml the pore volume was calculated as 64 ml with a porosity of 19% at room temperature.

The brine permeability of the core was estimated by the pressure drop across the core. After saturation, the two pore volumes of the same brine was injected into the core. During that time, the outlet was kept open to the atmosphere without backpressure and the effluent was collected in a waste container. By changing the injection flow rate and observing the pressure drop across the core via a pressure gauge connected to the inlet of the core, the steady state pressure drop data was collected and used to determine the brine permeability. For this experiment, brine permeability was 86.5 mD.

Chemical Composition

Formulation F1 was used in this experiment showed an ultra-low IFT around 4.0-5.0 wt% NaCl. For this experiment, the optimum salinity was chosen to be 4wt% NaCl.

The polymer drive salinity was designed to be 60wt% of surfactant slug salinity. A low polymer concentration was used since no oil was displaced. Table 4.3.2 lists the composition of the chemical slugs.

Table 4.3. 2 Composition of Chemical Flood Solutions for Experiment S-1

Injection Fluid	**Components**
Surfactant Slug	4 wt% NaCl
	0.5 wt% CH_3O 21PO 10EO SO_4
	0.5 wt% $C_{19\text{-}23}$ IOS
	1 wt% TEGBE
	0.15 wt% FP3330S
Polymer Drive	
	2.5 wt% NaCl
	0.15 wt% FP3330S

Chemical Flood

The chemical flood solutions were prepared based on the steps detailed in the previous chapter. Although, this experiment was only single phase flood, the polymer was used in both

the surfactant slug and the polymer drive to emulate the oil recovery coreflood. Surfactant slug was injected at 1ft/D and followed by the polymer drive, which was without any co-solvent. The lists and properties and injection volume information of chemical solutions are shown in the Table 4.3.3.

Table 4.3. 3 Surfactant Slug and The polymer drive Properties for Experiment S-1

	Surfactant Slug	**Polymer Drive**
PV Injected	0.6	2
Polymer	FP 3330S	FP 3330S
Polymer Concentration (ppm)	1500	1500
Frontal Velocity (ft/D)	1	1
Salinity (ppm TDS)	40,000	25,000
pH	6.8	6.5

Chemical Flood Results

During the chemical flood effluents were collected into the plastic graded tubes with 6 ml volume of liquid in each. After ~2.5 PV of injection, the chemical flood was ended. Surfactant retention was determined from the surfactant concentration data measured using the HPLC to be 0.235 mg/g-rock with 0.52mg/g-rock being injected. Surfactant broke-through at 0.93 PV and reached the peak at 1.66 PV with ~3700 ppm concentration (See Figure 4.3.3).

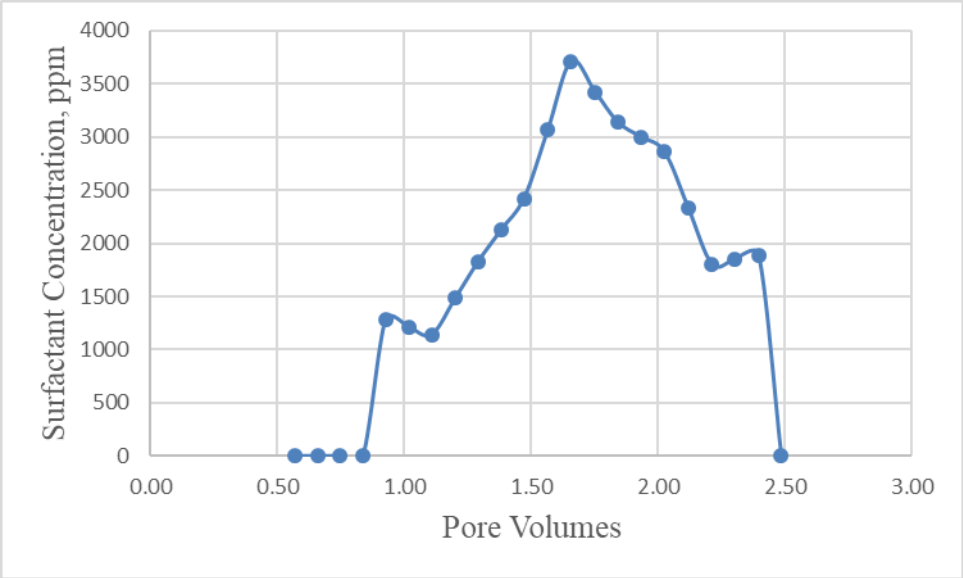

Figure 4.3. 1 Effluent Surfactant Concentration for Experiment S-1

4.3.1.2. Single Phase Flood Experiment (S-2)

The purpose of experiment S-2 was to determine the surfactant retention of formulation F2 on a Berea Sandstone. Similar to experiment S-1, this experiment was conducted without oil and co-solvent in the polymer drive. The core used in this experiment was a new outcrop core (never was a subject of any flood). After the core size was analyzed, the core was placed into the core holder and then saturated with 3.5wt% NaCl, optimum salinity. See Table 4.3.4 for the core properties.

Table 4.3. 4 Core Properties for Experiment S-2

Rock Type	Berea Sandstone	
Temperature	40.00	°C
Diameter	3.80	cm
Length	30.45	cm
Weight	701.81	g
Area X	11.33	cm^2
Pore Volume	74.00	ml
Bulk Volume	344.85	cm^3
Porosity	0.21	
Brine Viscosity @40°C	0.69	cP
Permeability	277.16	mD

Brine Flood and Pore Volume Calculations

3.5 wt% NaCl brine was injected to saturate the core, estimate the pore volume of the core and obtain brine permeability. After CO_2 injection and vacuuming, the system was pressurized to 200 psi same as experiment S-2, and with the pump volume, leak volume (0.85ml) and the dead-end volume (2.1ml) information the pore volume was determined as 74ml with a porosity of 21% at room temperature.

To determine the brine permeability of the core, the pressure drop across core at steady state was used in Darcy's Equation. The procedure was the same as experiment S-1. The brine permeability was estimated to be 277mD.

Chemical Composition

Formulation F2 showed a classical type of phase behavior, i.e., the transition between phase behavior types with salinity are similar to classical phase behavior (Type I phase behavior is observed at low salinities and as salinity increased type III is observed and flowed by Type II). Ultra-low IFT with low microemulsion viscosity was observed around 3.5-4.0 wt% NaCl. For this experiment, the optimum salinity was chosen to be 3.5wt% NaCl which is also aqueously stable at 40℃.

The polymer drive salinity was designed to be ~60wt% of surfactant slug salinity. Also, for the same reasons as experiment S-1, polymer concentration was low. See Table 4.3.5 for formulation of S-2.

Table 4.3. 5 Composition of Chemical Flood Solutions for Experiment S-2

Injection Fluid	**Components**
Surfactant Slug	3.5 wt% NaCl
	0.5 wt% TDA 13PO SO_4
	0.5 wt% $C_{19\text{-}23}$ IOS
	1 wt% TEGBE
	0.1 wt% FP3330S
The polymer drive	
	2 wt% NaCl
	0.1 wt% FP3330S

Chemical Flood

The chemical flood solutions were prepared based on the steps detailed in previous chapter. Although, this experiment was only single phase flood, the polymer was used into both surfactant slug and the polymer drive to emulate an oil recovery core flood. Surfactant slug and the polymer drive were injected at 1ft/D. The polymer drive did not have any co-solvent. See below the lists and properties and injection volume information of chemical solutions.

Table 4.3. 6 Surfactant Slug and Polymer Drive Properties for Experiment S-2

	Surfactant Slug	**Polymer Drive**
PV Injected	0.6	2
Polymer	FP 3330S	FP 3330S
Polymer Concentration (ppm)	1500	1500
Frontal Velocity (ft/D)	1	1
Salinity (ppm TDS)	35,000	20,000
pH	6.6	6.67

Chemical Flood Results

6 ml samples of effluent were collected in plastic graded tubes and after nearly 2.5 PV of chemical flood injection was stopped and effluents were analyzed by HPLC. Surfactant retention was determined to be 0.166 mg/g-rock with 0.65 mg/g-rock being injected. Surfactant

broke-through ~1 PV and reached the peak at 1.6 PV with ~7000 ppm concentration. See the figure below for surfactant concentration.

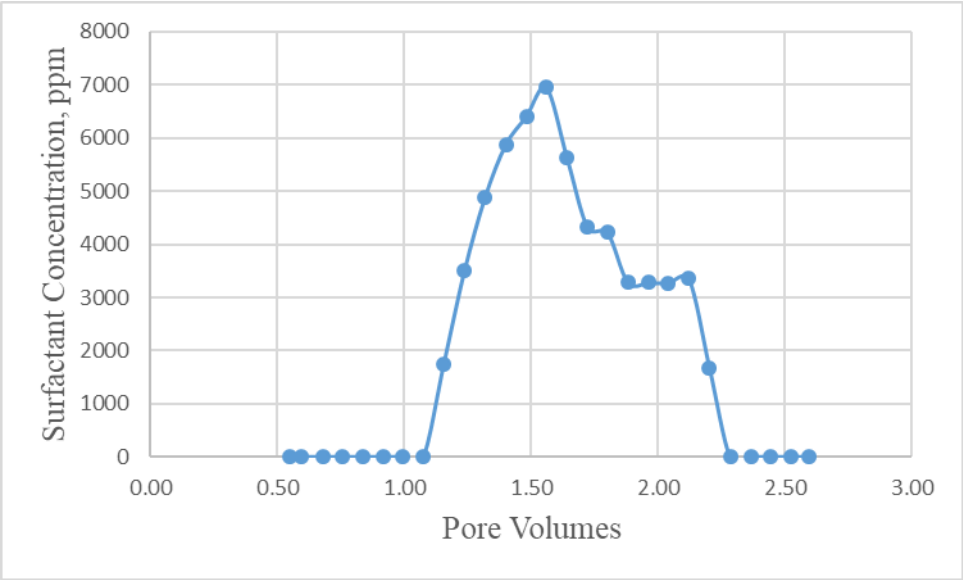

Figure 4.3. 2 Effluent Surfactant Concentration for Experiment S-2

4.3.1.3. Single Phase Flood Experiment (S-3)

The purpose of experiment S-3 was to determine the surfactant retention of Formulation #3 in a Berea Sandstone. This experiment was conducted without oil and co-solvent in the polymer drive. The core used in this experiment was a new outcrop core (never was a subject of any flood). After analyzing the core size and preparing the core as stated in previous chapters, the core was saturated with 4.5wt% NaCl, which is the optimum salinity for chosen formulation. See Table 4.3.7 for the detailed information about the core.

Table 4.3. 7 Core Properties for Experiment S-3

Rock Type	Berea Sandstone	
Temperature	40.00	°C
Diameter	3.78	cm
Length	30.35	cm
Weight	731.80	gr
Area X	11.25	cm^2
Pore Volume	65.00	ml
Bulk Volume	341.42	cm^3
Porosity	0.19	
Brine Viscosity @40°C	0.71	cP
Permeability	134.70	mD

Brine Flood and Pore Volume Calculations

Pore volume of the core was determined through saturation of 4.5wt% NaCl. The core was saturated with that brine at high pressure rate after the core was vacuumed for three hours. By knowing the pump injected liquid volume and leak volume (1.5ml) and the dead-end volume (2.1ml), the pore volume was calculated to be 65 ml with a porosity of 19% at 25°C.

Brine permeability of the core was determined by the same method as previous dynamic experiments, meaning steady state conditions' pressure drop was used in Darcy's equation. For this experiment, the permeability was determined to be 135mD.

Chemical Composition

Formulation F3 showed a classical type of phase behavior. The transition between phase behavior types with salinity are the same as classical phase behaviors,' i.e. Type I phase behavior is observed at low salinities and as salinity increased type III is observed and flowed by Type II. Ultra-low IFT with low microemulsion viscosity was observed around 4.0-4.5 wt% NaCl at 40℃. For this experiment, the optimum salinity was chosen to be 4.5wt% NaCl which is also aqueously stable at 40℃.

The polymer drive salinity was designed to be ~60wt% of surfactant slug salinity. Also, for the same reasons of S-1, and S-2 polymer concentration was low. See below the charts of summary of formulation and core properties.

Table 4.3. 8 Composition of Chemical Flood Solutions for Experiment S-3

Injection Fluid	**Components**
Surfactant Slug	4.5 wt% NaCl
	0.5 wt% TDA-7PO-SO_4
	0.5 wt% C_{1923} IOS
	1 wt% TEGBE
	0.1 wt% FP3330S
Polymer Drive	2.5 wt% NaCl
	0.1 wt% FP3330S

Chemical Flood

The chemical flood solutions were prepared based on the steps detailed in previous chapter. To emulate the oil production, the polymer was used into the both surfactant slug and polymer drive. The surfactant slug and polymer drive were injected with 1ft/D and the polymer drive did not include any co-solvent. Table 4.3.9 lists the properties of chemical solutions.

Table 4.3. 9 Surfactant Slug and Polymer Drive Properties for Experiment S-3

	Surfactant Slug	**Polymer Drive**
PV Injected	0.6	2
Polymer	FP 3330S	FP 3330S
Polymer Concentration (ppm)	1000	1000
Frontal Velocity (ft/D)	1	1
Salinity (ppm TDS)	45,000	25,000
pH	7.30	7.45

Chemical Flood Results

After nearly 2.5 PV of the chemical flood and collecting fractions of 6 ml of effluents in plastic centrifuge tubes, the injection was ended and effluents were analyzed. The surfactant retention for this experiment was determined to be 0.176 mg/g-rock with 0.53 mg/g-rock being injected. The surfactants broke-through at 1 PV of injection and reached the peak at 1.3 PV with ~6600 ppm concentration. See Figure 4.3.5 for the effluent surfactant concentrations.

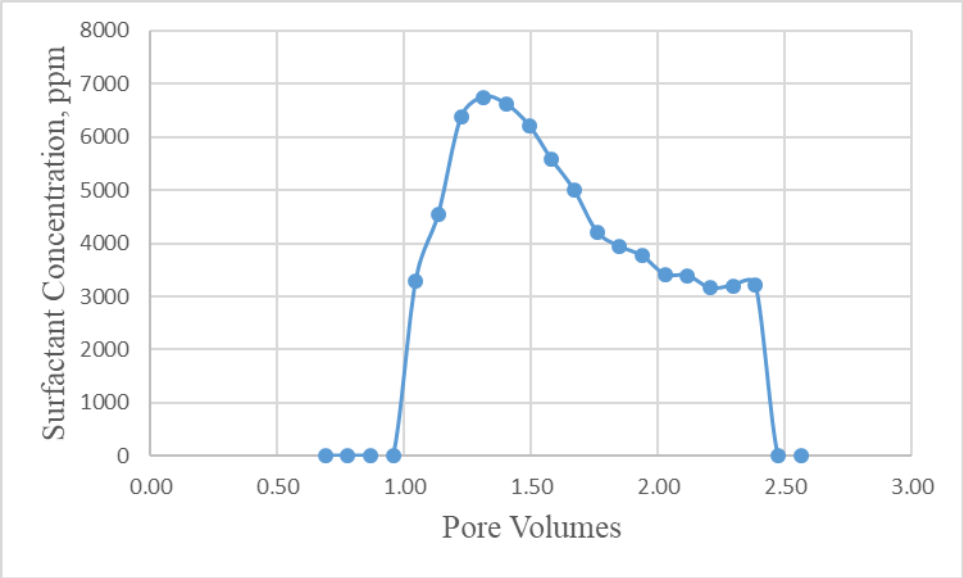

Figure 4.3. 3 Effluent Surfactant Concentration for Experiment S-3

4.3.1.4. Single Phase Flood Experiment (S-4)

The purpose of experiment S-4 was to measure the surfactant retention of formulation F4 on a Berea Sandstone. This experiment conducted without oil and co-solvent in the polymer drive. The core has been used in this experiment was a new outcrop core (never was a subject of any flood). The core was analyzed for the size and mass and prepared for the flood as described in Chapter III. The core was then saturated with the brine at optimum salinity (5wt% NaCl). See Table 4.3.10 below for core properties of this experiment.

Table 4.3. 10 Core Properties for Experiment S-4

Rock Type	Berea Sandstone	
Temperature	40.00	°C
Diameter	3.80	cm
Length	31.50	cm
Weight	737.35	g
Area X	11.32	cm^2
Pore Volume	72.17	ml
Bulk Volume	356.50	cm^3
Porosity	0.20	
Brine Viscosity @40°C	0.72	cP
Brine Permeability	59.62	mD

Brine Flood and Pore Volume Calculations

Pore volume of the core was determined through saturation of 5wt% NaCl. The core was saturated with that brine at high pressure after the core was vacuumed for three hours. By knowing the pump injected liquid volume and leak volume (1.5ml) and the dead-end volume (2.1ml), the pore volume was calculated to be 72 ml with a porosity of 20% at 25°C.

The brine permeability of the core was determined by the same method as previous dynamic experiments, meaning steady state conditions' pressure drop was used in Darcy's equation. For this experiment, the permeability was determined to be 60mD.

Chemical Composition

Formulation F4 showed a classical type of phase behavior. The transition between phase behavior types with salinity are the same as classical phase behaviors' (i.e. Type I phase behavior is observed at low salinities and as salinity increased type III is observed and flowed by Type II). Ultra-low IFT with low microemulsion viscosity was observed around 4.5-5.0wt% NaCl at 40℃. For this experiment, the optimum salinity was chosen to be 5.0wt% NaCl which is also aqueously stable at 40℃.

The polymer drive salinity was designed to be ~60wt% of the surfactant slug salinity. Also, for the same reasons of previous floods, polymer concentration kept low. See below the summary of formulation and core properties.

Table 4.3. 11 Composition of Chemical Flood Solutions for Experiment S-4

Injection Fluid	**Components**
Surfactant Slug	5 wt% NaCl
	0.5 wt% 2EH 7PO SO_4
	0.5 wt% C_{19-23} IOS
	1 wt% TEGBE
	0.1 wt% FP3330S
Polymer Drive	
	3 wt% NaCl
	0.1 wt% FP3330S

Chemical Flood

Chemical flood solutions were prepared as described in the previous chapter. In this experiment, surfactant slug and the polymer drive (without co-solvent) were injected at 1ft/D. Polymer was used in surfactant slug as well to maintain the required viscosity.

Table 4.3. 12 Surfactant Slug and Polymer Drive Properties for Experiment S-4

	Surfactant Slug	**Polymer Drive**
PV Injected	0.6	2
Polymer	FP 3330S	FP 3330S
Polymer Concentration (ppm)	1000	1000
Frontal Velocity (ft/D)	1	1
Salinity (ppm TDS)	50,000	30,000
pH	7.2	7.1

Chemical Flood Results

After about 2 PV injection the flood was stopped and then collected effluent samples were analyzed. Surfactant retention was estimated to be 0.234 mg/g-rock using HPLC. The injected amount of surfactant was 0.52 mg/g-rock. Surfactant broke-through around 1 PV and the peak was around 1.5 PV with ~4200 ppm concentration. See below the effluent analysis in terms of surfactant concentration.

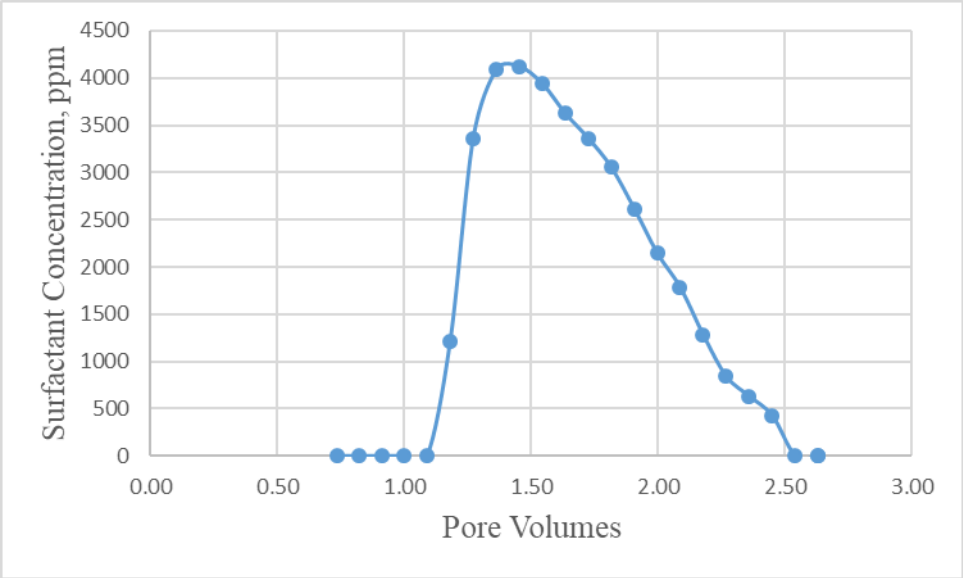

Figure 4.3. 4 Effluent Surfactant Concentration for Experiment S-4

4.3.1.5. Single Phase Flood Experiment (S-5)

The purpose of this flood is to determine the repeatability of the retention values. By using the same formulation as in S-1 with the same size and type of outcrop with the same polymer concentration under same conditions, the same experiment was repeated and retention value was calculated in the same way that of S-1. See below the formulation and the core properties for this particular experiment.

Table 4.3. 13 Core Properties for Experiment S-5

Rock Type	Berea Sandstone	
Temperature	40.00	°C
Diameter	3.79	cm
Length	30.60	cm
Weight	738.79	gr
Area X	11.29	cm^2
Pore Volume	67.58	ml
Bulk Volume	345.62	cm^3
Porosity	0.20	
Brine Viscosity @40°C	0.70	cP
Permeability	189.77	mD

Brine Flood and Pore Volume Calculations

For this flood the core was saturated with 5wt% KCl at 200 psi pressure to establish the pore volume. Once the dead-end volume of the core holder and leak volume was subtracted from the volume of injected brine into the core, the pore volume was determined to be 67.5ml with the porosity of 20% at room temperature. In addition to saturation method, the pore volume was also determined with tracer test after injection of 1wt% KCl at 3ml/min with a sample taken every 2 minutes for a samples size of 4ml. Based on the tracer test pore volume was determined to be 67.6ml, which is only 0.9ml lower than the saturation volume. For this experiment tracer test pore volume was used. The tracer brine broke-through at 0.32PV and took ~2PV for the effluent salinity to reach the injected salinity (See Figure 4.3.7) After tracer test 4wt% NaCl was injected to saturate the core with optimum salinity brine prior to chemical

flood. The pressure drop at steady state for different flow rates (1ml/min, 2ml/min and 3ml/min) were used to calculate brine permeability, which was equal to 190mD.

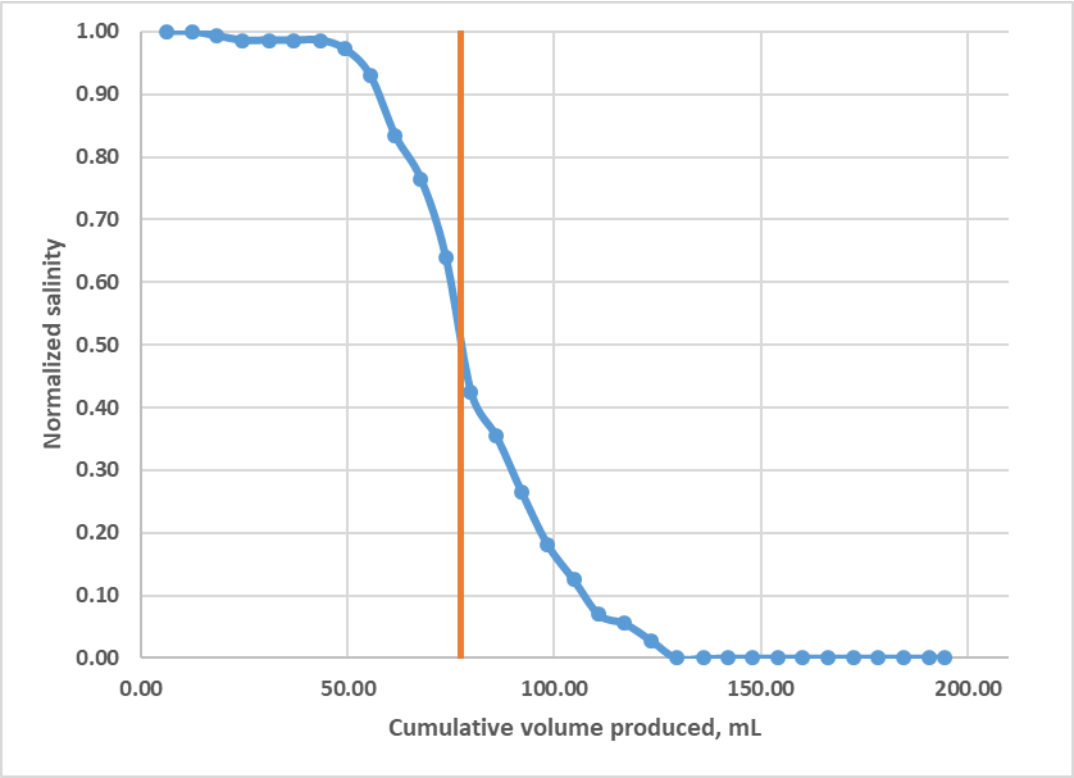

Figure 4.3. 5 Tracer Test for Experiment S-5

Chemical Composition

Formulation F1 was used in this experiment to compare the repeatability of the retention number.

Table 4.3. 14 Properties of Solutions for Experiment S-5

Injection Fluid	**Components**
Surfactant Slug	4 wt% NaCl
	0.5 wt% CH_3O 21PO 10EO SO_4
	0.5 wt% C_{19-23} IOS
	1 wt% TEGBE
	0.15 wt% FP3330S
Polymer Drive	2.5 wt% NaCl
	0.15 wt% FP3330S

Chemical Flood

As experiment S-1, the formulation of chemicals were kept the same and prepared in the way described in Chapter III. The Chemical solutions (surfactant slug and then the polymer drive) were injected at the same flow rate as experiment S-1 (1ft/D) and fraction of 6 ml of effluents were collected in plastic centrifuge tubes for the effluent analysis.

Table 4.3. 15 Surfactant Slug and The polymer drive Properties for Experiment S-5

	Surfactant Slug	**Polymer Drive**
PV Injected	0.6	2
Polymer	FP 3330S	FP 3330S
Polymer Concentration (ppm)	1500	1500
Frontal Velocity (ft/D)	1	1
Salinity (ppm TDS)	58000	25000
pH	7	7

Chemical Flood Results

Chemical flood was continued for ~2.5 PV and then stopped for effluent analysis. Effluents were analyzed in HPLC and the retention was determined to be 0.22mg/g-rock with 0.58mg/gr-rock being injected. Surfactant broke-through at 0.7PV and reached the peak of concentration of 5600 ppm at 1.45PV (See Figure 4.3.8).

.

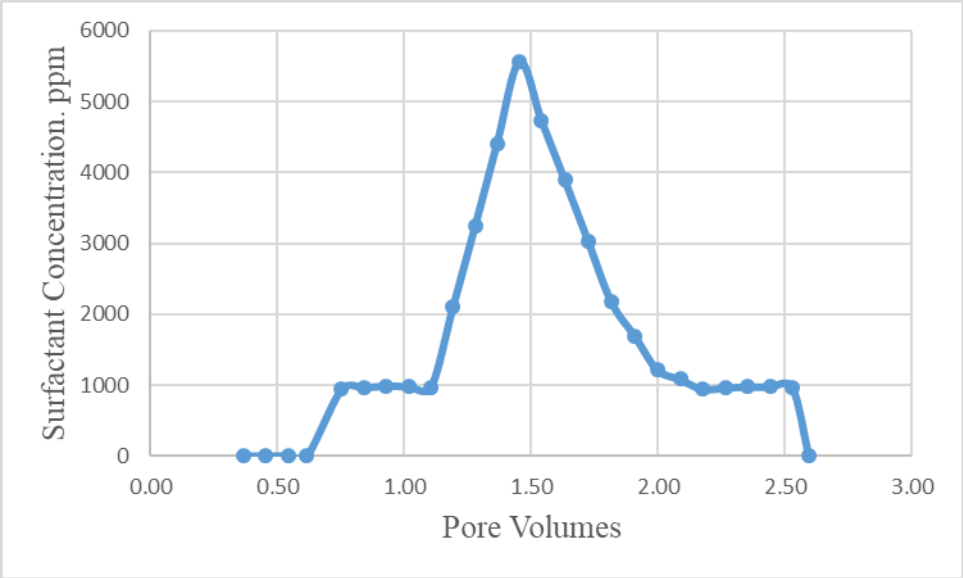

Figure 4.3. 6 Effluent Surfactant Concentration for experiment S-5

Effluent samples were analyzed for salinity propagation during chemical slug. In this experiment, effluent salinity reached a peak salinity of 55000 ppm TDS at 1.4PV (Figure 4.3.9). This indicates that the salinity of the slug propagated well throughout the core.

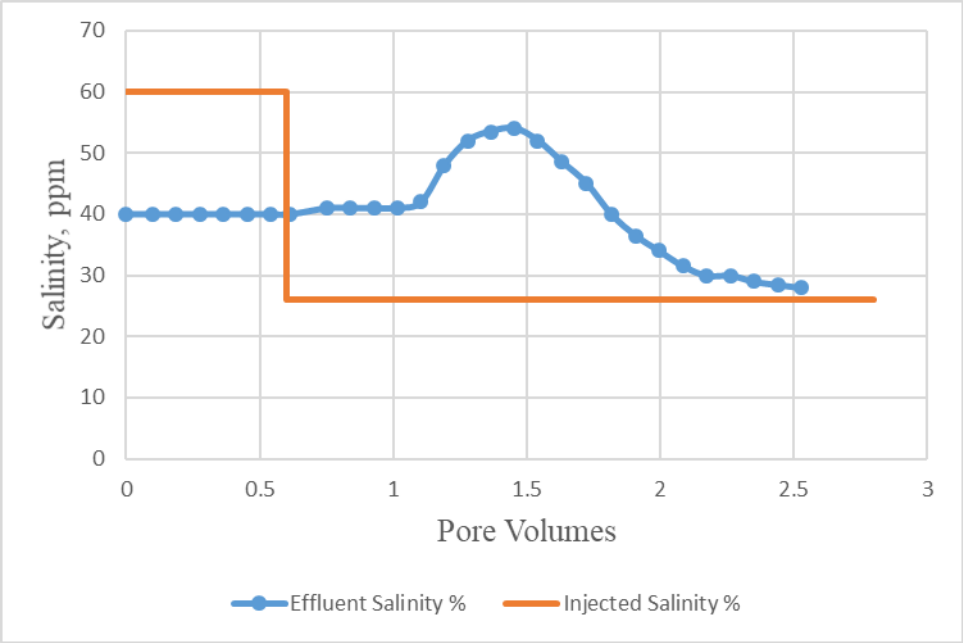

Figure 4.3. 7 Chemical Flood Effluent Salinity for Experiment S-5

Discussion of Results S-5

For this experiment, the retention of surfactant Formulation F1 was determined to be 0.22mg/g-rock. The main purpose of this experiment was to determine the repeatability of the dynamic experiment for the same conditions with the same formulation. Based on the obtained surfactant retention value, since the retention for experiment S-1 was estimated to be 0.235mg/g-rock, it can be clearly stated that the dynamic experiments are repeatable with 5% error when mineralogical composition of the cores and conditions were the same.

4.3.8 Single Phase Flood Experiment (S-6)

This experiment was conducted to determine the retention of formulation F5 through single phase flood dynamic experiment. After the determination of pore volume and permeability of the core the chemical flood has been conducted at 1ft/D. By arranging the pH of slugs to be between 6.5 and 8, the neutral conditions are targeted. Polymer concentration was kept low (1500ppm FP 3330S) as previous single phase dynamic floods.

Table 4.3. 16 Core Properties for Experiment S-6

Rock Type	Berea Sandstone	
Temperature	40	°C
Diameter	3.80	cm
Lenght	31.50	cm
Weight	722	g
Area X	11.25	cm^2
Pore Volume	70.0	ml
Bulk Volume	354.36	cm^3
Porosity	0.20	
Brine Viscosity @40°C	0.72	cP
Permeability	171	mD

Brine Flood and Pore Volume Calculations

2wt%KCl used to saturate the core and 5.3wt% NaCl injected at 2ml/min into the core for tracer test. Tracer test was conducted at 2ml/min and fractions of 6ml of effluents were collected into 15ml plastic graded tubes. Tracer brine broke-through around 0.7PV and reached injected salinity after 1.7PV (Figure 4.3.10). After tracer test brine permeability calculation was conducted. 5.3wt% NaCl was injected at different flow rates (1ml/min, 2ml/min and 3ml/min) until it reached steady state and then by using Darcy's Law, the permeability was calculated as 171mD at 40℃.

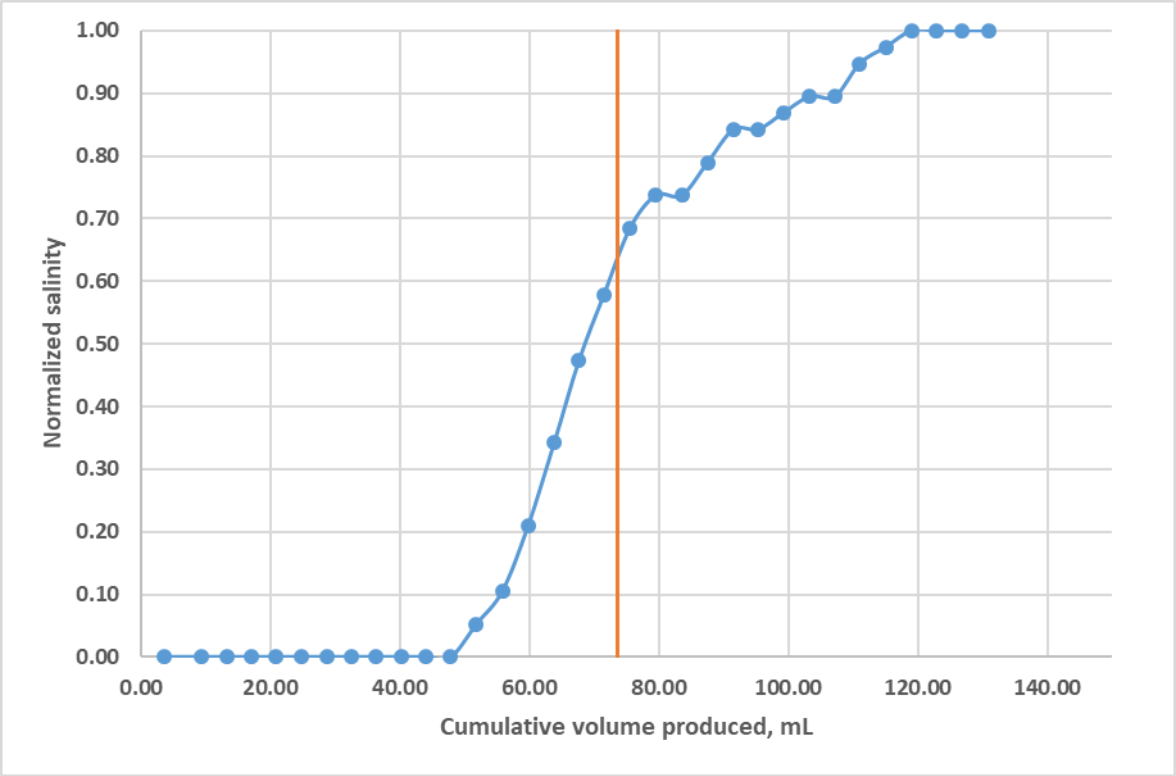

Figure 4.3. 8 Tracer Test for Experiment S-6

Chemical Composition

Formulation F5 was used in this experiments. See Table 4.3.17 for chemical composition in details.

Table 4.3. 17 Composition of Chemical Flood Solutions for Experiment S-6

Injection Fluid	**Components**
Surfactant Slug	5.3 wtwt% NaCl
	0.6 wt% TDA 13PO SO_4
	0.3 wt% $C_{15\text{-}18}$ IOS
	0.25 wt% TEGBE
	0.15 wt% FP3330S
Polymer Drive	0.15 wt% FP3330S
	3.7 wt% NaCl

Chemical Flood

Chemical flood solutions are prepared as described in Chapter III. Surfactant slug and the polymer drive (without co-solvent) were injected after filtration by using argon gas. Polymer was used in surfactant slug as well to maintain the required viscosity. Injection parameters can be seen from Table 4.3.18.

Table 4.3. 18 Surfactant Slug and Polymer Drive Properties for Experiment S-6

	Surfactant Slug	**Polymer Drive**
PV Injected	0.5	2
Polymer	FP 3330S	FP 3330S
Polymer Concentration (ppm)	1500	1500
Frontal Velocity (ft/D)	1	1
Salinity (ppm TDS)	64	37
pH	8.00	7.80
Viscosity at 10 s^{-1} & 40°C	7	8

Chemical Flood Results

Chemical flood was continued for 2.5PV and the effluents were collected in plastic centrifuge tubes. The effluents were analyzed in HPLC for surfactant retention. Surfactant breakthrough was observed at 0.5PV and the concentration reached the peak at 0.7PV and 3745 ppm. See Figure 4.3.10 for effluent surfactant concentration.

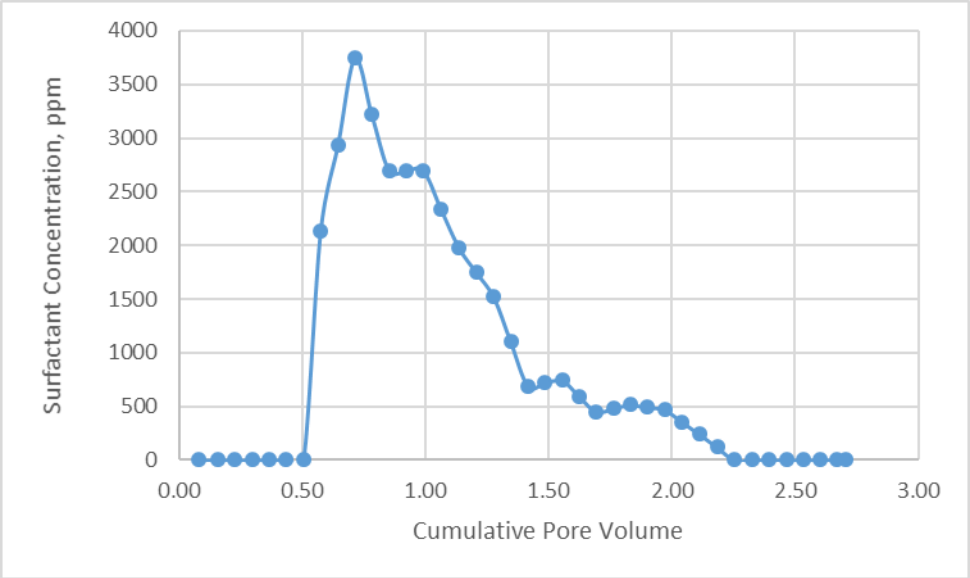

Figure 4.3. 9 Effluent Surfactant Concentrations for experiment S-6

The salinity propagation of the chemical slugs was also tested via refractometer. Effluent salinity reached the peak at 61000 ppm TDS at 1.3PV. The Figure 4.3.11 indicates that the salinity of the slug propagated well through the core.

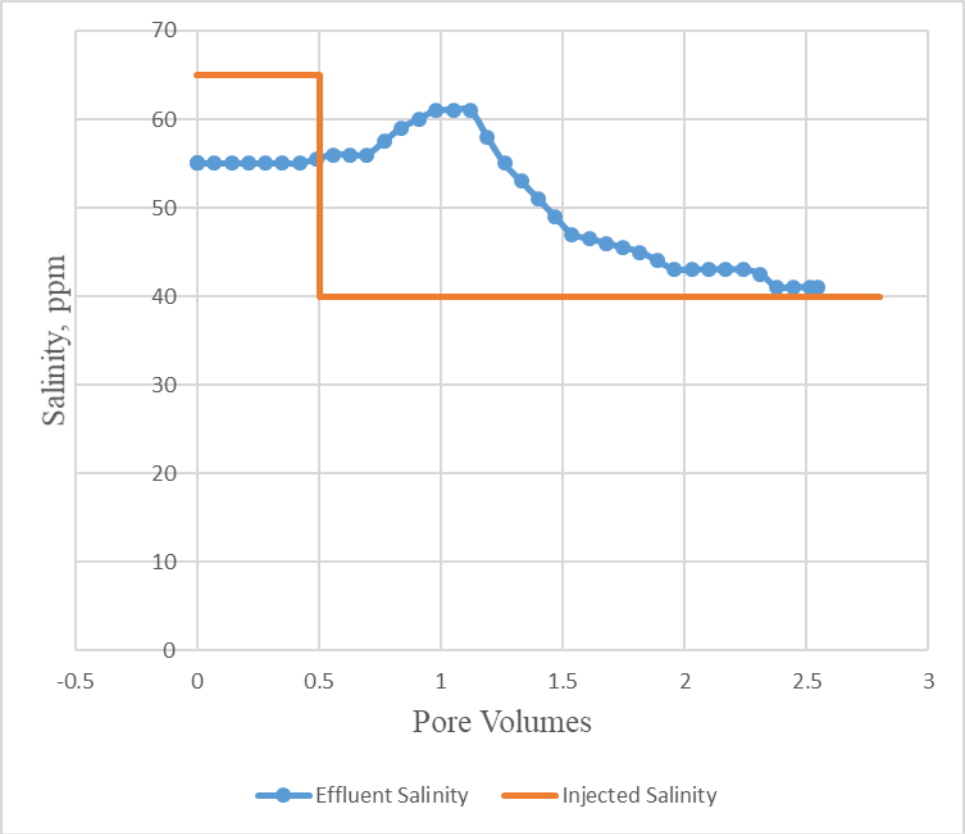

Figure 4.3. 10 Chemical Flood Effluent Salinity for Experiment S-6

The pH propagation of effluents were measured via pH meters and the pH propagation. See Figure 4.3.12. The effluent pH is higher than the injected pH because of the buffering capacity of the core.

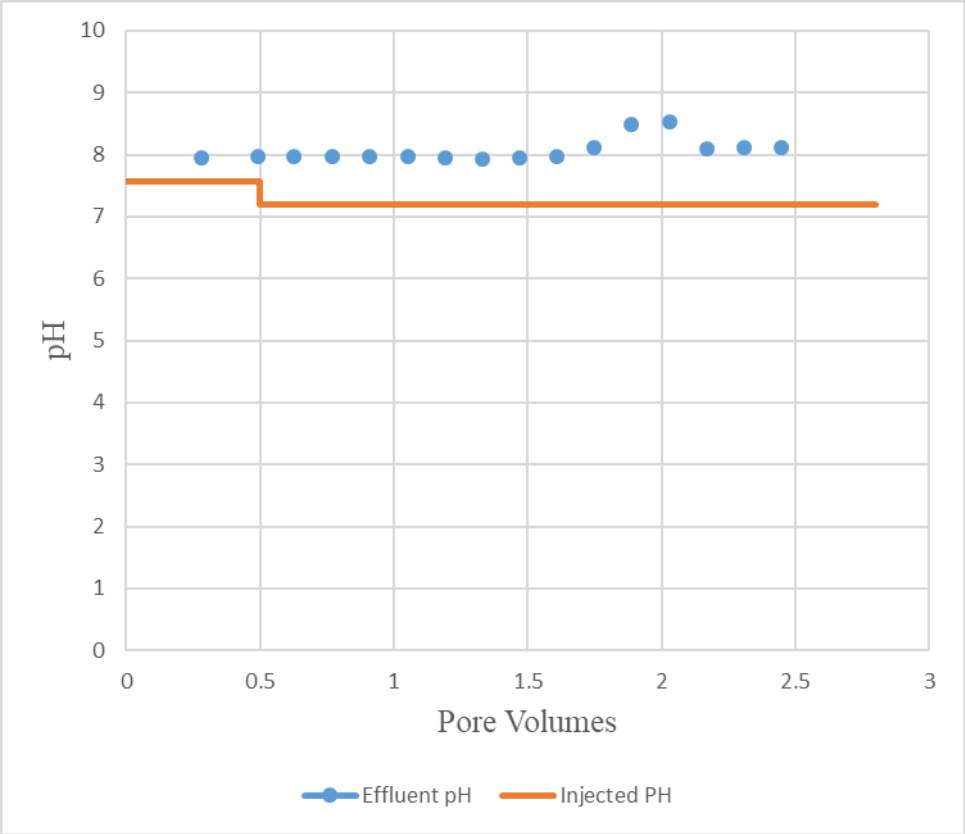

Figure 4.3. 11 Chemical Flood Effluent pH for Experiment S-6

The pressure drop during the chemical flood was indicated in Figure 4.3.13. The pressure drop of whole core increased up to ~0.9PV and then stabilized for 1.5PV of the chemical injection.

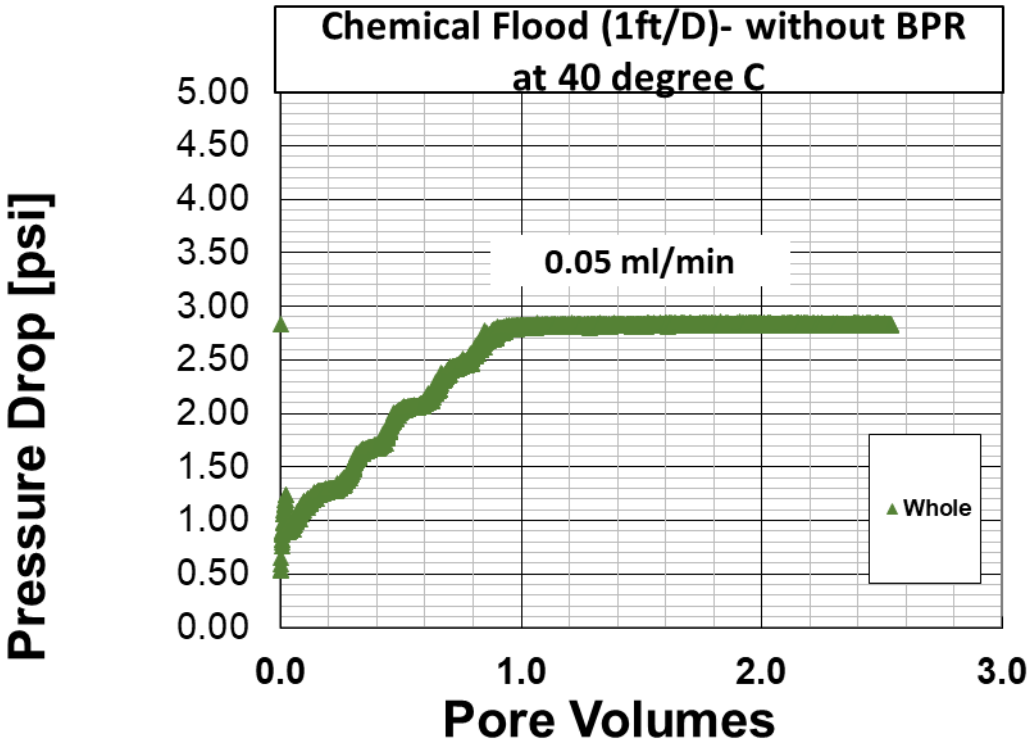

Figure 4.3. 12 Pressure Drop for Experiment S-6

The effluent viscosity started to increase at 0.6PV and took 2.5PV to reach its maximum value which is the almost exact same viscosity of injected the polymer drive viscosity. Thus, polymer degradation was not observed.

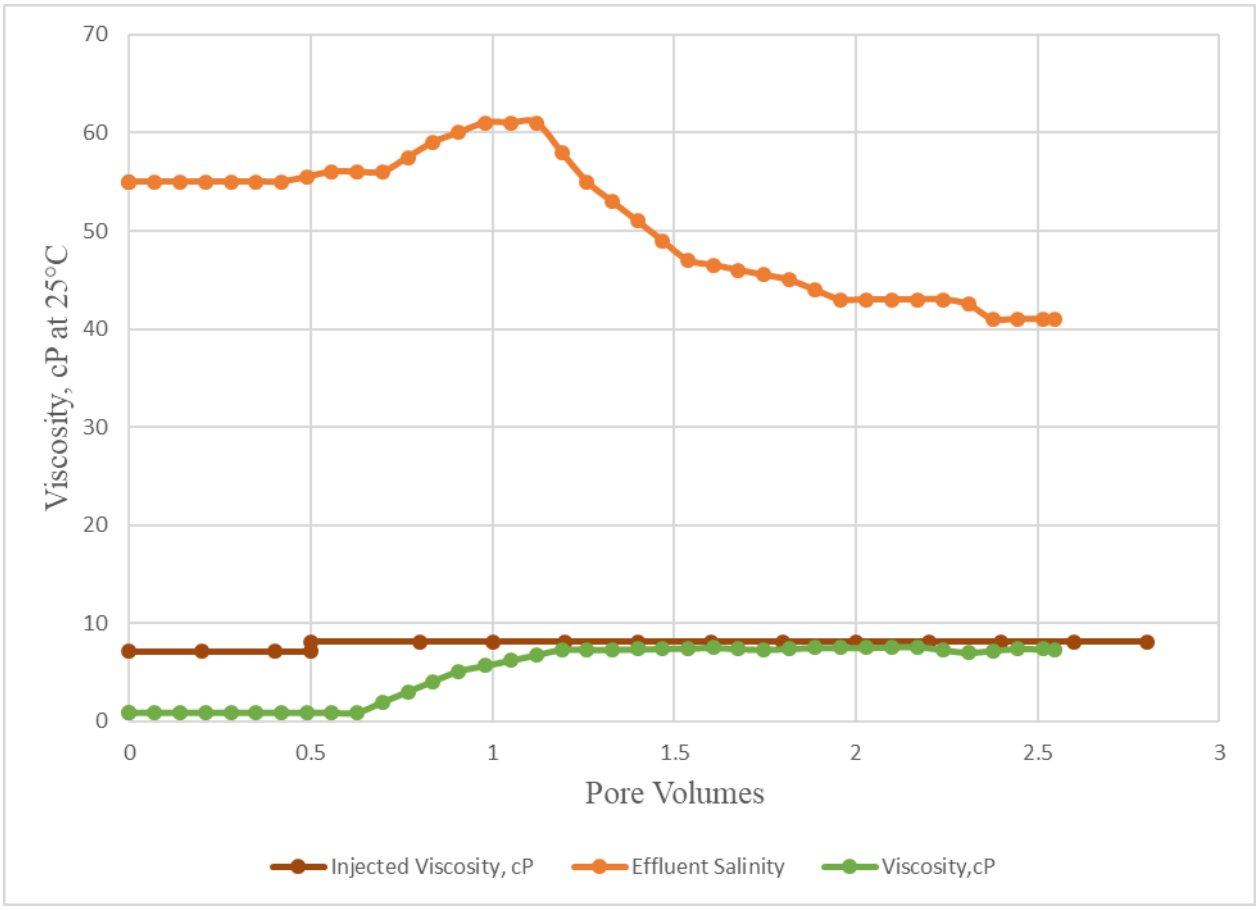

Figure 4.3. 13 Chemical Flood Effluent Salinity, Effluent Viscosity and Injected Viscosity for Experiment S-6

Discussion of Results S-6

During the tracer test, the tracer brine did not breakthrough earlier than 0.5PV, so it was concluded that the Berea sandstone was a homogeneous sandstone. Also, the pressure drop profile showed an increase in pressure drop as surfactant slug and the polymer drive injected and stayed stable during the polymer drive and the effluent viscosity reached the injected viscosity indicating stable polymer drive. The stability of the polymer is attributed to successful vacuuming and saturation and argon bubbling for 3 hours.

The S-6 surfactant retention was determined to be 0.20mg/g-rock. In order to decrease the surfactant retention further SN-1 was conducted with 1wt% NaPA to observe the effect of NaPA on the surfactant retention in Berea sandstone.

4.3.2. Single Phase Dynamic Experiments with NaPA

4.3.2.1. Single Phase Flood Experiment (SN-1)

After the repeatability test (S-6), reducing the retention for formulation F1 without alkali was targeted. As a sacrificial agent, sodium polyacrylate (NaPA) with the concentration of 10,000 ppm was tested. See Table 4.3.19 for the core properties.

Table 4.3. 19 Core Properties for Experiment SN-1

Rock Type	Berea Sandstone	
Temperature	40	°C
Diameter	3.80	cm
Length	30.40	cm
Weight	728.49	gr
Area X	11.33	cm^2
Pore Volume	70.06	ml
Bulk Volume	344.40	cm^3
Porosity	0.20	
Brine Viscosity @40°C	0.70	cP
Permeability	233.69	mD

Brine Flood and Pore Volume Calculations

For this experiment, the core was saturated with 0.5wt%KCl and then 4wt% NaCl was injected to the core at 2ml/min for the tracer test as to collect 6 ml fractions of effluents in each tube. The tracer brine (4wt% NaCl) broke-through at 0.7PV and took 1.7PV of injection to displace the in-situ brine completely (Figure 4.3.16). The tracer test was followed by the brine permeability determination. For the brine permeability, brine was injected at different flow rates (1ml/min, 2ml/min and 3ml/min) and the pressure drops at steady state, for each flow rate, were used in Darcy's Equation and the brine permeability determined as 234mD at 40℃

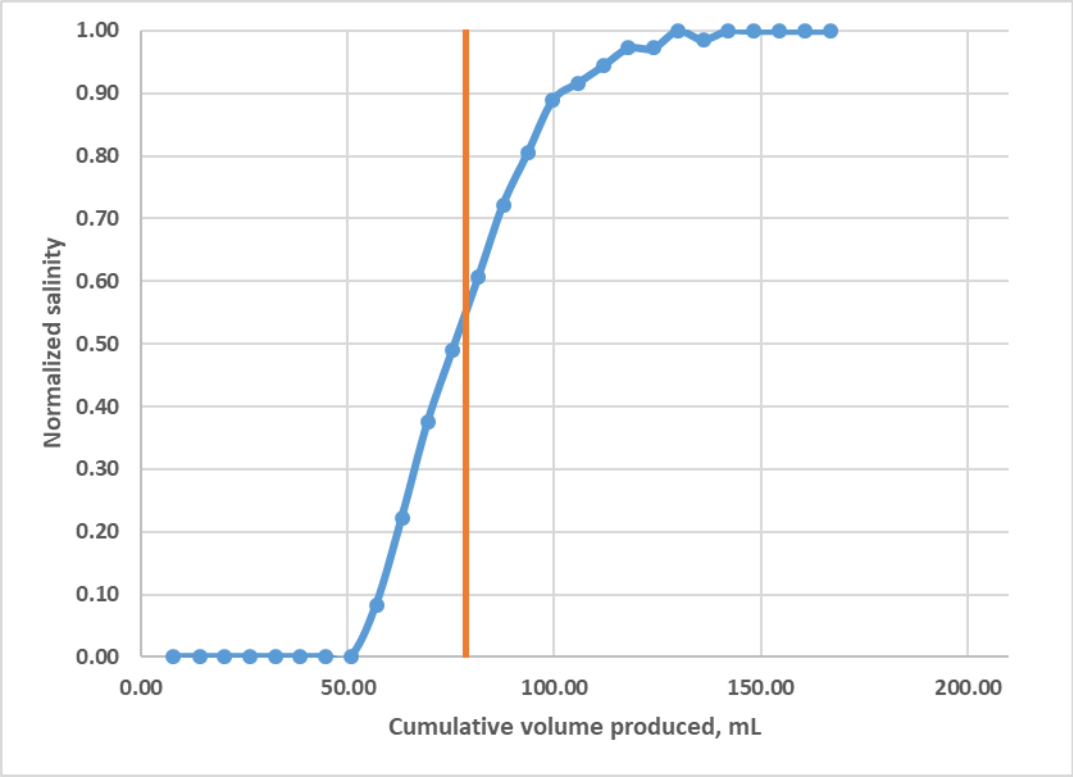

Figure 4.3. 14 Tracer Test for Experiment SN-1

Chemical Composition

Formulation F1 was used in this study to determine the effect of NaPA on the surfactant retention. As in previous experiments, a negative salinity gradient was applied. The compositions of the surfactant slug and the polymer drive are listed in Table 4.3.20.

Table 4.3. 20 Composition of Chemical Flood Solutions for Experiment SN-1

Injection Fluid	**Components**
Surfactant Slug	4 wt% NaCl
	0.5 wt% CH_3O 21PO 10EO SO_4
	0.5 wt% C1923 IOS
	1 wt% TEGBE
	0.3 wt% FP3330S
	1 wt% NaPA
Polymer Drive	
	2.5 wt% NaCl
	0.3 wt% FP3330S

Chemical Flood

The chemical flood solutions were prepared as described in Chapter III. In this experiment, the surfactant slug and the polymer drive (without co-solvent in PD) were injected at 1ft/D. The polymer, FP3330s was used in the surfactant slug as well to maintain the required viscosity.

Table 4.3. 21 Surfactant Slug and Polymer Drive Properties for Experiment SN-1

	Surfactant Slug	**Polymer Drive**
PV Injected	0.6	2
Polymer	FP 3330S	FP 3330S
Polymer Concentration (ppm)	3000	3000
Frontal Velocity (ft/D)	1	1
Salinity (ppm TDS)	75	30
pH	6.8	6.75
Viscosity at 10 s^{-1} & 25°C	27	32

Chemical Flood Results

The chemical flood was continued for 2.5PV of injection and fraction of 6ml of effluents were collected in plastic centrifuge tubes. Effluents were analyzed via HPLC for the surfactant retention and the surfactant breakthrough was observed at 0.7PV and the concentration reached the peak at 1.3PV and 8000 ppm. Even though, unlike experiment S-1 and S-5, in this experiment NaPA was used, the surfactant retention stayed almost the same (~0.23mg/g-rock). See Figure 4.3.17 for the effluent surfactant concentrations.

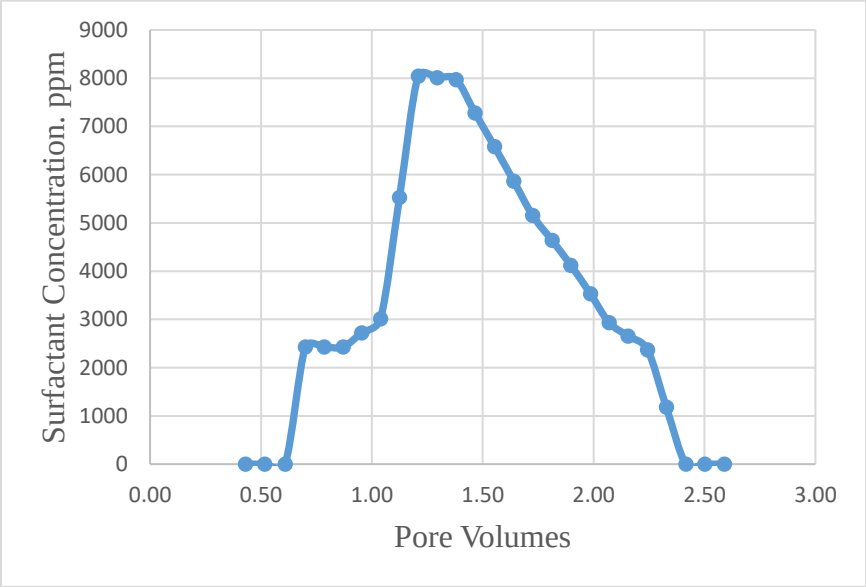

Figure 4.3. 15 Effluent Surfactant Concentration for experiment SN-1

The salinity propagation of the chemical slugs was also tested by a refractometer. The effluent salinity reached the peak at 60,000 ppm TDS at 1.3PV and reached the polymer drive salinity before 2.5PV of injection. The Figure 4.3.18 indicates that the salinity propagated well through the core.

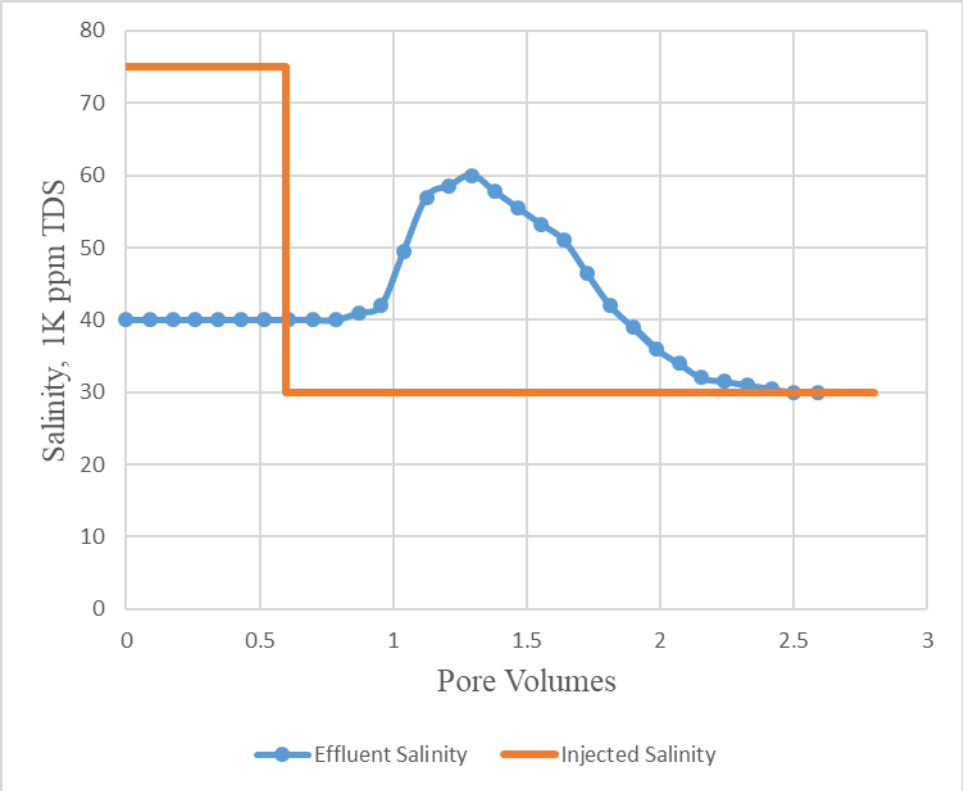

Figure 4.3. 16 Chemical Flood Effluent Salinity for Experiment SN-1

The pressure drop data during the chemical flood are shown in Figure 4.3.18. The pressure drop of the whole core increased until 0.7PV and then stabilized until 2.3PV of chemical injection. Towards the end of the flood the lower pressure drop was observed (See Figure 4.3.25)

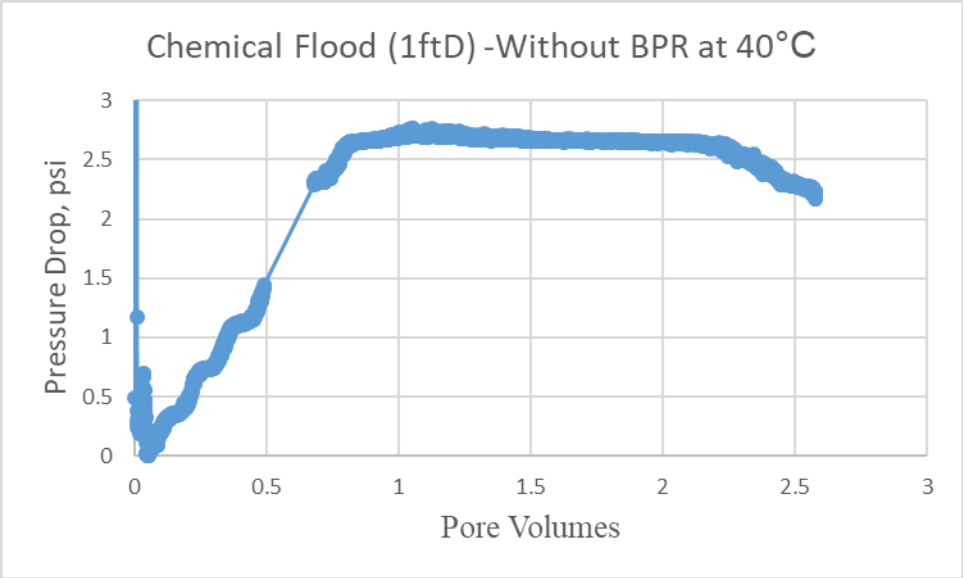

Figure 4.3. 17 Pressure Drop for Experiment SN-1

Effluent viscosity started to increase at 1.6PV and took 2.8PV to reach its maximum value which is 10wt% lower than influent viscosity (Figure 4.3.26), indicating some degradation in the core.

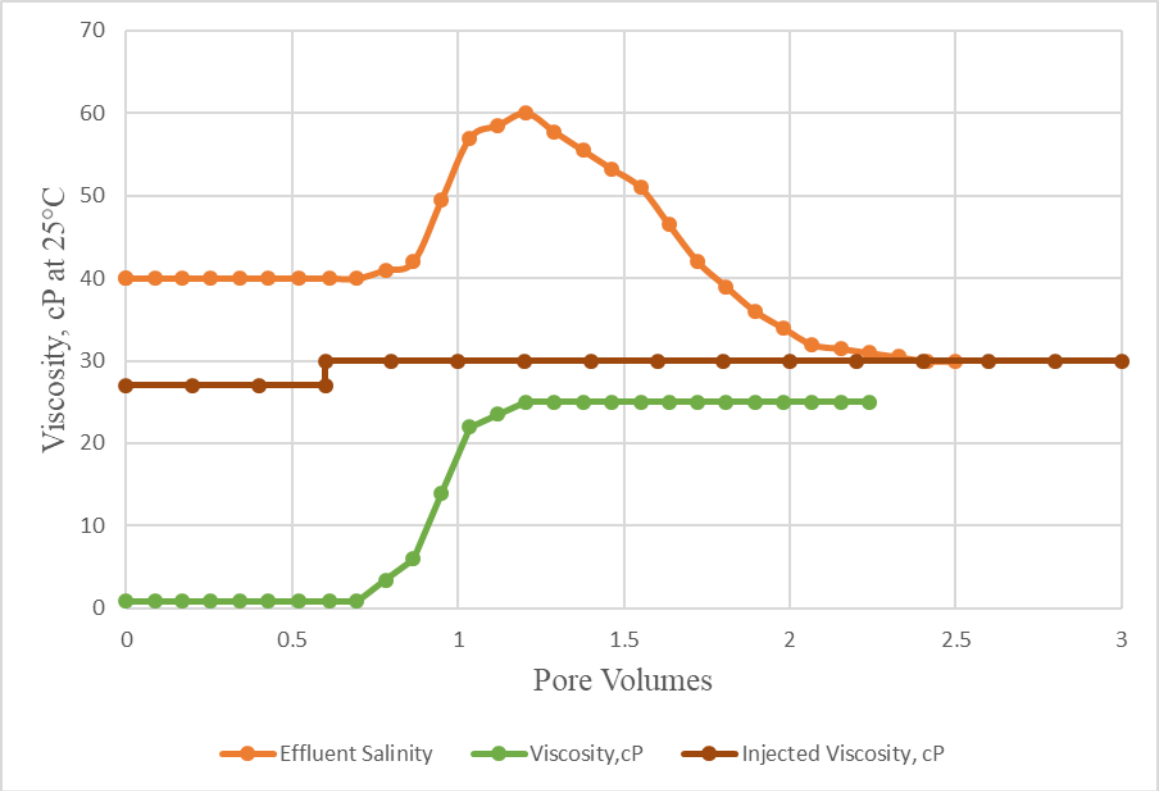

Figure 4.3. 18 Chemical Flood Effluent Salinity, Effluent Viscosity and Injected Viscosity for Experiment SN-1

Discussion of Results SN-1

The SN-1 surfactant retention was determined to be the same as experiment S-1 and S-5. In this experiment, the usage of NaPA did not change the retention of surfactant. Thus, it was concluded that, either this outcrop had much more clay content than the previous experiments and /or 0.5wt% KCl brine saturation was not enough to remove some of divalent cations from the core and this caused higher retention.

The decrease in pressure drop towards the end of the chemical flood and the effluent viscosity profile indicated polymer degradation. Since the temperature (40°C) is not a concern for polymer degradation, the decrease in the pressure drop at the end of experiment was

attributed to the presence of iron and its reaction with oxygen in the core. In order to prevent this effect in the future experiments, the argon bubbling time was increased.

4.3.2.2 Single Phase Flood Experiment (SN-2)

The formulation F2 was chosen to see the effect of NaPA in reduction on the surfactant retention in a formulation with the conventional surfactants. Other variables were kept similar to experiment S-2 to obtain a reliable comparison. See Table 4.3.22 for the core properties.

Table 4.3. 22 Core Properties for Experiment SN-2

Rock Type	Berea Sandstone	
Temperature	40	°C
Diameter	3.76	cm
Length	30.70	cm
Weight	717.09	gr
Area X	11.10	cm^2
Pore Volume	70.67	ml
Bulk Volume	340.74	cm^3
Porosity	0.21	
Brine Viscosity @40°C	0.61	cP
Permeability	193.20	mD

Brine Flood and Pore Volume Calculations

2wt%KCl was injected for the core saturation and 5wt%NaCl was injected at 2ml/min flow rate for the tracer test. 6ml of the tracer test effluents were collected in plastic graded centrifuge tubes and analyzed for the salinity propagation. Brine salinity broke-through after 0.7PV and took 1.8PV for the effluent salinity to reach the injected salinity (Figure 4.3.21). The

tracer test was followed by 3.5wt%NaCl, which was the optimum salinity, and brine permeability was determined to be 193mD. The brine permeability was determined by using the steady state pressure drop values at 2ml/min and 4ml/min at 40°C. The brine flood pressure drop can be seen in Figure 4.3.22.

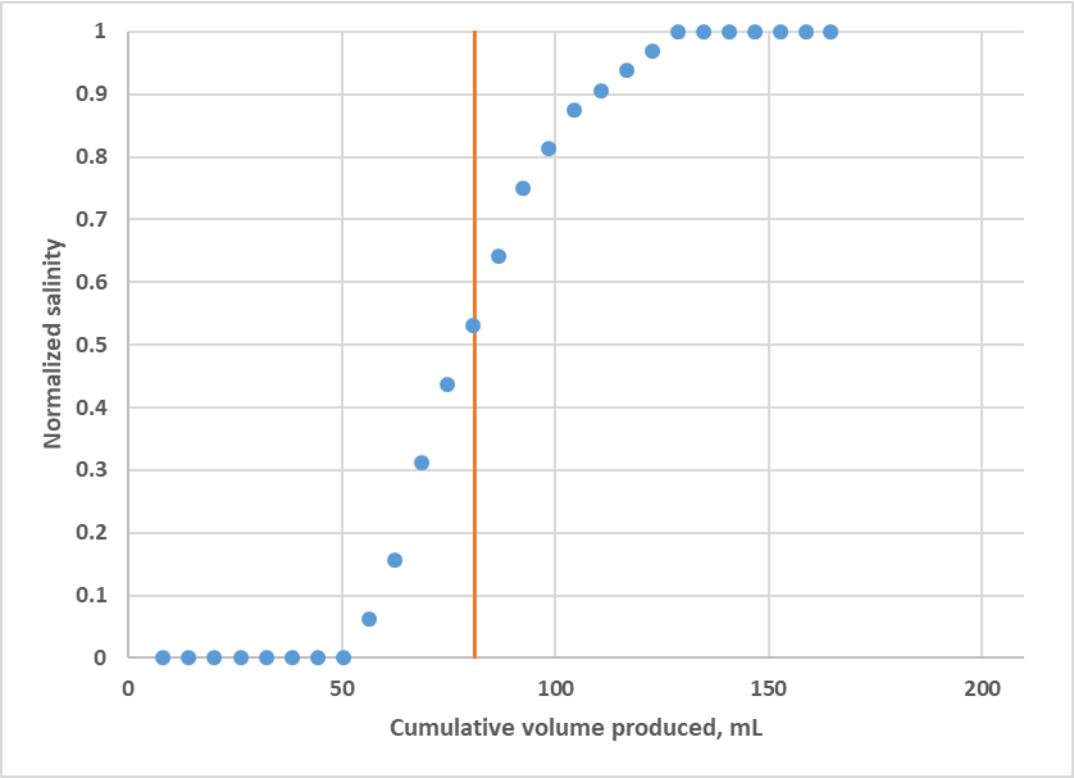

Figure 4.3. 19 Tracer Test for Experiment SN-2

Chemical Composition

Formulation F2 was used in this experiment to see the surfactant retention difference between the formulations with and without NaPA. See Table 4.3.23 for the chemical composition of the surfactant slug.

Table 4.3. 23 Composition of Chemical Flood Solutions for Experiment SN-2

Injection Fluid	**Components**
Surfactant Slug	3.5 wt% NaCl
	0.5 wt% TDA 13POSO$_4$
	0.5 wt% C1923 IOS
	1 wt% TEGBE
	0.1 wt% FP3330S
	0.5 wt% NaPA
Polymer Drive	2.0 wt% NaCl
	0.1 wt% FP3330S

Chemical Flood

The chemical flood for this experiment was designed in the same way that of experiment S-2. The chemical flood was performed at 1ft/D (0.05ml/min) as previous experiments. The polymer drive did not include any co-solvents. See below the Table 4.3.24 for the chemical flood properties.

Table 4.3. 24 Surfactant Slug and Polymer Drive Properties for Experiment SN-2

	Surfactant Slug	**Polymer Drive**
PV Injected	0.6	2
Polymer	FP 3330S	FP 3330S
Polymer Concentration (ppm)	1000	1000
Frontal Velocity (ft/D)	1	1
Salinity (ppm TDS)	62	22
pH	7.54	6.06
Viscosity at 10 s^{-1} & 25°C	5.5	13

Chemical Flood Results

After injecting 2.5PV of chemical solutions, collecting 6ml in plastic graded centrifuge tubes, the flood was ended and effluents were analyzed. By HPLC, the surfactant concentration in effluents was determined first and then the retention was calculated to be 0.103mg/g-rock with 0.57mg/g-rock being injected. Surfactant broke-through around 0.9PV of injection and reached the peak at 1.3PV with the concentration of 7500 ppm (see Figure 4.3.22).

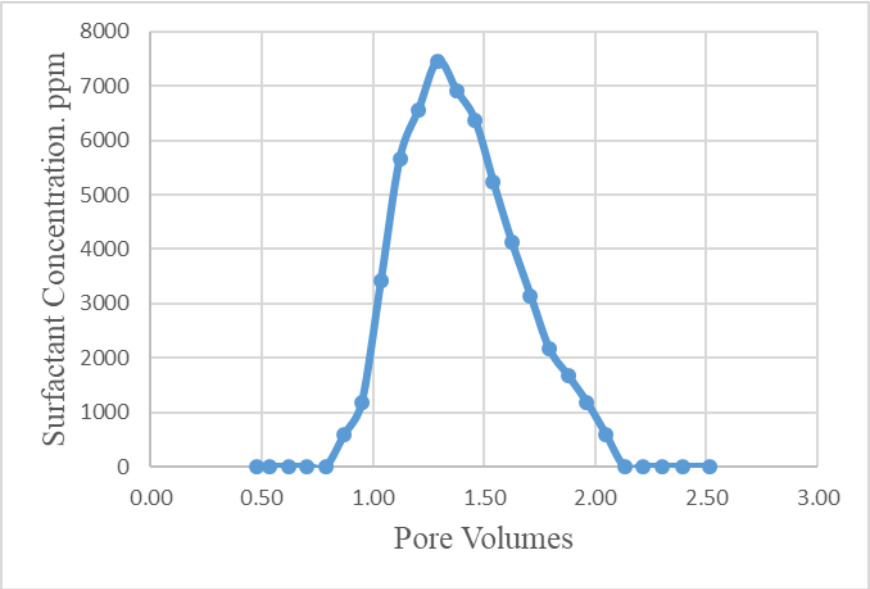

Figure 4.3. 20 Effluent Surfactant Concentration for experiment SN-2

The pressure drop during the chemical flood is presented in Figure 4.3.24. The pressure drop for the chemical flood increased up to 1PV and then slightly decreased and stabilized at about 1.5PV.

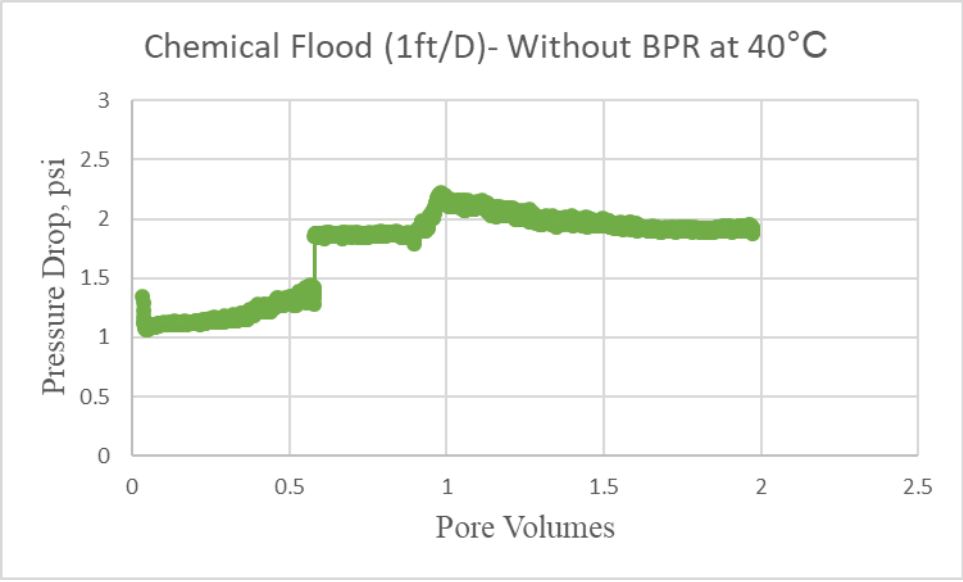

Figure 4.3. 21 Pressure Drop for Experiment SN-2

By using a refractometer, the salinity of the effluent samples were also analyzed and a good propagation of the salinity were observed. The effluent salinity reached the peak at 1.3PV at the concentration of 56,000ppm. Effluents reached the polymer drive salinity before 2.5PV of injection, indicating the salinity propagation was efficient.

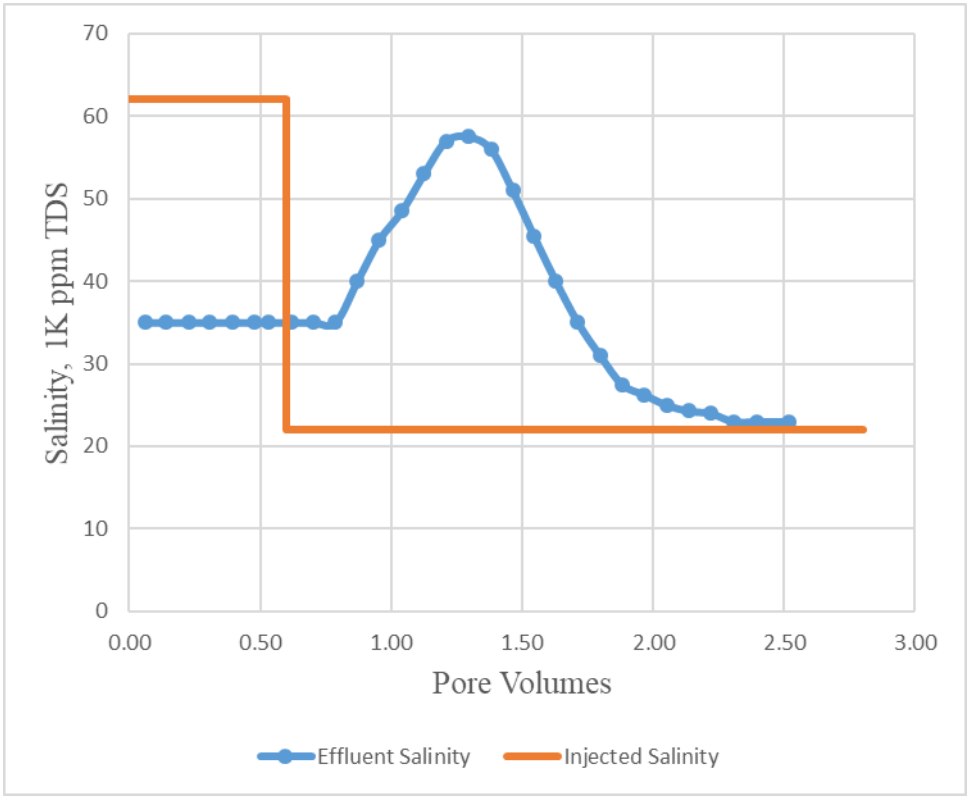

Figure 4.3. 22 Chemical Flood Effluent Salinity for Experiment SN-2

The effluent viscosity started to increase at 0.8PV and reached the maximum value at 1.63PV and stayed stable towards the end of flood (Figure 4.3.26). Within the error range, the effluent viscosity reached the injected polymer viscosity at 1.5PV. Therefore, it was concluded that the viscosity propagated well.

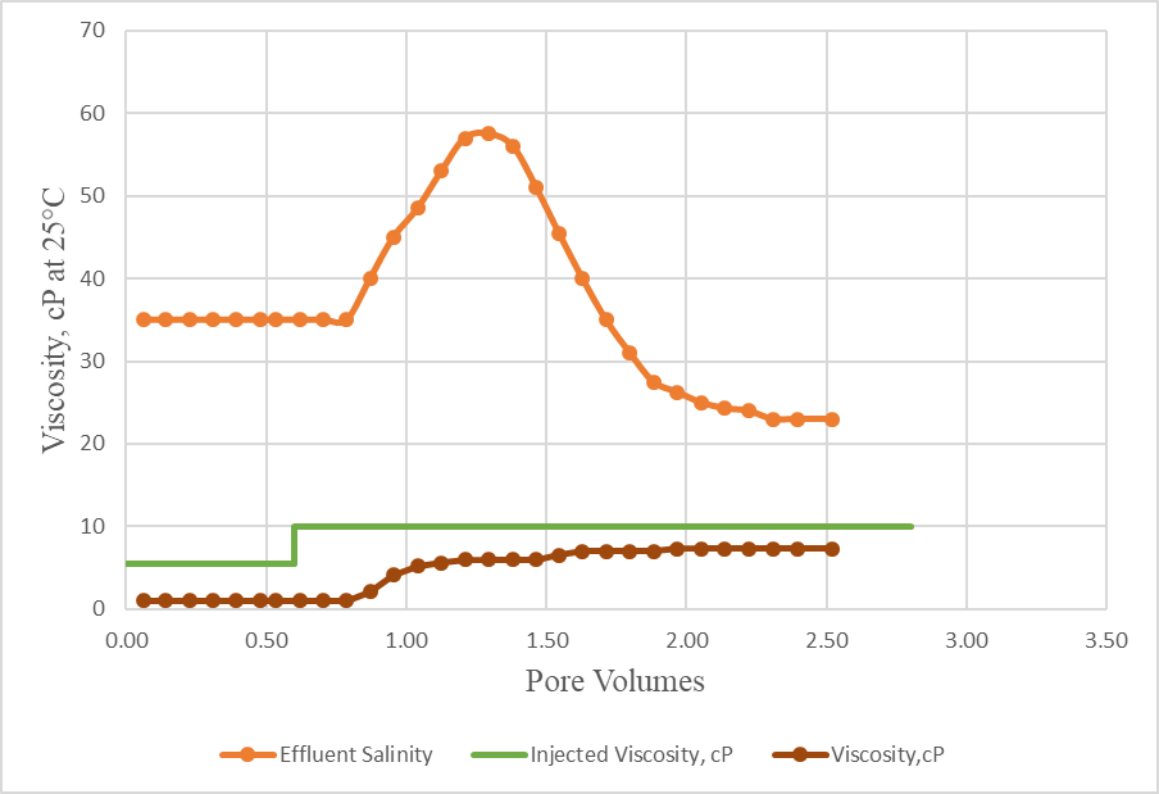

Figure 4.3. 23 Effluent Viscosity for Experiment SN-2

4.3.2.3. Single Phase Flood Experiment (SN-3)

The purpose of this experiment was to determine the effect of NaPA on the surfactant retention in formulation F5. After the analysis of the core as described in Chapter III, the core was saturated and the tracer test was conducted. For the chemical flood, polymer concentration, surfactant concentration and amount of the injection were kept the same as experiment S-5 to obtain a good comparison between the two SPF experiments. A new outcrop Berea sandstone from the same lot of previous experiments was used. See Table 4.3.25 for the core properties.

Table 4.3. 25 Core Properties for Experiment SN-3

Rock Type	Berea Sandstone	
Temperature	40	°C
Diameter	3.80	cm
Length	30.05	cm
Weight	695.6	gr
Area X	11.25	cm^2
Pore Volume	68.6	ml
Bulk Volume	354.36	cm^3
Porosity	0.19	
Brine Viscosity @40°C	0.72	cP
Permeability	107	mD

Brine Flood and Pore Volume Calculations

The saturation and the tracer test conducted in the same way that experiment S-5 was performed (saturated with 2wt%KCl followed by 5.3wt%NaCl injection at 2ml/min for the tracer test). The tracer brine broke-through around 0.6PV and the pore volume determined to be 67ml. The brine permeability test was conducted by using Darcy's equation for pressure drops at different flow rates. The brine permeability determined to be 107mD at 40℃. See Figure 4.3.25 for the tracer test.

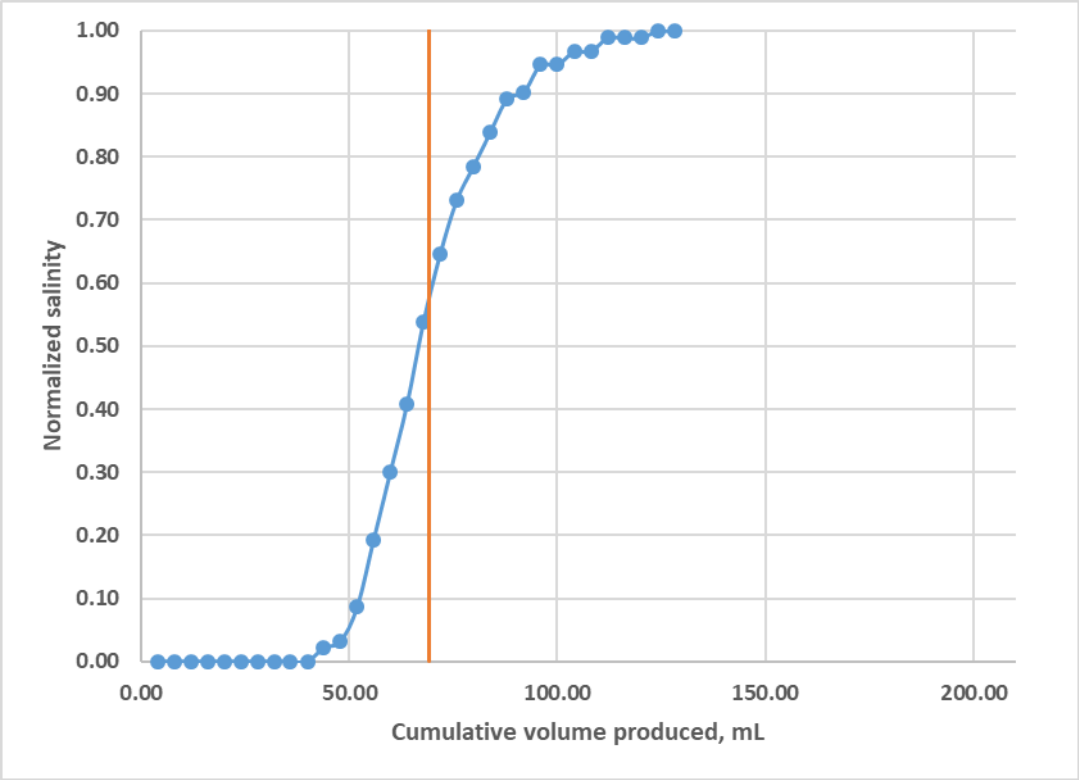

Figure 4.3. 24 Tracer Test for Experiment SN-3

Chemical Composition

Formulation F5 and 1wt% NaPA was used in this experiments. See Table 4.3.24 for chemical composition in details.

Table 4.3. 26 Composition of Chemical Flood Solutions for Experiment SN-3

Injection Fluid	**Components**
Surfactant Slug	4.5 wt% NaCl
	0.6 wt% TDA 13PO SO_4
	0.3 wt% C1518 IOS
	0.25 wt% TEGBE
	0.15 wt% FP3330S
	1wt%NaPA
Polymer Drive	0.15 wt% FP3330S
	3wt% NaCl

Chemical Flood

By following the standard chemical solution preparation procedure as described in Chapter III, the surfactant slug and the polymer drive solutions were prepared and filtered through the Nitrocellulose filters and after pH was arranged be neutral, the solutions injected to the core at 40℃. See Table 4.3.27 for the injection parameters.

Table 4.3. 27 Surfactant Slug and Polymer Drive Properties for Experiment SN-3

	Surfactant Slug	**Polymer Drive**
PV Injected	0.5	2
Polymer	FP 3330S	FP 3330S
Polymer Concentration (ppm)	1500	1500
Frontal Velocity (ft/D)	1	1
Salinity (ppm TDS)	68	32
pH	8.08	7.39
Viscosity at 10 s^{-1} & 40℃	7	8

Chemical Flood Results

Chemical flood was continued for 2.5PV and the effluents were collected in plastic centrifuge tubes with the fraction of 5ml effluent. The effluents were analyzed by HPLC for the surfactant retention, and the surfactant breakthrough was observed at 0.5PV, and the concentration reached the peak at 1.5PV and 6500 ppm with 0.1mg/g-rock surfactant retention. See Figure 4.3.26 for the effluent surfactant concentration.

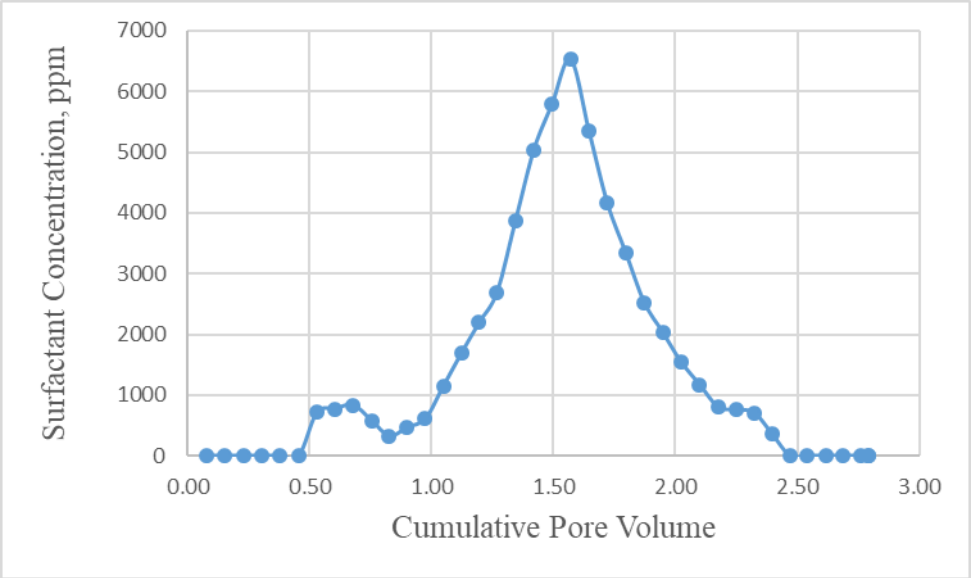

Figure 4.3. 25 Effluent Surfactant Concentration for Experiment SN-3

The salinity propagation of the chemical slugs was also tested via refractometer. The effluent salinity reached the peak at 65,000 ppm TDS at 1.3PV of injection. The Figure 4.3.29 indicates that the salinity of the chemicals propagated well through the core.

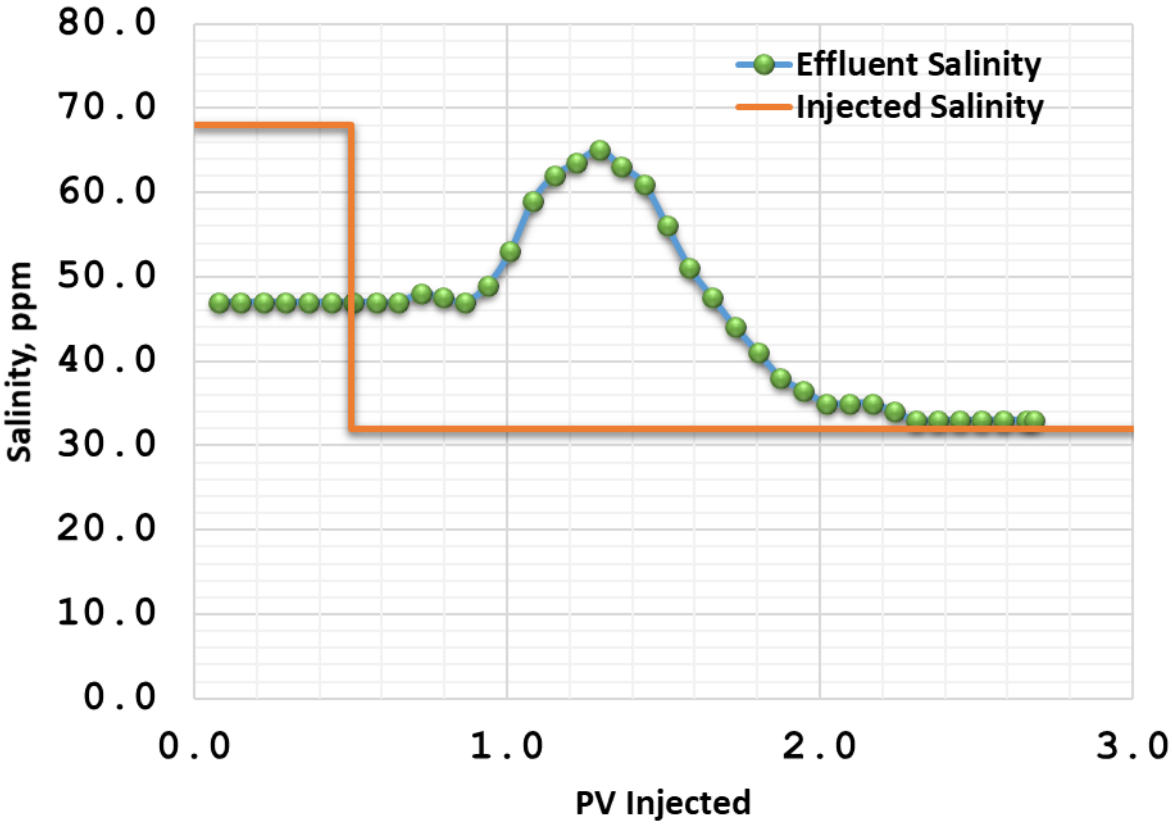

Figure 4.3. 26 Chemical Flood Effluent Salinity for Experiment SN-3

The effluent pH was significantly higher than the injected pH (Figure 4.3. 28).

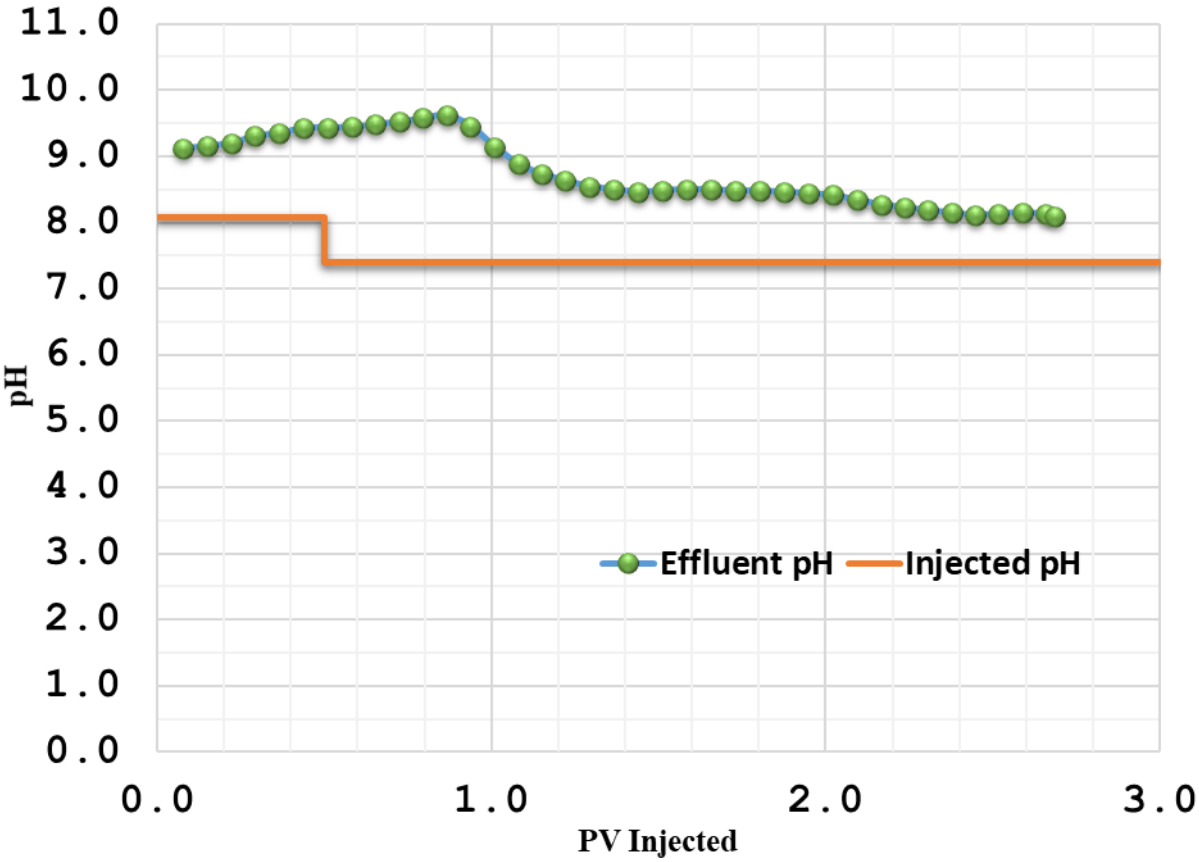

Figure 4.3. 27 Chemical Flood Effluent pH for Experiment SN-3

The pressure drop during the chemical flood was demonstrated in Figure 4.3.31. The pressure drop of whole core increased up to ~1PV and then stabilized for 1.5PV of the chemical flood injection as the polymer drive started to be produced.

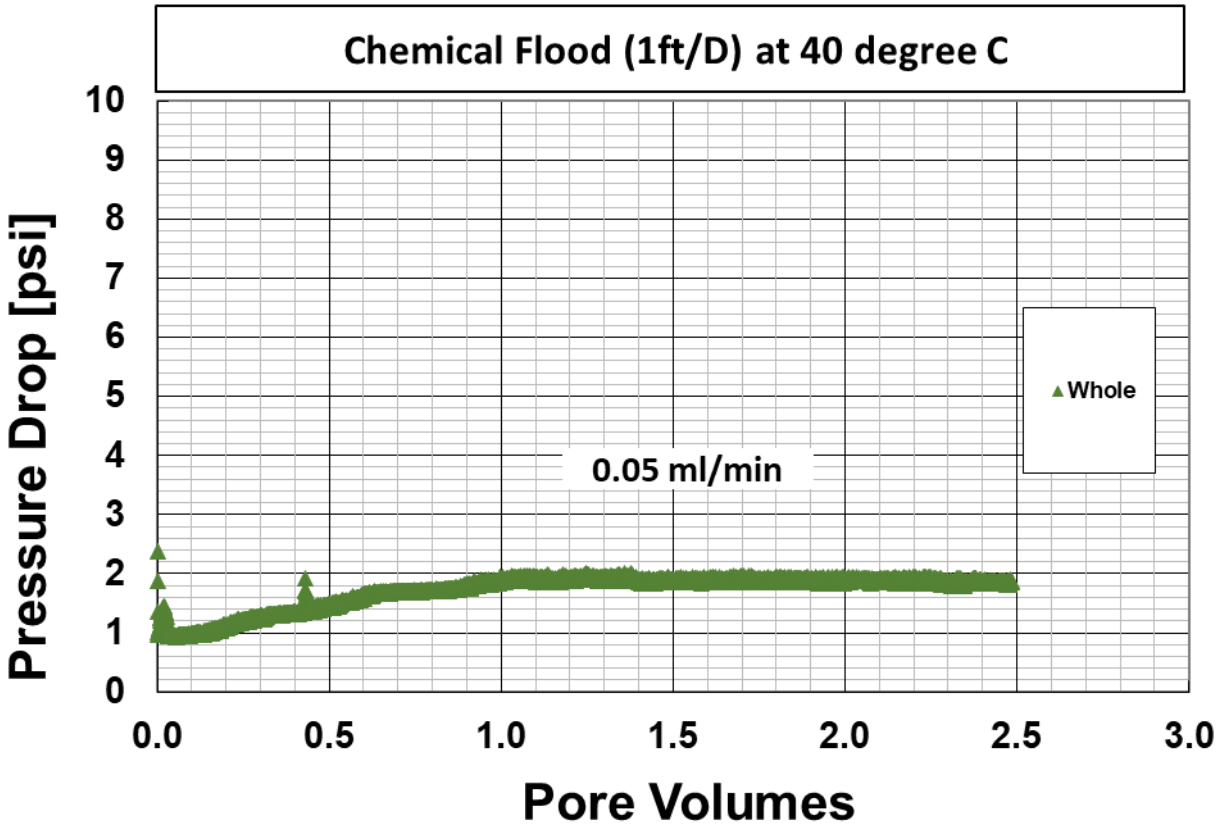

Figure 4.3. 28 Pressure Drop for Experiment SN-3

The effluent viscosity started to increase around 0.4PVof injection; however, this early breakthrough was attributed to the measurement errors, since early breakthrough was not observed in other tests such as the tracer test and the salinity test. The increase in viscosity was observed around 0.9PV and reached its maximum value at 1.4PV and stayed stable at the polymer drive viscosity before 1.5PV of injection (See Figure 4.3.32).

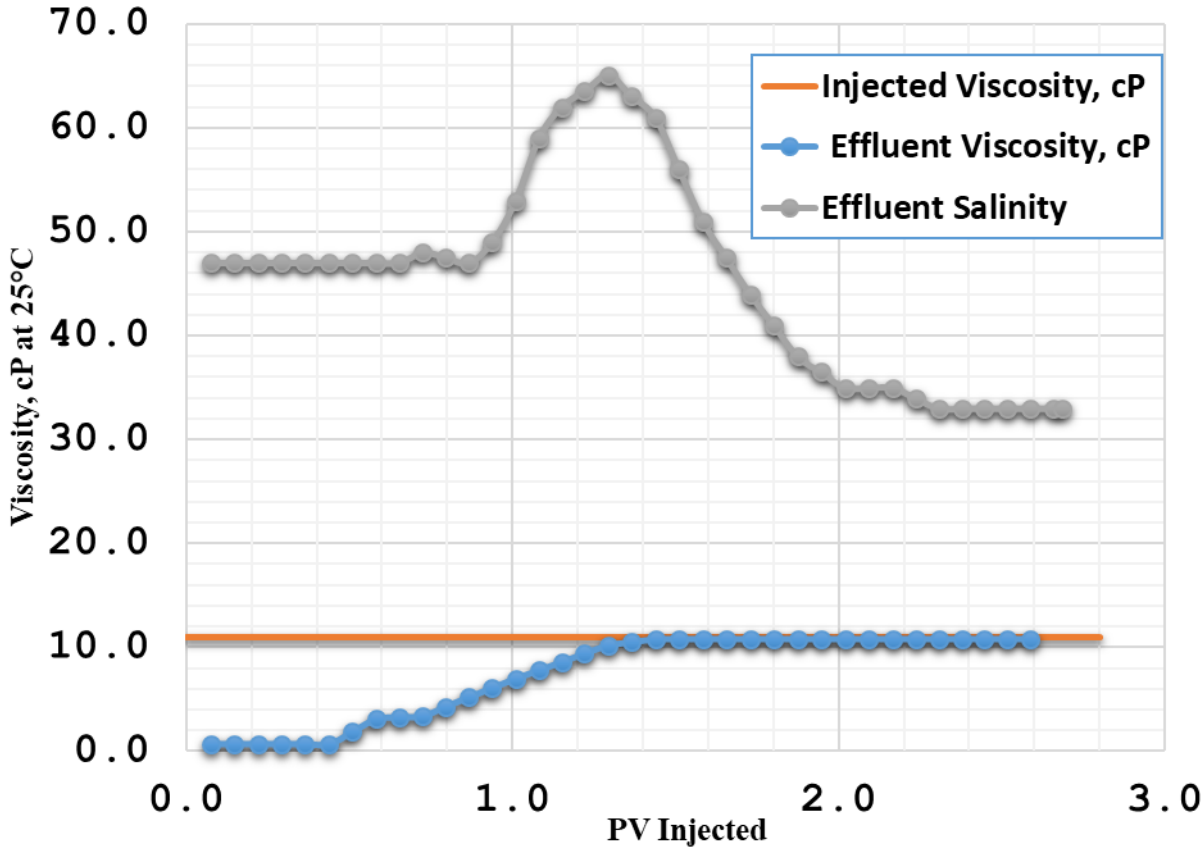

Figure 4.3. 29 Chemical Flood Effluent viscosity for Experiment SN-3

Discussion of Results

The tracer brine broke-through around 0.6PV, indicating that the core is a homogenous outcrop. Due to the homogeneity of the core, a good propagation of the pH and salinity was observed. Viscosity was also propagated well throughout the core.

The effluent samples were analyzed by HPLC for the determination of the surfactant retention. Based on the measured surfactant concentrations in the effluent samples, retention was calculated to be very low (0.1mg/g-rock). Most of the injected surfactants was produced by 2.5PV of chemical flood. The low surfactant retention might be due to the sodium polyacrylate or it might be due to the higher effluent pH, or a combination of the two effects.

Table 4.3. 28 Summary of Single Phase Dynamic Experiments

Formulation	Surfactant		Co-Surfactant		Co-Solvent		SPF Experiments Without NaPA		SPF Experiments With NaPA	
	Name	wt%	Name	wt%	Name	wt%	Name	Ads, mg/g-rock	Name	Ads, mg/g-rock
F1	CH3O 21PO 10 EO SO4	0.5	C19-23IOS	0.5	TEGBE	1	S-1 & S-5	0.23-0.22	SN-1	0.23
F2	TDA 13PO SO4	0.5	C19-23IOS	0.5	TEGBE	1	S-2	0.17	SN-2	0.1
F3	TDA 7PO SO4	0.5	C19-23IOS	0.5	TEGBE	1	S-3	0.18		
F4	2EH 7PO SO4	0.5	C19-23IOS	0.5	TEGBE	1	S-4	0.23		
F5	TDA 13PO SO4	0.6	C15-18 IOS	0.3	TEGBE	0.25	S-6	0.2	SN-3	0.1

4.3. SURFACTANT RETENTION IN OIL RECOVERY EXPERIMENTS

4.4.1. Oil Recovery Experiment C-1

The purpose of this experiment was to determine the surfactant retention in the presence of the oil and measure the oil production using formulation F1 in Berea outcrop sandstone. The core was prepared as described in Chapter III, after the dimensions and mass of the core were noted. The core initially saturated with 2wt% KCl at 40℃.

Table 4.3. 29 Core Properties for Experiment C-1

C-1		
Core Properties		
Core Name	ABC	
Rock Type	Berea Sandstone	
Diameter	3.80	Cm
Length	30.70	Cm
Mass	738.74	G
Bulk vol.	345.36	cm3
Porosity	0.2032	
Area	11.25	cm^2
PV	70	Ml
Length (Section 1)	8.13	cm
Length (section 2)	7.62	cm
Length (section 3)	7.62	cm
Length (section 4)	7.24	cm
Temperature	40	°C

Tracer Test and Brine Permeability

2wt%KCl was injected at different ratios (1ml/min, 2ml/min and 3ml/min) to determine the brine permeability at 40℃ when the flow reached steady state conditions. Afterwards, 5wt% NaCl tracer brine was injected to determine the pore volume of the core. The tracer brine broke-through at 0.7PV of injection, and it took 1.6PV of injection to reach its maximum value. This shows that the core is a homogeneous core. For this core the pore volume was determined to be 70ml and the average brine permeability at 40℃ was calculated as 168mD. For the sectional permeability see Table 4.3.29.

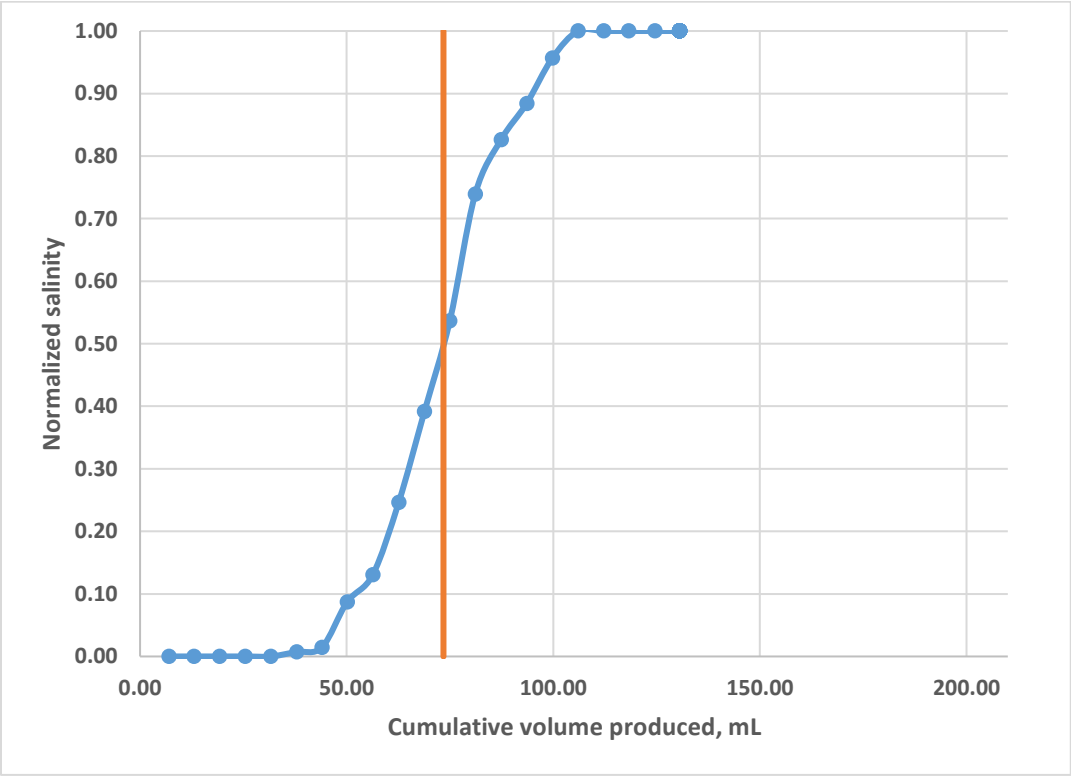

Figure 4.3. 30 Normalized Salinity Tracer for Experiment C-1

Oil Flood

The core was oil flooded at 40℃ with oil O-1. The oil is filled into a stainless steel column and displaced by argon gas at 140psi. The BPR was set to ~50psi, allowing for a 90psi pressure differential. Injection of the oil continued until the oil cut was zero. When the water

saturation reached to residual value, the oil injection was continued to determine the oil pressure drop at the steady state conditions and determine the end point oil relative permeability k_{ro}^{o} (1.0). From the displaced water volume by oil, S_{oi} was estimated to be 0.62.

Water Flood

After the dilution tests at 40°C, the water flood salinity was determine to be 6.5wt%NaCl. At this salinity, the diluted phase behavior showed ultra-low IFT near the optimum salinity. Injection was continued at 2ft/D (0.1ml/min) until the oil cut was less than 1% and the pressure drop reached steady state. The pressure drops at steady state used to estimate the end point water relative permeability k_{rw}^{o} as 0.13. S_{orw} was calculated to be 0.31 (See Table 4.3.30).

Table 4.3. 30 Summary of Brine Flood, Oil Flood and Water Flood permeability and Relative Permeability for Experiment C-1

	Average Brine Permeability @40°C	**Average Oil Permeability @40°C**	**k_{ro}^{o}**	**Average Water Permeability @40°C**	**k_{rw}^{o}**
Whole	168	187	1	22	0.13
Section1	163	197	1	26	0.16
Section2	214	175	1	30	0.14
Section3	202	186	1	21	0.11
Section4	211	199	1	20	0.09

Table 4.3. 31 Summary of Oil Flood and Water flood for Experiment C-1

Oil Flood		**Water Flood**	
k_{ro}^{o}	1	**k_{rw}^{o}**	0.13
S_{oi}	0.62	**S_{orw}**	0.31

Mobility Control

At the end of the water flood, the required minimum viscosity for a stable displacement was designed by using the total mobility curve. The inverse of minimum mobility was estimated and set as the required minimum viscosity for chemical slugs and with safety factor 1.2, the chemical flood viscosity was designed to be more than 18cp. See Table 4.3.31 for the parameters used in this calculation.

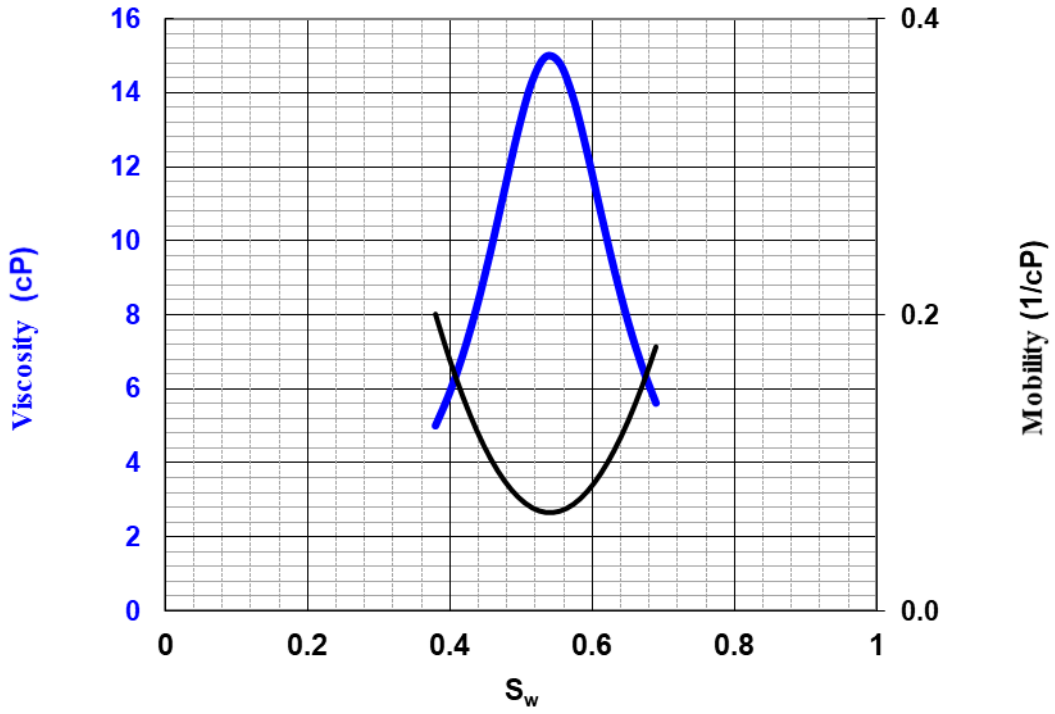

Figure 4.3. 31 Total Relative Mobility Curve for Experiment C-1

Table 4.3. 32 Total Relative Mobility Curve Parameters for Experiment C-1

k_{rw}^{o}	0.130	
k_{ro}^{o}	1.00	
n_w	2.5	
n_o	2.5	
S_{wr}	0.38	
S_{or}	0.31	
μ_w	0.73	cp
μ_o	5	cp

The equivalent shear rate in the core was estimated to be $8.7s^{-1}$. Viscosity of the SP slug and the polymer drive were tested with different concentrations of polymer FP3330S and chosen to be 3000ppm, which was the concentration needed for the required viscosity at the target shear rate.

Chemical Flood

The SP slug and the polymer drive were prepared by following the procedure described in Chapter III. Slugs were prepared and placed inside the oven to heat them up to the 40℃ and afterwards, injection started at 1ft/D (0.05ml/min) at 40℃. The effluents were collected with 5ml in each tube. At the end of the flood, the effluents were analyzed for retention, pH, viscosity and salinity.

Table 4.3. 33 Surfactant Slug and Polymer Drive Properties for Experiment C-1

	Surfactant Slug	**Polymer Drive**
PV Injected	0.5	2
Polymer	FP 3330S	FP 3330S
Polymer Concentration (ppm)	3000	3000
Frontal Velocity (ft/D)	1	1
Salinity (ppm TDS)	70	37
pH	7	6
Viscosity at 10 s^{-1} & 40°C	23	23

Chemical Flood Results

After 2.5PV of chemical flood, the effluent samples were analyzed visually for oil recovery after centrifuging them for 10mins at 2000rpm at room temperature. Amount of the oil collected was determined as ~48% with S_{orc} 0.14. Due to the low oil recovery, the chemical flood continued for additional 0.7PV at higher flow rate and additional 2% of oil recovery was obtained.

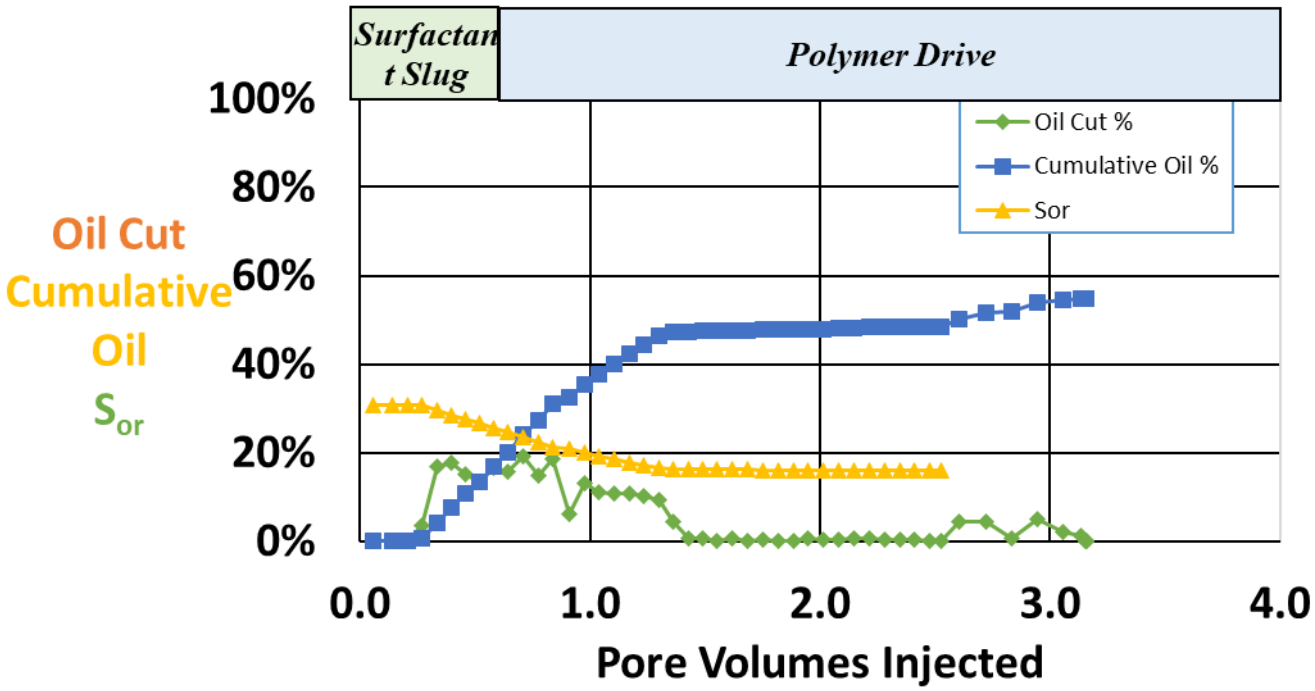

Figure 4.3. 32 Oil Recovery for Experiment C-1

The effluent surfactant concentration was measured by HPLC and the surfactant retention was determined to be 0.31mg/g-rock. The surfactant break thorough was observed at 0.75PV and continued producing for 1.5PV. The surfactant retention for experiment C-1 was higher than that of single phase dynamic experiments S-1 and S-5, which had the same formulation with lower polymer concentration.

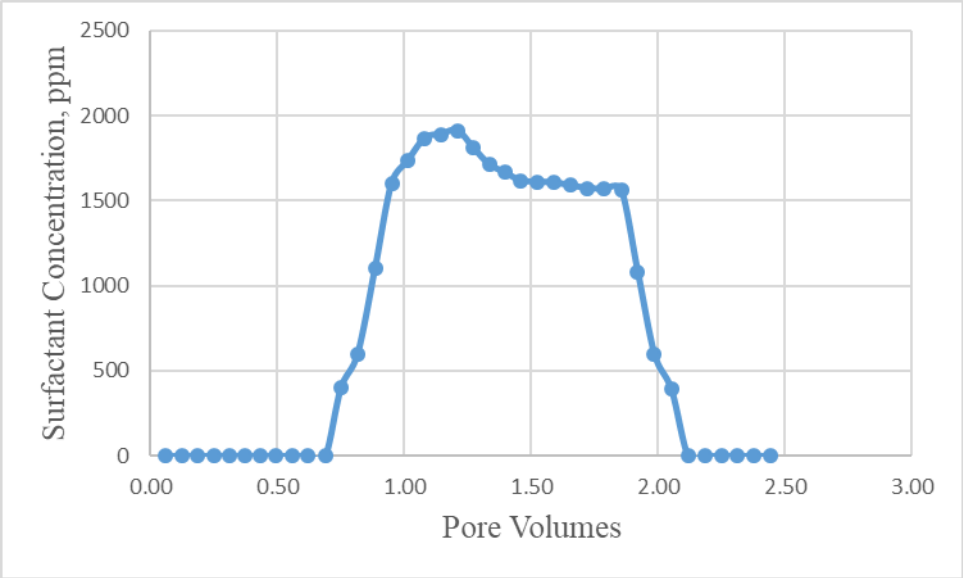

Figure 4.3. 33 Effluent Surfactant Concentration for experiment C-1

The salinity propagation was determined using a refractometer. Salinity front broke-through at 0.5PV of injection and continued decreasing. Salinity propagated well through the core as effluents salinity reached injected salinity at 2PV.

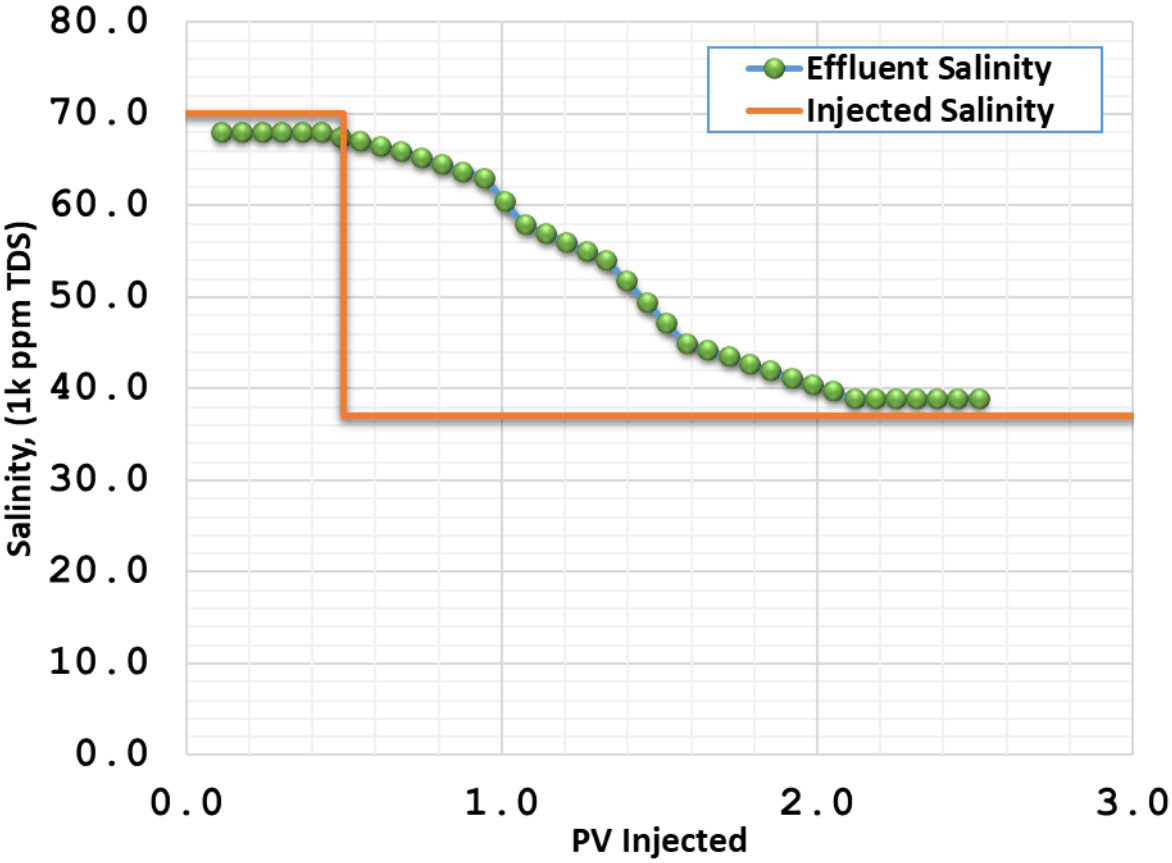

Figure 4.3. 34 Chemical Flood Effluent Salinity for Experiment C-1

The effluent pH was measured and compared to the pH of the injected solutions. The pH of injected chemical solutions were arranged to neutral values, prior to the flood. The pH of effluents were higher than the injected pH.

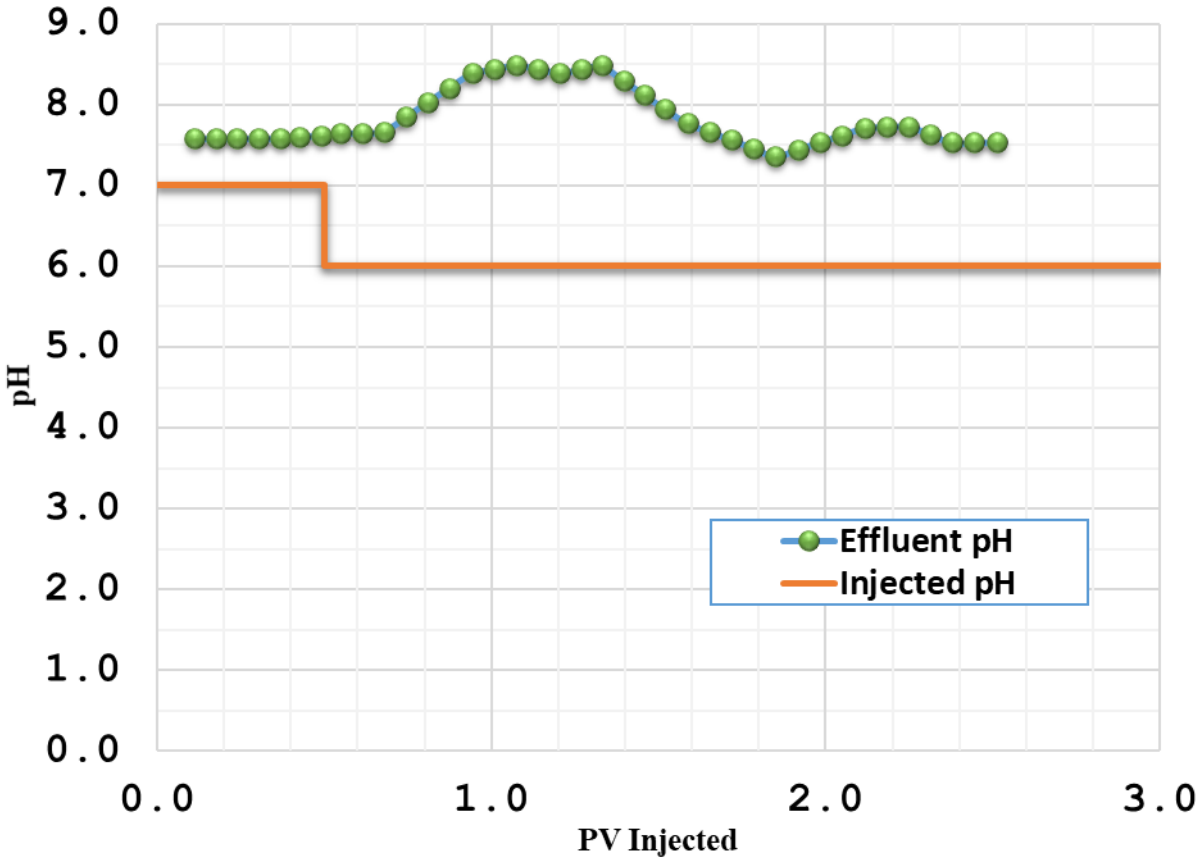

Figure 4.3. 35 Chemical Flood Effluent pH for Experiment C-1

The viscosity of the effluents began increasing at 0.6PV of injection and reached the injected polymer drive viscosity near 2.5PV of injection. This showed that viscosity propagated slowly.

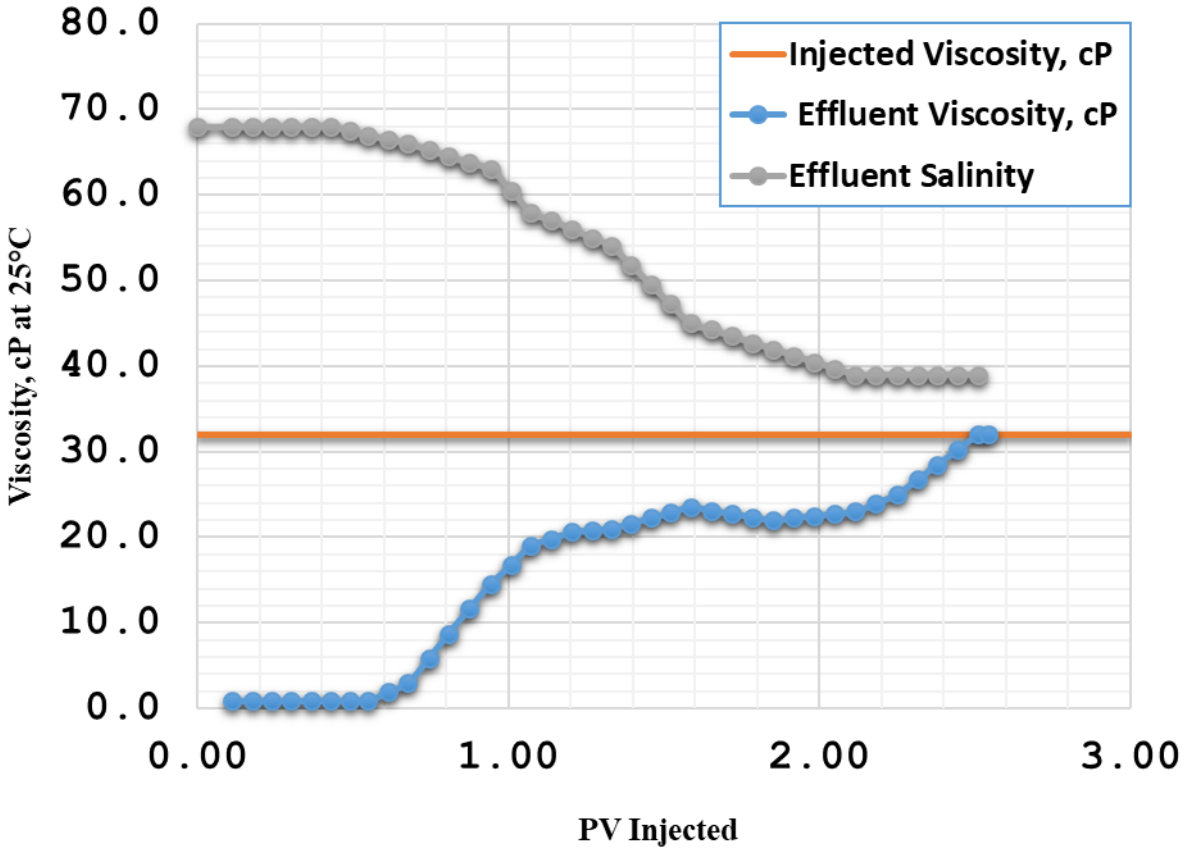

Figure 4.3. 36 Chemical Flood Effluent viscosity and salinity for Experiment C-1

Based on pressure drop data, there was no plugging observed and the pressure drop reached the steady state after 1.5PV of chemical injection. The pressure drop, at the beginning increased as both the high viscosity of chemical slug injection and the oil displacement through the core. Figure 4.3.46 shows sectional pressure drop data.

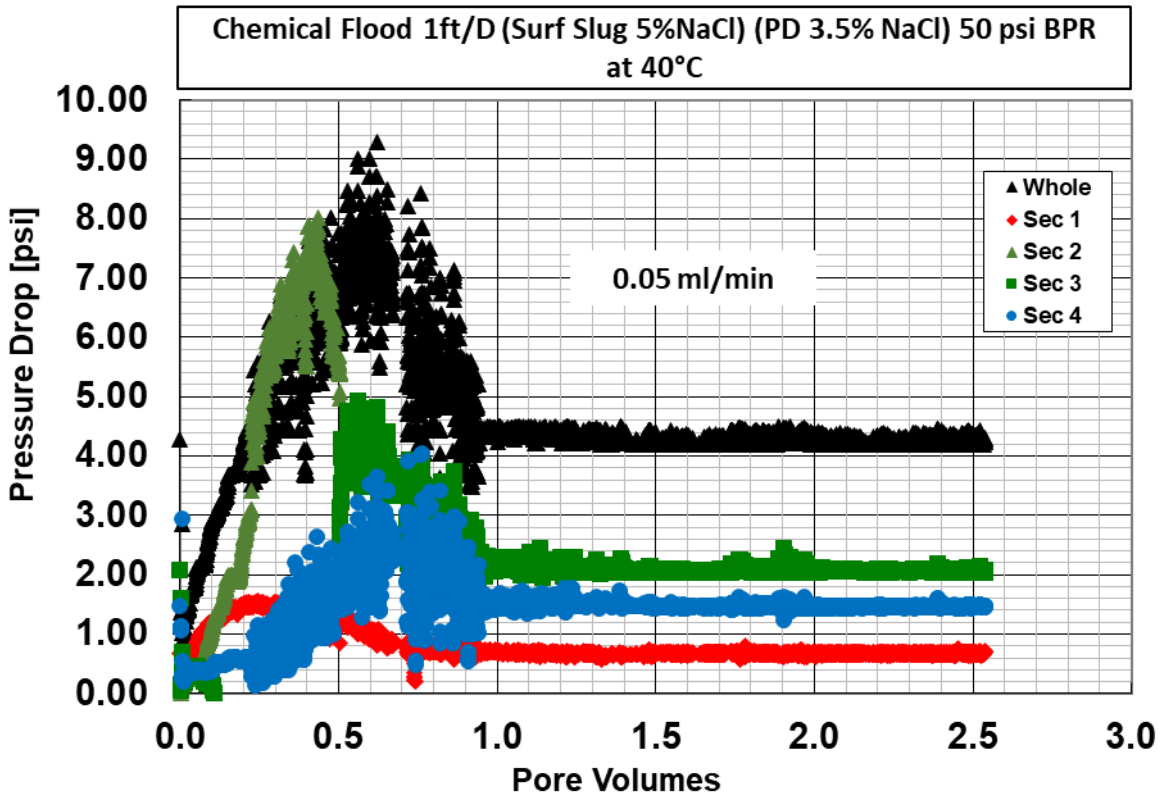

Figure 4.3. 37 Pressure Drop Data for Experiment C-1

Discussion of Results

The failure of experiment C-1 with a low oil recovery and a high surfactant retention (0.31mg/g-rock) was attributed to the unstable displacement. The viscosity propagation was retarded and until 2.5PV of injection viscosity did not reach the injected value. It was hypothesized that the injected viscosity was insufficient to account for the uncertainty in calculated total mobility of the oil bank. Corey exponents used in calculating the relative permeability for oil bank were highly uncertain as full relative permeability curves for the core ABC were not available. The value of 2.5 was used for both oil and water exponents to calculate the minimum total mobility of the oil bank, but retroactive inspection showed that even a value of 3.0 could have resulted in two fold decrease in the mobility of the oil bank. In highly uncertain situations like this, a viscosity safety factor of 2 would be preferred for a laboratory coreflood. Furthermore, a large amount of oil was not swept by the chemical flood and it is

most likely that the injected surfactant was retained by phase trapping due to poor mobility control.

4.4.2. Oil Recovery Experiment C-2

Formulation F2 was used in this experiment to determine the surfactant retention in the presence of oil and oil production in Berea sandstone. The core was prepared as described in Chapter III, after the dimensions and mass of the core were noted. The core was initially saturated with 2wt% KCl at 40℃. See Table 4.3.33 for the core properties.

Table 4.3. 34 Core Properties for Experiment C-2

C-2		
Core Properties		
Core Name	DEF	
Rock Type	Berea Sandstone	
Est. k	150	md
Diameter	1.49	inch
Length	30.40	cm
Mass	722.54	g
Bulk vol.	341.98	cm3
Porosity	0.21	
Area	11.25	cm^2
PV	72.52	ml
Length (Section 1)	8.13	cm
Length (section 2)	7.67	cm
Length (section 3)	7.67	cm
Length (section 4)	6.99	cm
Temperature	40	°C

Tracer Test and Brine Permeability

2wt% KCl was injected at different ratios (1ml/min, 2ml/min and 3ml/min) to determine the brine permeability at steady state at 40°C. Afterwards, 5wt% NaCl tracer brine was injected to determine the pore volume of the core. The tracer brine broke-through at 0.55PV of injection, and it took 1PV of injection to reach its maximum value. The pore volume was determined to be 72.5ml. The average brine permeability at 40°C was calculated as 265mD for the core. For the sectional permeability see Table 4.3.34.

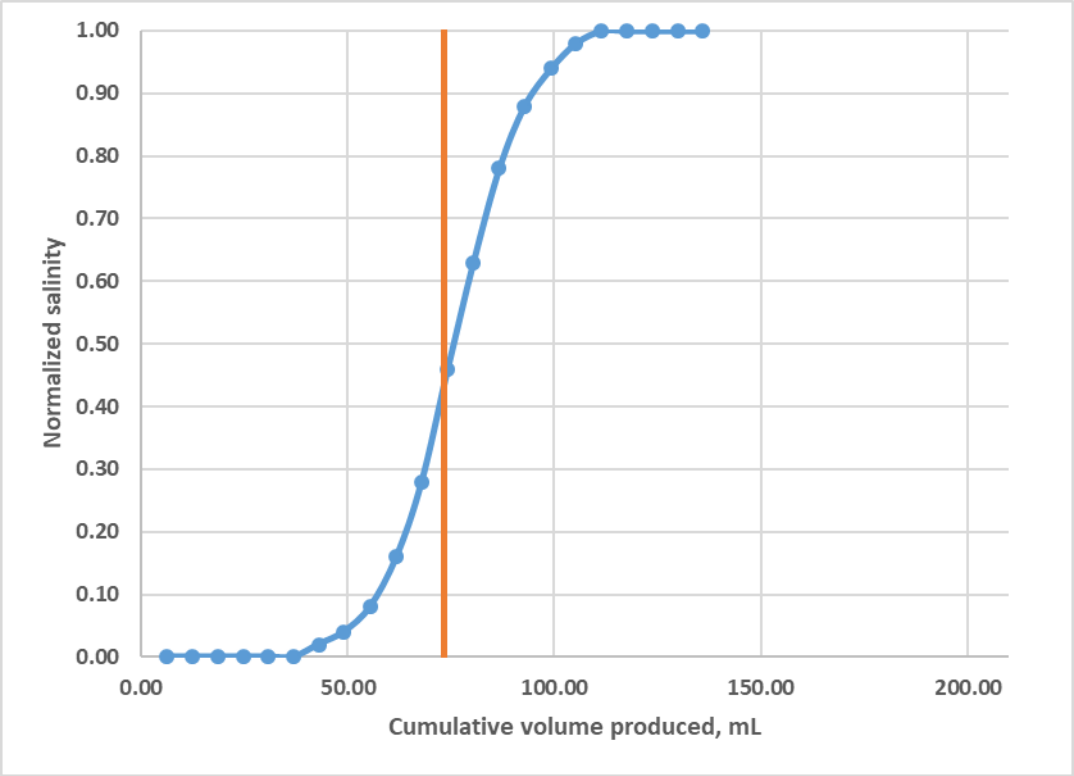

Figure 4.3. 38 Normalized Salinity Tracer for Experiment C-2

Oil Flood

The core was oil flooded at 40°C. The oil is filled into a stainless steel column and displaced by argon gas at 140psi. The BPR was set to ~55psi, allowing for a 95psi pressure differential. Injection of the oil continued until the oil cut was zero. When the water saturation reached the residual value, the oil injection was continued to determine the oil pressure drop at

steady state conditions and to determine the end point oil relative permeability k_{ro}^{o} (0.8). By volume balance, S_{oi} was estimated to be 0.73.

Water Flood

After the dilution tests at 40°C, the water flood salinity was determined to be 4.5wt%NaCl. At this salinity, diluted phase behavior showed ultra-low IFT near the optimum salinity. Injection was continued at 2ft/D (0.1ml/min) until the oil cut was less than 1% and the pressure drop reached steady state. The pressure drops at steady state (SS) used to estimate the end point water relative permeability k_{rw}^{o} as 0.08. S_{orw} was calculated to be 0.42 (Table 4.3.35).

Table 4.3. 35 Summary of Brine Flood, Oil Flood and Water Flood permeability and Relative Permeability for Experiment C-1

	Average Brine Permeability @40°C	**Average Oil Permeability @40°C**	**k_{ro}^{o}**	**Average Water Permeability @40°C**	**k_{rw}^{o}**
Whole	264.705	214	0.81	22	0.08
Section1	203.808	278	1.36	27	0.13
Section2	306.655	230	0.75	28	0.09
Section3	328.029	204	0.62	27	0.08
Section4	314.606	167	0.53	24	0.08

Table 4.3. 36 Summary of Oil Flood and Water flood for Experiment C-2

Oil Flood		**Water Flood**	
k_{ro}^{o}	0.81	**k_{rw}^{o}**	0.08
S_{oi}	0.71	**S_{orw}**	0.49

Mobility Control

At the end of the water flood, the required minimum viscosity for a stable displacement is designed by using the total mobility curve. The inverse of minimum mobility was estimated and set as the minimum viscosity for chemical slugs with safety factor of 1.2. Due to the failure

of experiment C-1, the value of 3, instead of 2.5, was used for both oil and water exponents to calculate the total mobility of the chemical slug and the required minimum viscosity for the chemical slug was determined to be 36cp. See Table 4.3.36 the parameters used in this calculation.

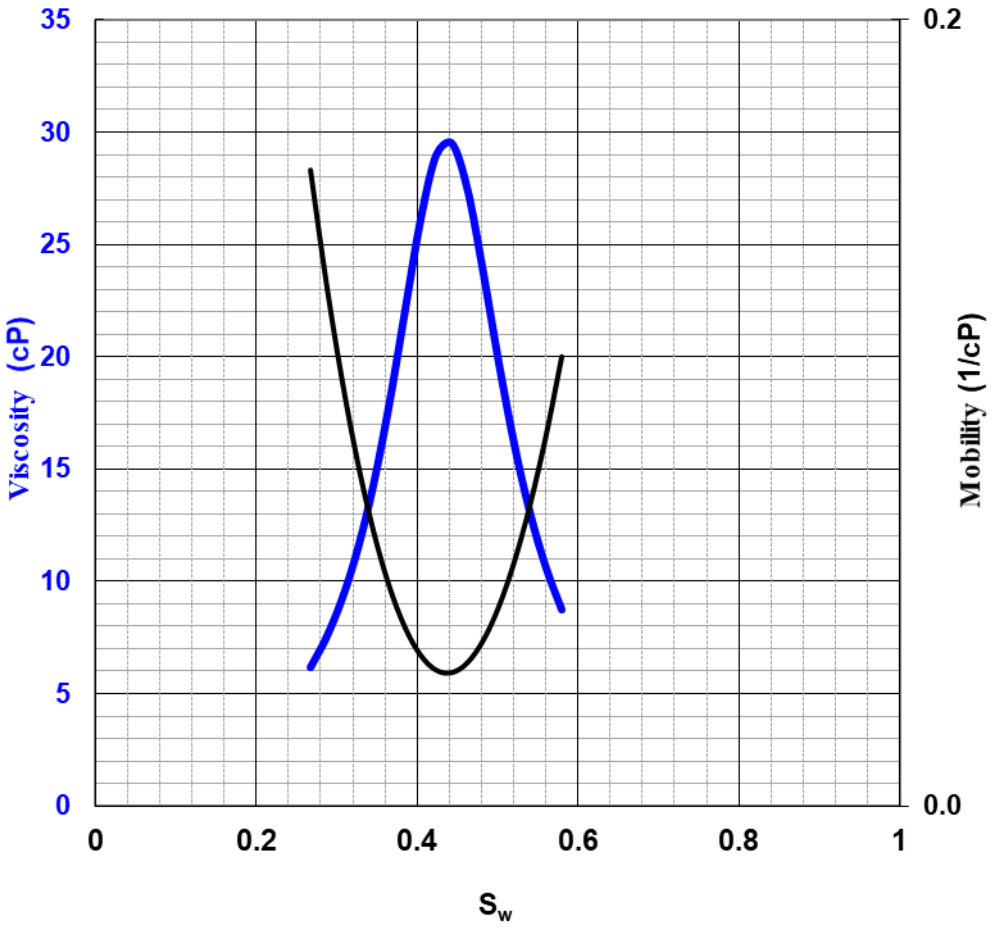

Figure 4.3. 39 Total Relative Mobility Curve for Experiment C-2

Table 4.3. 37 Total Relative Mobility Curve Parameters for Experiment C-2

k_{rw}^o	0.080	
k_{ro}^o	0.81	
n_w	3	
n_o	3	
S_{wr}	0.27	
S_{or}	0.42	
μ_w	0.70	cP
μ_o	5	cP

The equivalent shear rate in the core was estimated to be 10.7 s^{-1} when n is 0.6 and C is 3. The constant C was also kept higher for this experiment because of the failure of experiment C-1. Higher C constant caused higher equivalent shear rate calculation, which is an additional safety precaution to obtain a robust displacement. Viscosity of the surfactant slug and the polymer drive were tested with different concentrations of polymer (FP3330S). The required viscosity was obtained with 3000ppm of polymer (FP3330S) at target shear rate.

Chemical Flood

The SP slug and the polymer drive were prepared by following the procedure described in Chapter III. Slugs were prepared and placed inside the oven to heat them up to the 40℃ and afterwards, injection started at 1ft/D (0.05ml/min) at 40℃. The effluents were collected with 5ml in each tube. At the end of the chemical flood, the effluent samples were analyzed for the surfactant retention and for the effluent pH, viscosity and salinity propagation through the core.

Table 4.3. 38 Surfactant Slug and Polymer Drive Properties for Experiment C-2

	Surfactant Slug	**Polymer Drive**
PV Injected	0.5	2
Polymer	FP 3330S	FP 3330S
Polymer Concentration (ppm)	3000	3000
Frontal Velocity (ft/D)	1	1
Salinity (ppm TDS)	61	24
pH	6	6.5
Viscosity at 10 s^{-1} & 40°C	38	53

Chemical Flood Results

At the end of the chemical flood of 2.5PV of injection, the effluents were analyzed after centrifuging them for 10mins at 2000rpm and room temperature, and amount of oil collected was estimated as ~63wt%ROIP with a S_{orc} 0.18. Due to low oil recovery, for a high permeability sandstone Berea outcrop, this chemical flood was considered to be a poor flood.

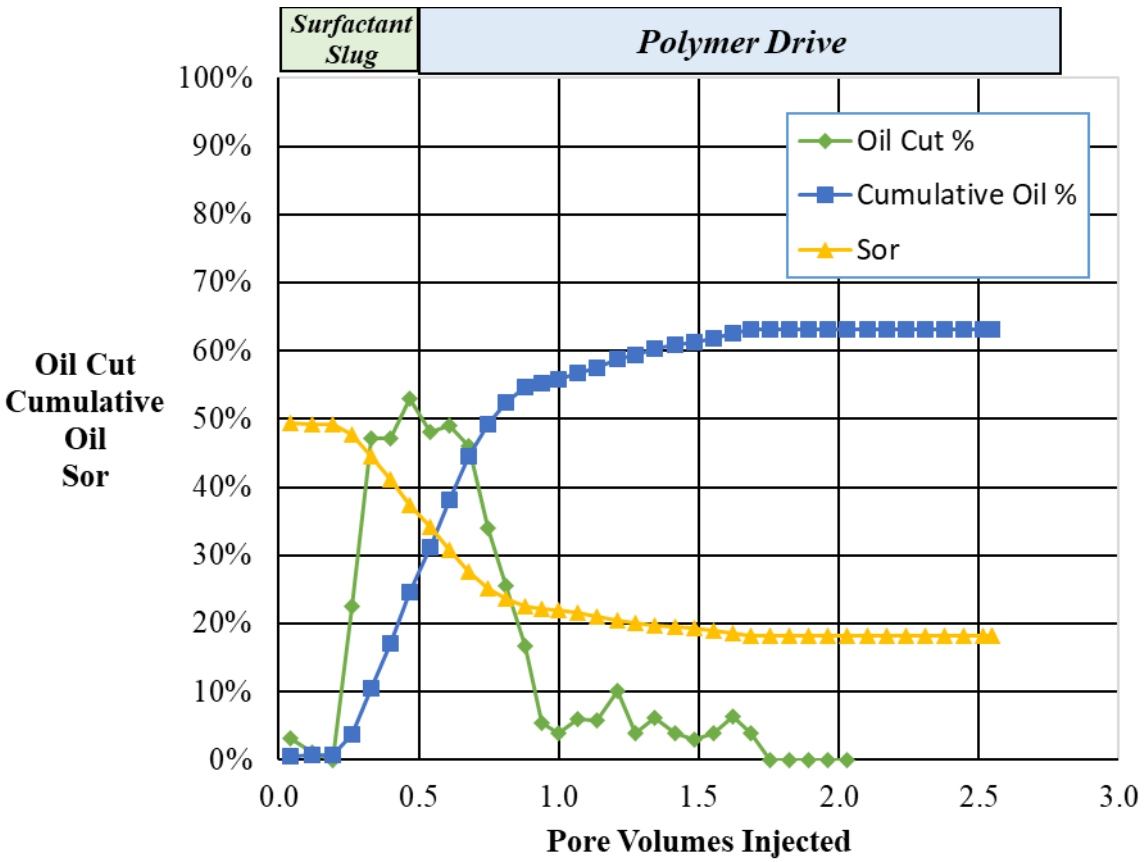

Figure 4.3. 40 Oil Recovery for Experiment C-2

The effluent surfactant concentration was measured by HPLC, and the surfactant retention was determined to be between 0.08-0.1mg/g-rock. The surfactant break-thorough was observed at 0.9PV and continued producing for ~1PV.

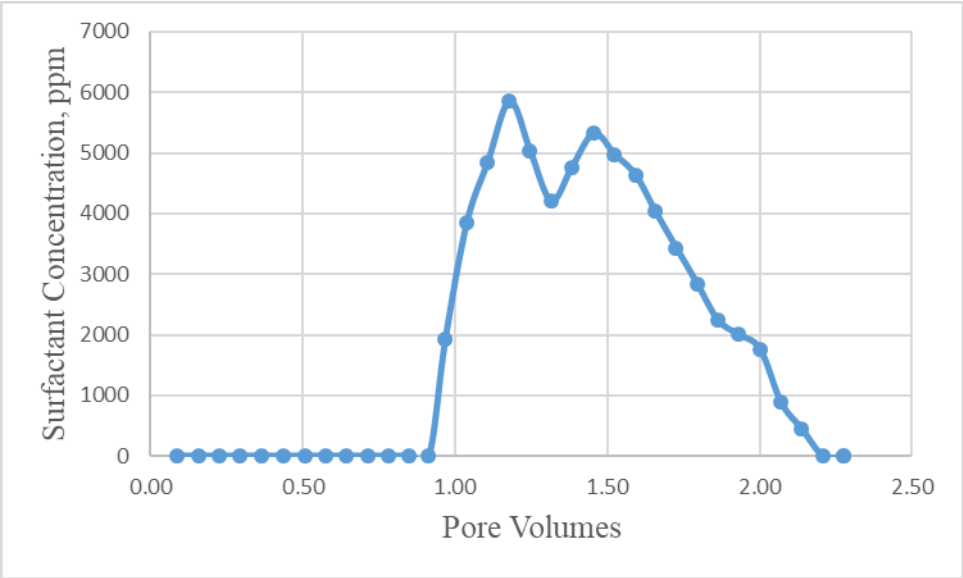

Figure 4.3. 41 Effluent Surfactant Concentration for experiment C-2

The salinity propagation was determined by a refractometer. The effluent salinity broke-through decreasing at 0.7PV of injection and increased to 50000ppm as the surfactant slug was injected and after 1PV of injection, the effluent salinity started decreasing. The effluent salinity reached the polymer drive salinity after 2PV of injection.

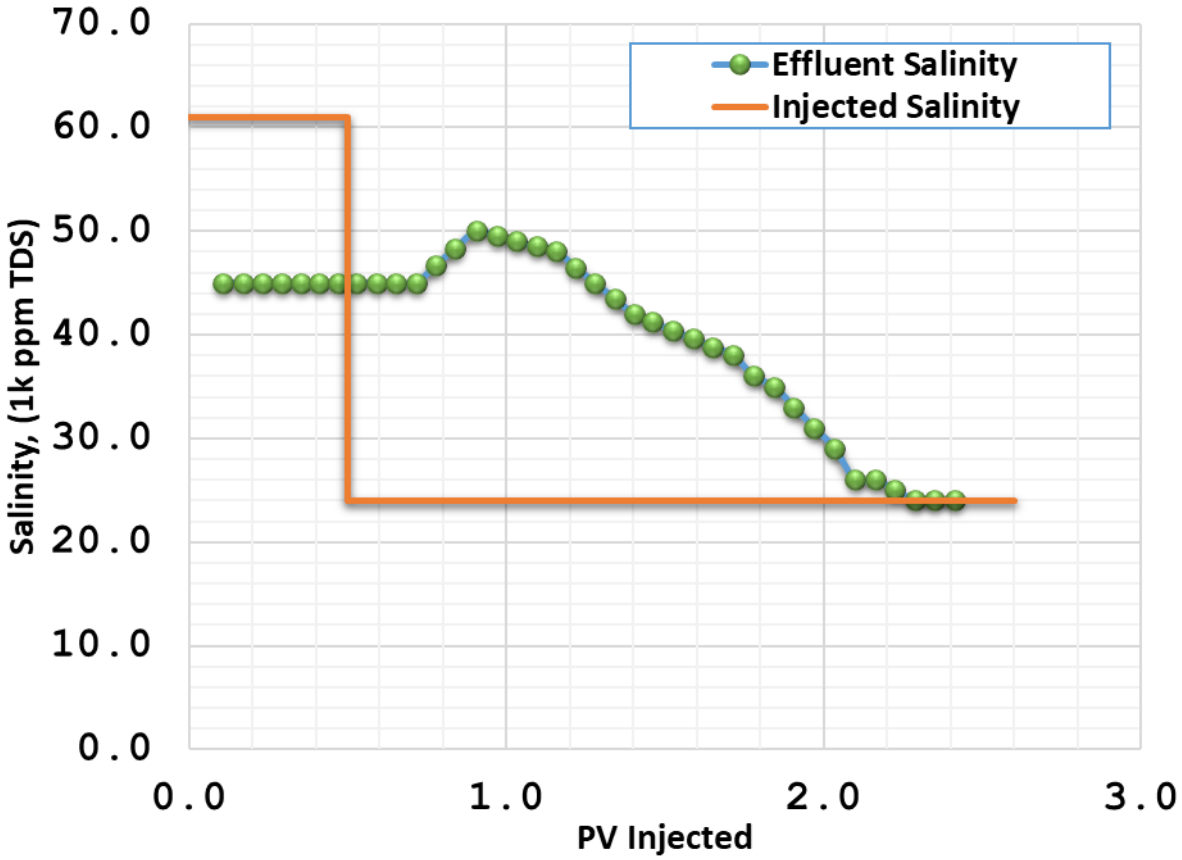

Figure 4.3. 42 Chemical Flood Effluent Salinity for Experiment C-2

The effluent pH was measured and compared to the pH of injected solutions. The pH of injected chemical solutions were arranged to neutral values, prior to the flood. The pH of effluents were higher than the injected pH; however, it was still neutral.

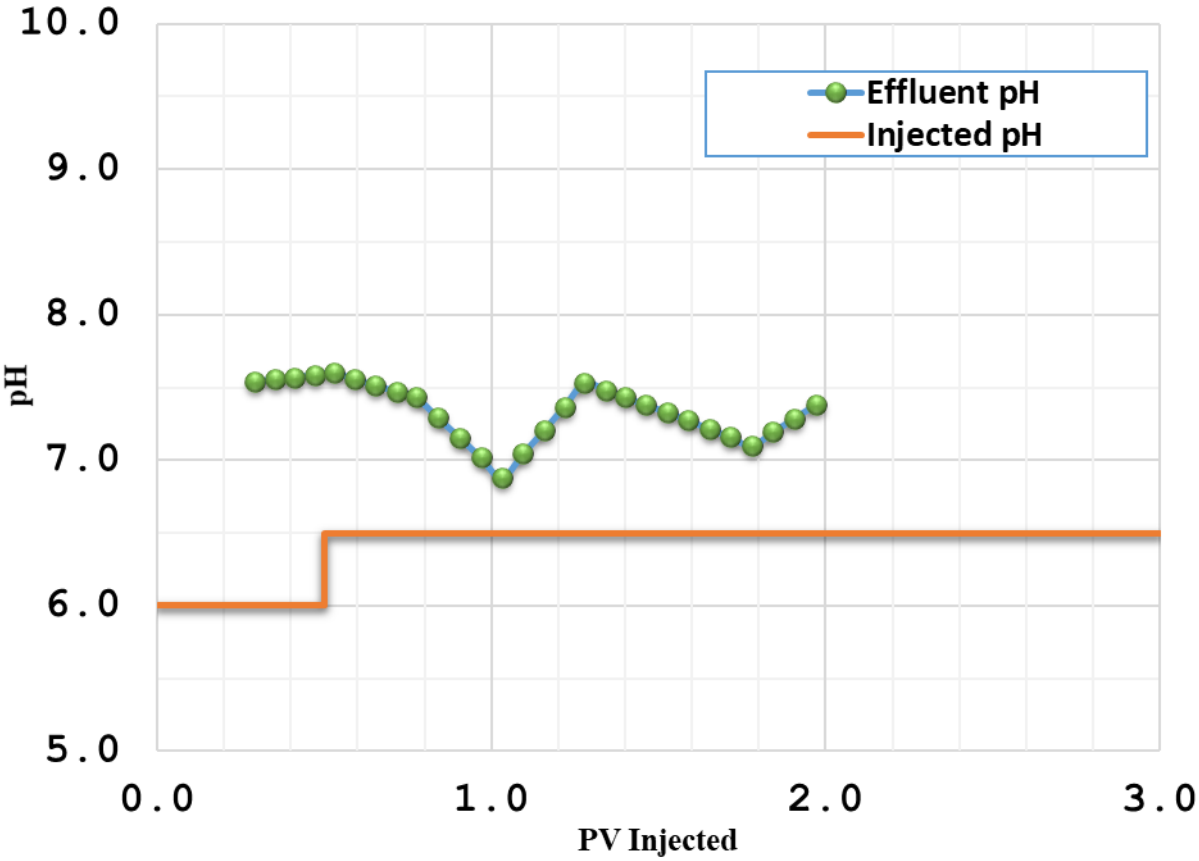

Figure 4.3. 43 Chemical Flood Effluent pH for Experiment C-2

The viscosity of effluents began increasing at 0.7PV of injection and reached the injected polymer drive viscosity near 2.5PV of injection. This showed that viscosity propagated efficiently through the core.

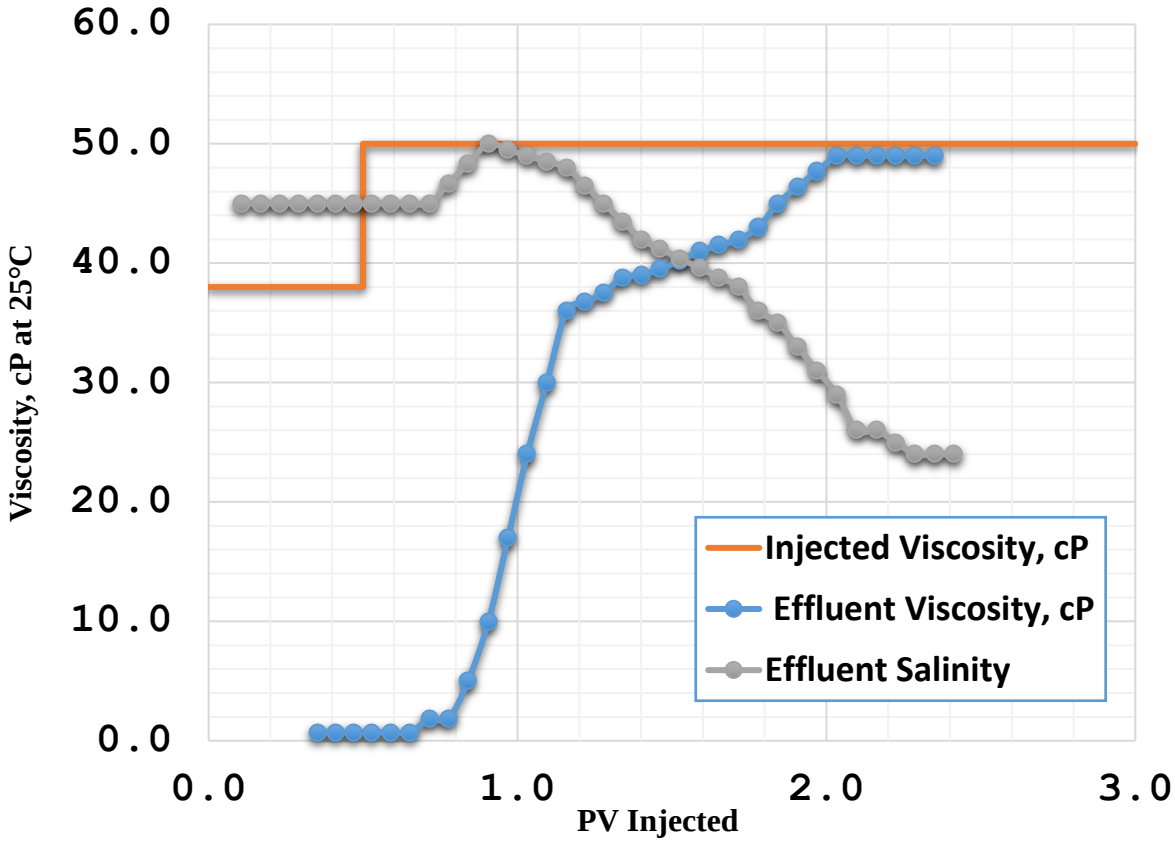

Figure 4.3. 44 Chemical Flood Effluent viscosity and salinity for Experiment C-2

Based on the pressure drop data, there was no plugging observed and the pressure drop reached the steady state after 1.5PV of chemical injection. The pressure drop at the beginning increased due to both the high viscosity of chemical slug injection and the oil displacement through the core. Section 3 pressure transducer line plugged during the flood. For that reason, section 3 and section 2 pressure drops were observed as a combined middle section, which was represented as section 2 in Figure 4.3.46.

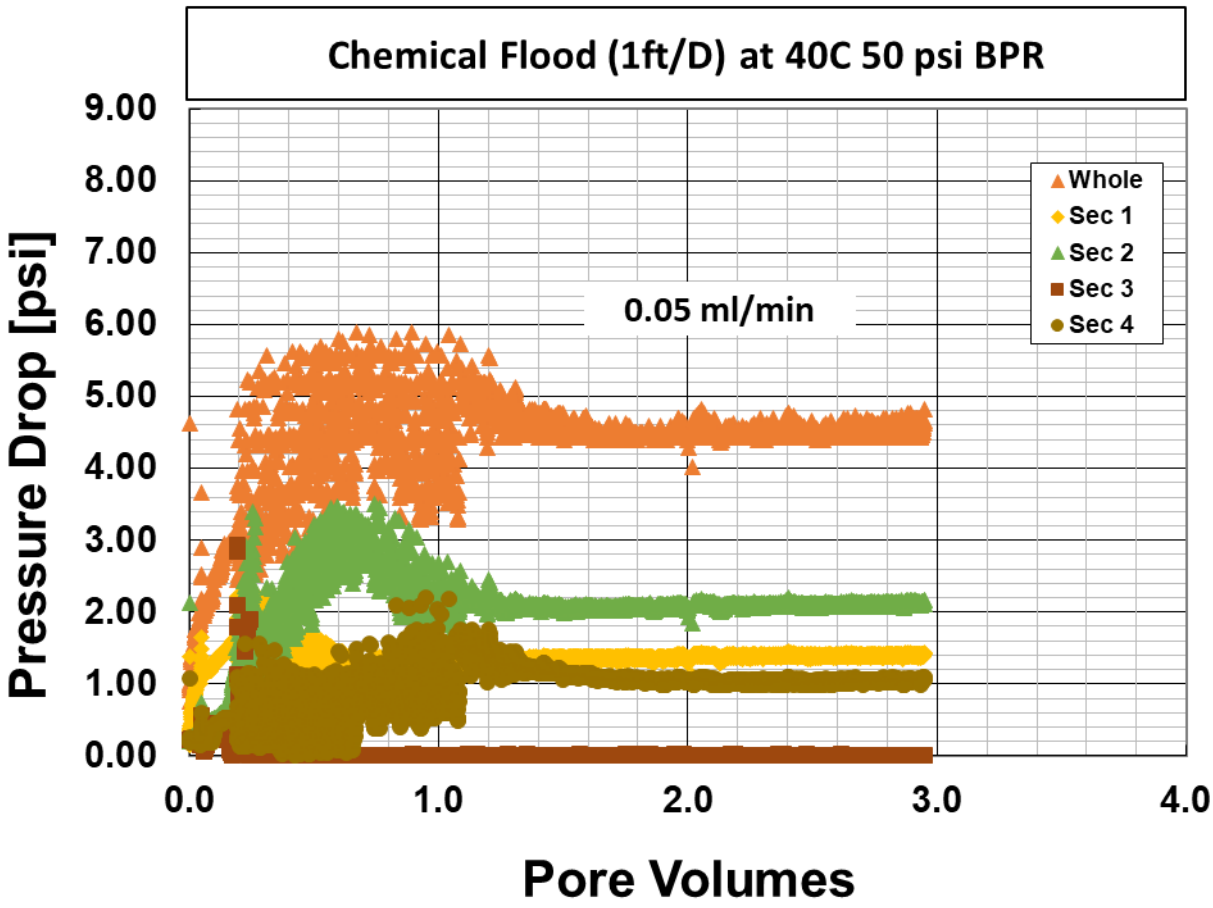

Figure 4.3. 45 Pressure Drops for Experiment C-2

Discussion of Results C-2

The chemical flood was continued for 2.5PV. Overall, the data for this experiment showed that the viscosity and salinity propagated well through the core. Even though, the oil recovery was low, the retention of surfactant was obtained to be low for an SP flood. This high surfactant production was attributed to the efficient viscosity and salinity propagation inside the core. The effluents reached the polymer drive viscosity towards the end of the chemical flood, which was necessary to increase the affinity of surfactants to the aqueous phase and produce the surfactants by diminishing the phase trapping of surfactants to the oil. Additionally, the effluents reached to the polymer drive viscosity before the chemical flood was ended. Combination of these effects resulted in a very low surfactant retention. On the other hand oil

production was very low, too, and this low production was not compatible with the data obtained during the flood. Thus, only hypothesis could be claimed was in situ phase behavior. In porous medium microemulsions can behave differently. Depending on the pH of the oil and the oil composition, in porous medium, the interaction between oil and the mineralogical components of the rock can result in different microemulsion behaviors. Therefore, the oil recovery experiments were continued with oil O-2, afterwards.

4.4.3. Oil Recovery Experiment C-3

The purpose of this experiment was to determine the surfactant retention in the presence of oil O-2 and measure the oil production using formulation F5 in Berea outcrop. After the failed experiment C-1 and non-satisfactory oil recovery results from experiment C-2, the formulation F5 in a medium viscosity oil (O-2) was used for this oil recovery experiment. The core is prepared as described in Chapter III after the core's dimensions and mass were measured. Due to the broken piece of the drilling pit inside the core on section 4 pressure tap, pressure drops for section 4 was analyzed in the combination of section 3. The core initially saturated with 2wt% KCl at 40°C.

Table 4.3. 39 Core Properties for Experiment C-3

C-3		
Core Properties		
Core Name	GHJ	
Rock Type	Berea Sandstone	
Est. k	150	md
Diameter	3.80	cm
Length	30.10	cm
Mass	723.91	g
Bulk vol.	338.61	cm3
Porosity	0.20	
Area	11.25	cm^2
PV	67.5	ml
Length (Section 1)	8.13	cm
Length (section 2)	7.62	cm
Length (section 3)	14.22	cm
Temperature	40	°C

Tracer Test and Brine Permeability

2wt%KCl was injected at different ratios to determine the brine permeability at 40℃ when the flow reached steady state conditions. Afterwards, 5.3wt% KCl tracer brine was injected to determine the pore volume of the core. The tracer brine broke-through at 0.4PV of injection, and it took almost 2PV for the influent brine to completely displace the in-situ brine. This shows that the core was a very heterogeneous core with the pore volume of 67.5ml. The average brine permeability of the core at 40℃ was calculated as 208mD. For the sectional permeability see Table 4.3.39.

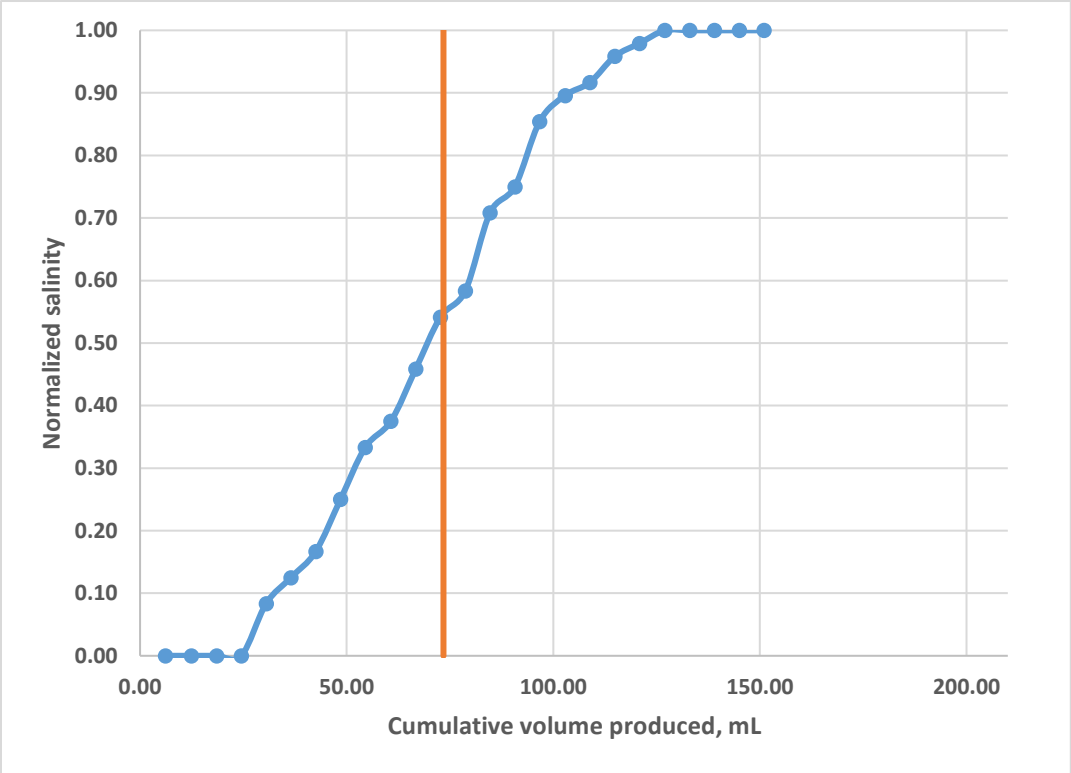

Figure 4.3. 46 Normalized Salinity Tracer for Experiment C-3

Oil Flood

The core was oil flooded at 40℃. The oil was filled into a stainless steel column and displaced by argon gas at 90psi. The BPR was set to ~15psi, allowing for a 75psi pressure differential. Injection of the oil continued until the oil cut was zero. When water saturation reached to residual value, the oil injection was continued to determine oil pressure drop at steady state conditions and determine the end point oil relative permeability k_{ro}^{o}, which is 1.0. By using displaced water volume by oil O-2, S_{oi} was estimated to be 0.60.

Water Flood

Water flood was conducted at optimum salinity of the formulation (5.3% NaCl). Water flood continued at 2ft/D (0.1ml/min) until the oil cut was less than 1% and pressure drop reached steady state. The pressure drops at steady state were used to estimate the end point water relative permeability k_{rw}^{o} as 0.05. S_{orw} was calculated to be 0.30 (Table 4.3.40).

Table 4.3. 40 Summary of Brine Flood, Oil Flood and Water Flood Permeability and Relative Permeability for Experiment C-3

	Average Brine Permeability @40°C	**Average Oil Permeability @40°C**	**k_{ro}^{o}**	**Average Water Permeability @40°C**	**k_{rw}^{o}**
Whole	208.796	309.98	1	10	0.05
Section1	203.033	301.72	1	10	0.05
Section2	206.116	271.27	1	11	0.05
Section3	218.158	339.34	1	11	0.05

Table 4.3. 41 Summary of Oil Flood and Water flood for Experiment C-3

Oil Flood		**Water Flood**	
k_{ro}^{o}	1	**k_{rw}^{o}**	0.05
S_{oi}	0.60	**S_{orw}**	0.30

Mobility Control

At the end of the water flood, the required minimum viscosity for a stable displacement was designed by using the total mobility curve. The inverse of minimum mobility was estimated and set as the minimum viscosity for the chemical slugs and with safety factor 1.2, the chemical flood viscosity was designed to be more than 60cp. See Table 4.3.41 for the parameters used in this calculation.

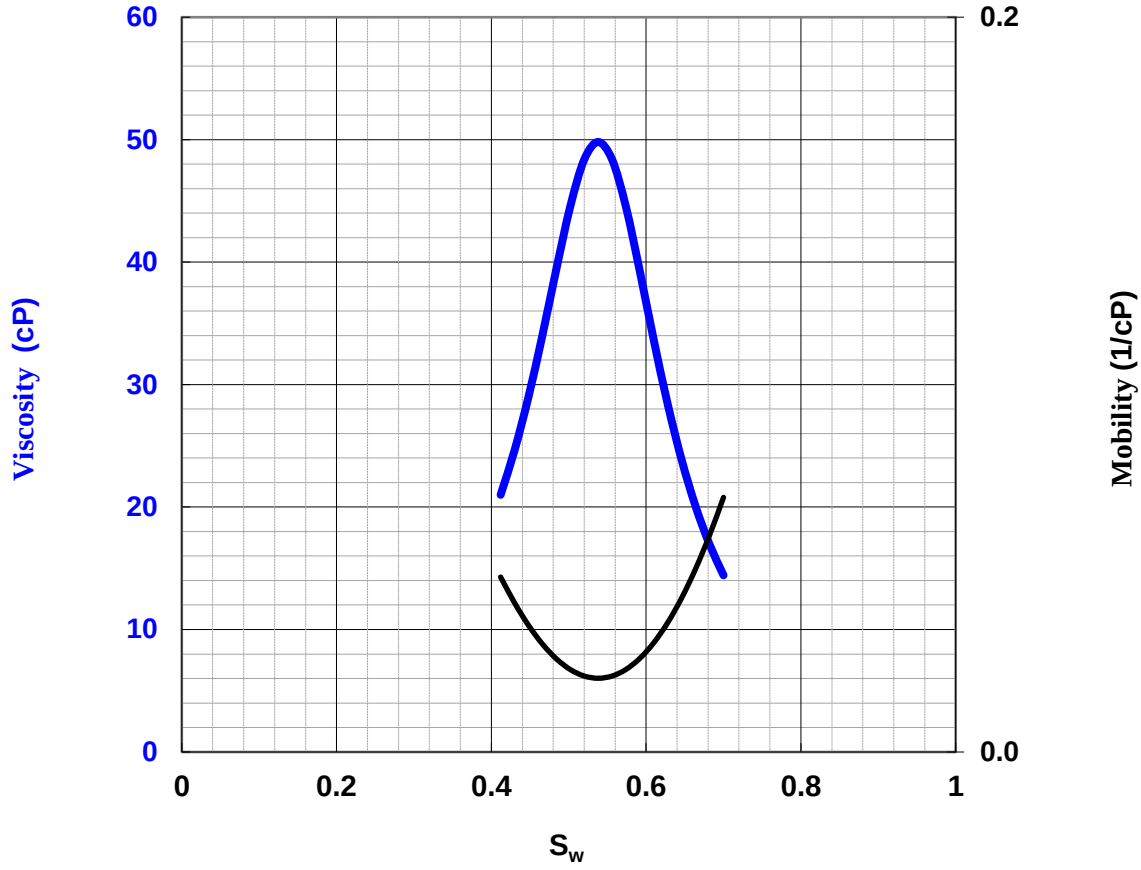

Figure 4.3. 47 Total Relative Mobility Curve for Experiment C-3

Table 4.3. 42 Total Relative Mobility Curve Parameters for Experiment C-1

k_{rw}^{o}	0.050	
k_{ro}^{o}	1.00	1.286
n_w	2.5	
n_o	2.5	
S_{wr}	0.41	
S_{or}	0.30	
μ_w	0.72	cP
μ_o	21	cP

The equivalent shear rate in the core was estimated to be $11.7s^{-1}$ when n is 6 and as an additional safety parameter C value was 3 instead of 2. Viscosity of surfactant slug was tested with different concentrations of FP3330S. With polymer concentration of 4,500ppm, the required viscosity was obtained at the target shear rate.

Chemical Flood

The surfactant slug and the polymer drive were prepared by following the procedure described in Chapter III. The injection of chemical solutions was conducted at 1ft/D (0.05ml/min) at 40℃. The effluents were collected with the fraction of 5ml. At the end of the flood, the effluents were analyzed for the surfactant retention and effluent pH, viscosity and salinity.

Table 4.3. 43 Surfactant Slug and Polymer Drive Properties for Experiment C-3

	Surfactant Slug	**Polymer Drive**
PV Injected	0.5	2
Polymer	FP 3330S	FP 3330S
Polymer Concentration (ppm)	4500	4500
Frontal Velocity (ft/D)	1	1
Salinity (ppm TDS)	70	42
pH	7.30	7.30
Viscosity at 10 s^{-1} & 40°C	53	53

Chemical Flood Results

After 2.5PV of the chemical flood, still Type I salinity was not achieved. Thus, the polymer drive was continued for additional 0.3 PV. At the end of the chemical flood, the effluents were analyzed visually for the oil recovery after centrifuging them for 10mins at 2000rpm at room temperature. Amount of oil collected was determined as ~92% ROIP with S_{orc} 0.025.

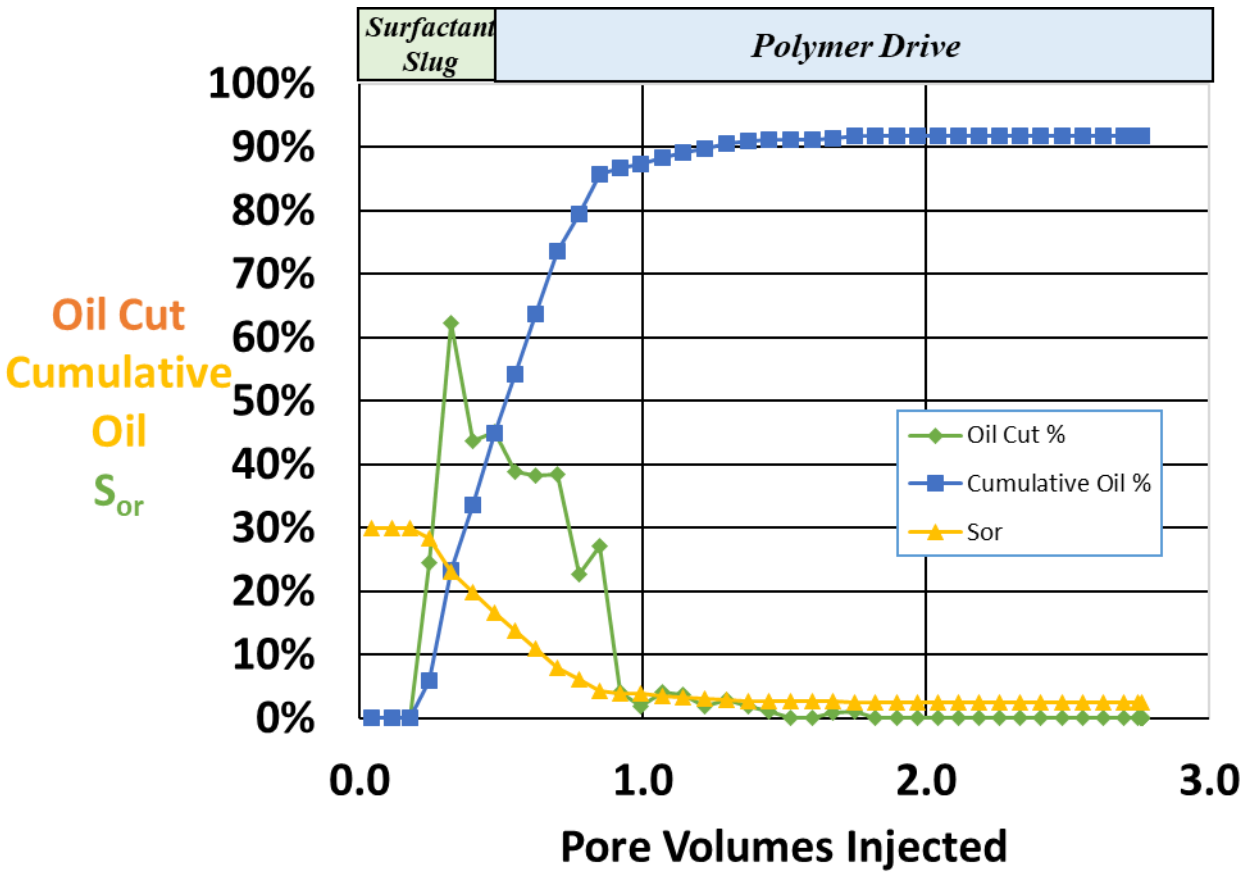

Figure 4.3. 48 Oil Recovery for Experiment C-3

The effluent surfactant concentration was measured by HPLC and the surfactant retention was determined to be between 0.18mg/g-rock-0.20mg/g-rock. The surfactant break-thorough was observed at 0.8PV and reached the peak value at 1.4PV and 1.75PV and continued producing up to 2.7PV.

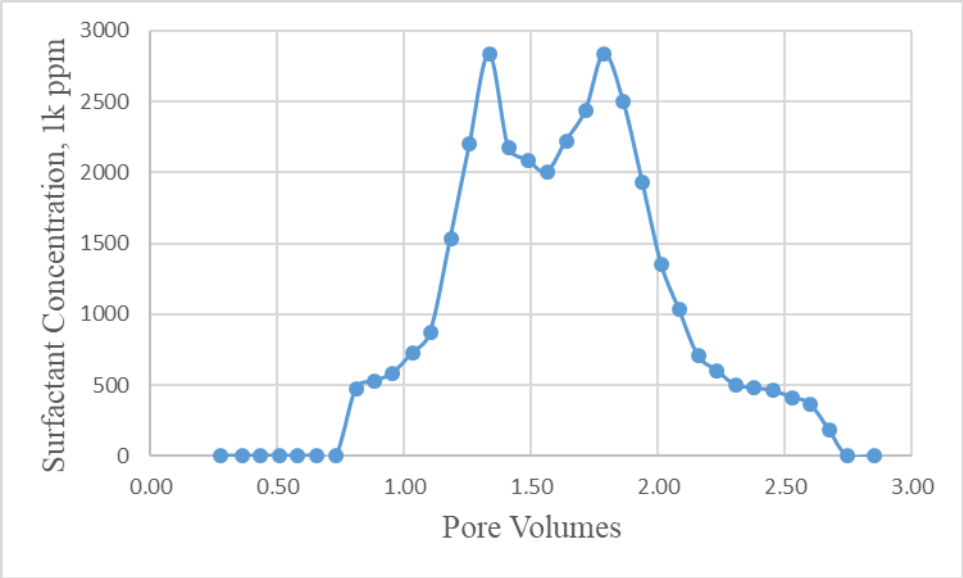

Figure 4.3. 49 Effluent Surfactant Concentration for experiment C-3

The salinity propagation was determined using a refractometer. The effluent salinity broke-through at 0.8PV of injection and increased at the beginning to reach the salinity of surfactant slug and then decreased as the polymer drive at lower salinity injected. The effluents reached Type I condition (the polymer drive salinity) at 2.5 PV of the chemical injection.

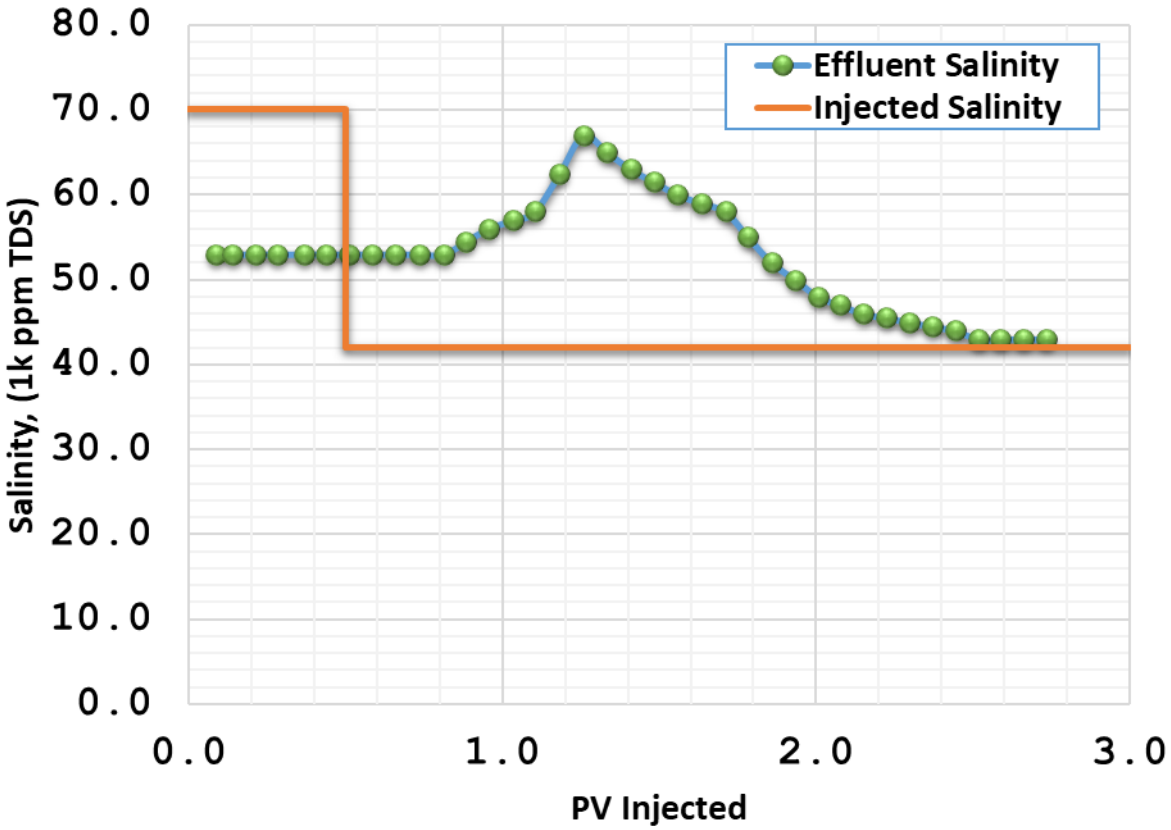

Figure 4.3. 50 Chemical Flood Effluent Salinity for Experiment C-3

The effluent pH was measured and compared to the pH of injected solutions. The pH of chemical solutions were arranged to neutral values, prior to the injection. The pH of effluents were higher than the injected pH; however, it was still the neutral. Only one effluent showed the pH of 8.90 which was accounted for a measurement error.

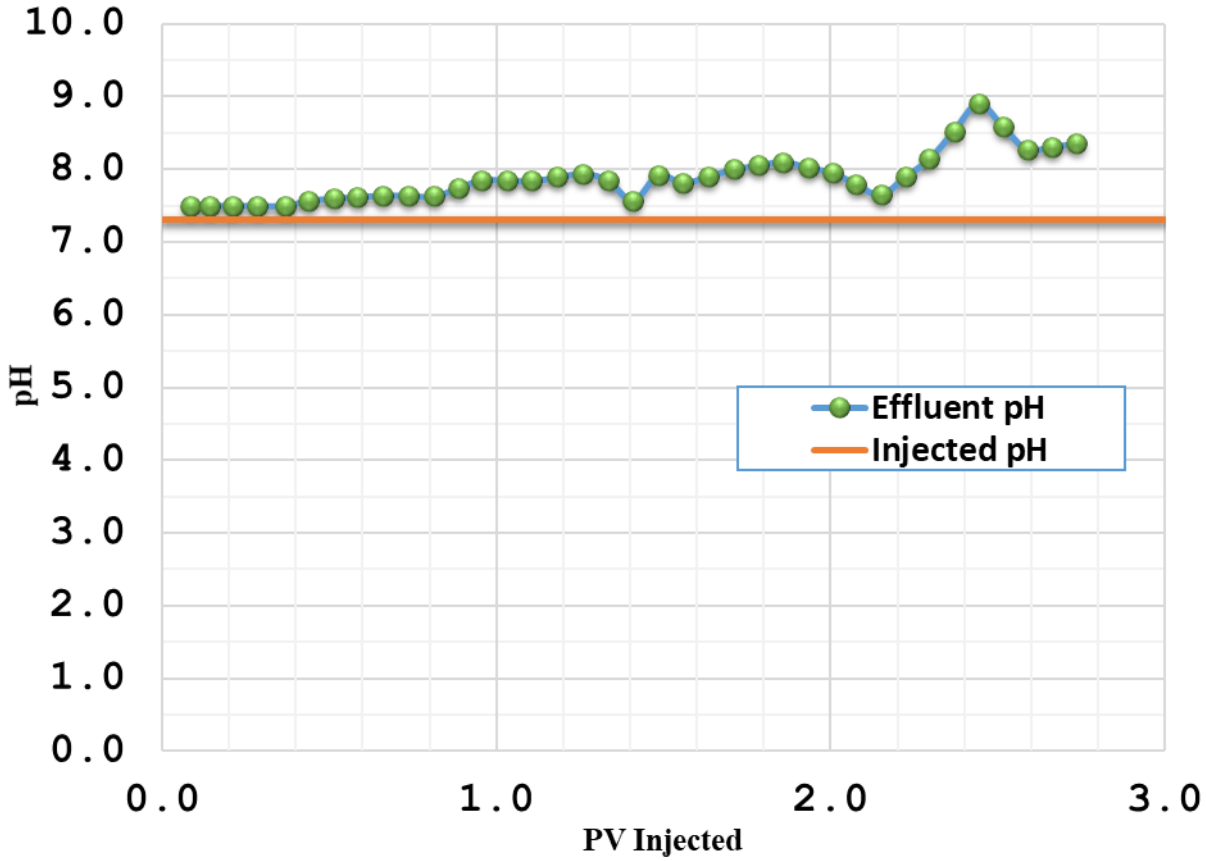

Figure 4.3. 51 Chemical Flood Effluent pH for Experiment C-3

The injected viscosity was lower than the target viscosity (60cp). Even though, the chemical slugs were prepared to be 60cp from the beginning, during the filtration (by using 1.2micons of Nitrocellulose membrane) viscosity decreased to 53cp. The viscosity of effluents began increasing at 0.8PV of injection and plateaued at the injected polymer drive viscosity at 2.3PV of injection. Thus, the viscosity propagation shows that polymer did not degraded throughout the core and efficient displacement was obtained.

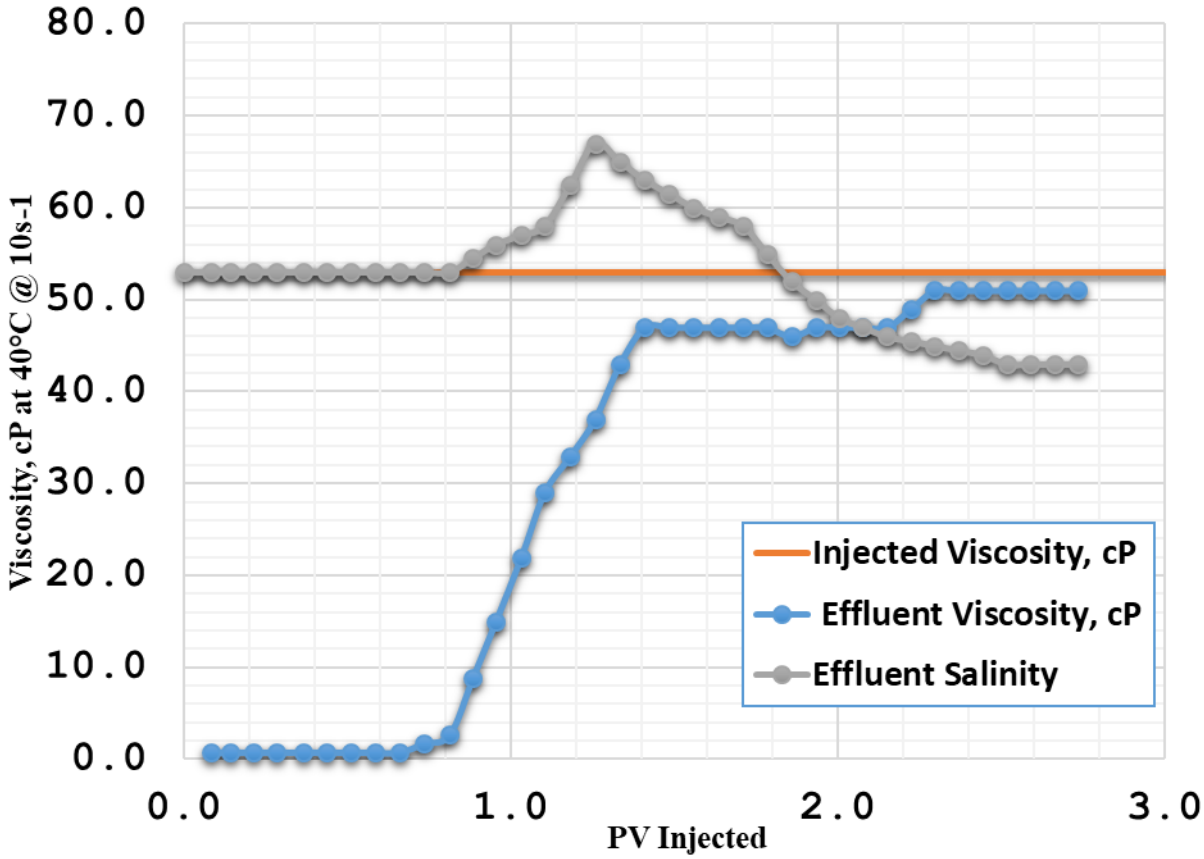

Figure 4.3. 52 Chemical Flood Effluent viscosity and salinity for Experiment C-3

Despite the high polymer concentration, plugging was not observed and polymer was transported well through the core. During the chemical flood, the pressure drop reached the steady state after 1.5PV of chemical injection. The pressure drop at the beginning increased due to both the high viscosity of chemical slug injection and the oil displacement through the core. Figure 4.3.54 shows the sectional pressure drop data.

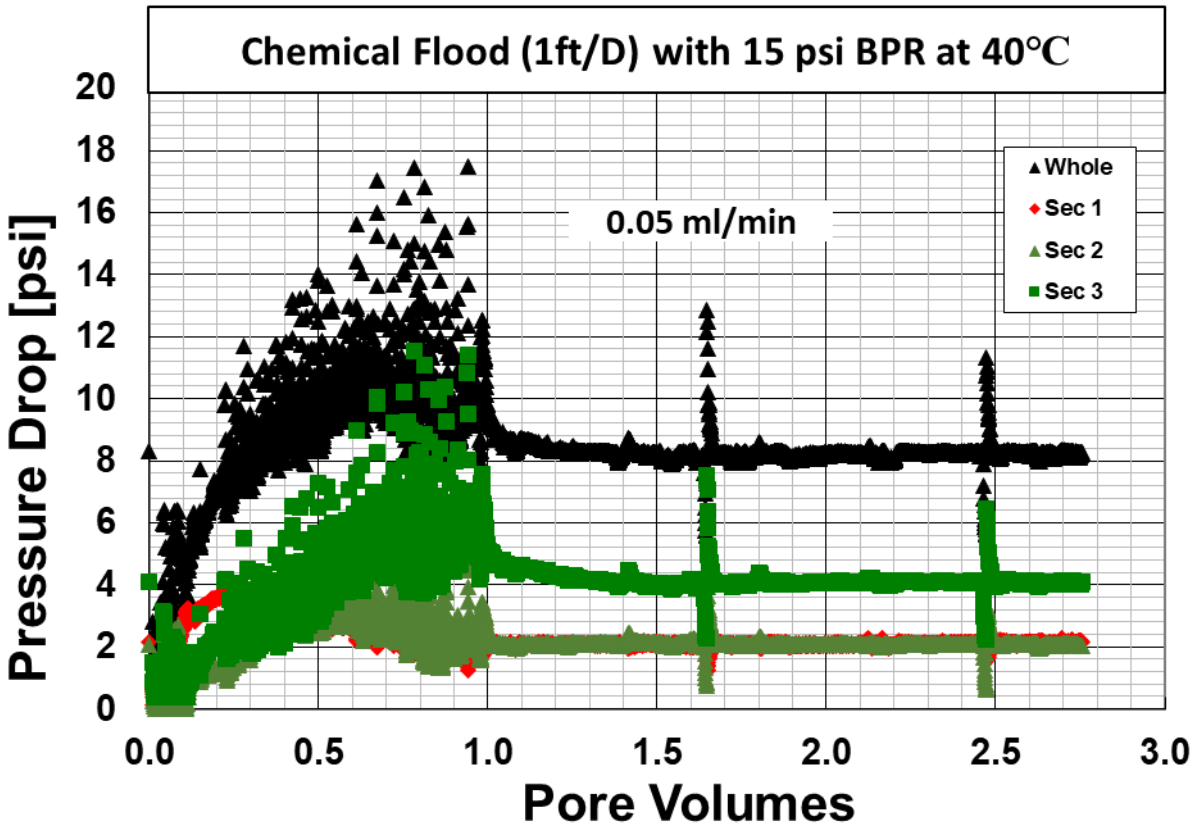

Figure 4.3. 53 Pressure Drops for Experiment C-3

Discussion of Results

For this experiment, 92% of the oil recovery was obtained before 1.5PV of the chemical injection, indicating a robust experimental design and successful displacement of the oil. The viscosity of effluents and salinity of effluents reached to that of the polymer drive after 2.5 PV of injection. This retardation was an indication of a narrow negative salinity gradient. Despite the fact that dilution tests showed Type I behavior at and near the selected salinity of the polymer drive, during the core flooding, Type I behavior in the effluent was delayed. This result was attributed to the long Type III behavior inside the core. In addition to the pre-flushing the core at optimum salinity for the water flood, the polymer flood at a salinity close to the optimum salinity was injected after the surfactant slug, and caused a retardation in forming Type I behavior. Another plausible reason for that delay can be the core heterogeneity which

can be explained by tracer test. After almost 2PV of injection, the resident brine could totally be displaced by the injecting brine due to the heterogeneity of the core.

Although, the emulsion production continued up to 2.6PV, most of the surfactants were produced before 2.5PV of injection. The surfactant concentration of effluents were measured by HPLC, and the surfactant retention was estimated as 0.18mg/g-rock, which was considered to be low for an SP formulation without alkali.

Furthermore, the formulation F5 was tested with 1wt% NaPA in surfactant slug to observe the effect of NaPA on surfactant retention. NaPA was previously observed to be useful in terms of diminishing the retention of surfactant, but these experiments were only single phase dynamic experiments. The behavior of NaPA was also tested in the presence of oil in the next experiment (experiment C-4).

4.4.4. Oil Recovery Experiment C-4

Formulation F5 with 1wt% NaPA was used in this experiment to determine the surfactant retention in the presence of oil and measure the oil production in Berea outcrops. The core was prepared as described in Chapter III, after the core's dimensions and mass were noted. The core was initially saturated with 2wt% KCl at 40°C. For this experiment, the pressure drop data was only observed throughout the core, sectional pressure drops could not observed due to the lack of experimental set up.

Table 4.3. 44 Core Properties for Experiment C-4

C-4		
Core Properties		
Core Name	**KLM**	
Rock Type	**Sandstone**	
Est. k	**100**	**md**
Diameter	**1.49**	**inch**
Length	**30.23**	**cm**
Mass	**726.75**	**g**
Bulk vol.	**340.02**	cm3
Porosity	**0.1973**	
Area	**11.25**	cm^2
PV	**66.04**	**ml**
Temperature	**40**	°C

Tracer Test and Brine Permeability

2wt%KCl was injected at different ratios (1ml/min, 2ml/min and 3ml/min) to determine the brine permeability at 40℃ when the flow reached steady state. Afterwards, 5.3wt% NaCl tracer brine was injected to determine the pore volume of the core. The tracer brine broke-through at 0.6PV of injection, and it took 1.7PV of injection to reach its maximum value. This shows that the core was not very homogeneous core and the pore volume determined to be 66ml. The average brine permeability at 40℃ was calculated as 154mD.

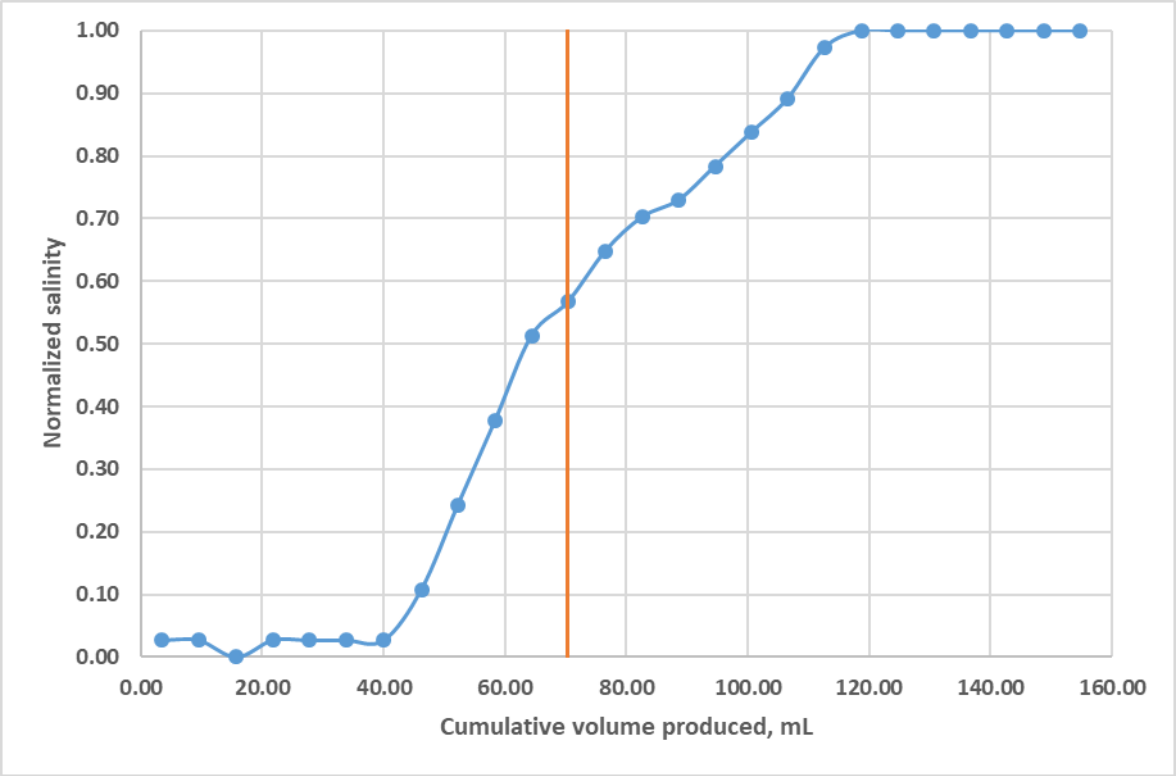

Figure 4.3. 54 Normalized Salinity Tracer for Experiment C-4

Oil Flood

The core was oil flooded at 40°C. The oil wass filled into a piston accumulator and displaced by pumps at 200psi without BPR. Injection of the oil continued until the oil cut was nearly zero. When water saturation reached to residual value, the oil injection was continued to determine the oil pressure drop at steady state and determine the end point oil relative permeability k_{ro}^{o} (1.0). By volume balance, S_{oi} was estimated to be 0.68.

Water Flood

5.3% NaCl was injected as water flood at 2ft/D (0.1ml/min) until the oil cut was less than 1wt%, and the pressure drop reached steady state. The pressure drops at steady state was

used to estimate the end point water relative permeability k_{rw}^{o} as 0.13. S_{orw} was calculated to be 0.20 (Table 4.3.45)

Table 4.3. 45 Summary of Brine Flood, Oil Flood and Water Flood permeability and Relative Permeability for Experiment C-4

	Average Brine Permeability @40°C	**Average Oil Permeability @40°C**	**k_{ro}^{o}**	**Average Water Permeability @40°C**	**k_{rw}^{o}**
Whole	154.51	237	1	6	0.03696

Table 4.3. 46 Summary of Oil Flood and Water flood for Experiment C-4

Oil Flood		**Water Flood**	
k_{ro}^{o}	1.0	**k_{rw}^{o}**	0.037
S_{oi}	0.68	**S_{orw}**	0.33

Mobility Control

At the end of the water flood, the required minimum viscosity for a stable displacement was designed by using the total mobility curve. The inverse of minimum mobility was estimated and set as the minimum viscosity for the chemical slugs with safety factor 1.2. The value of 2.5 was used for both oil and water exponents to calculate the minimum total mobility of the oil bank. Thus, required the minimum viscosity of chemical slug was determined to be 70cp. See Table 4.3.46 for the parameters used in this calculation.

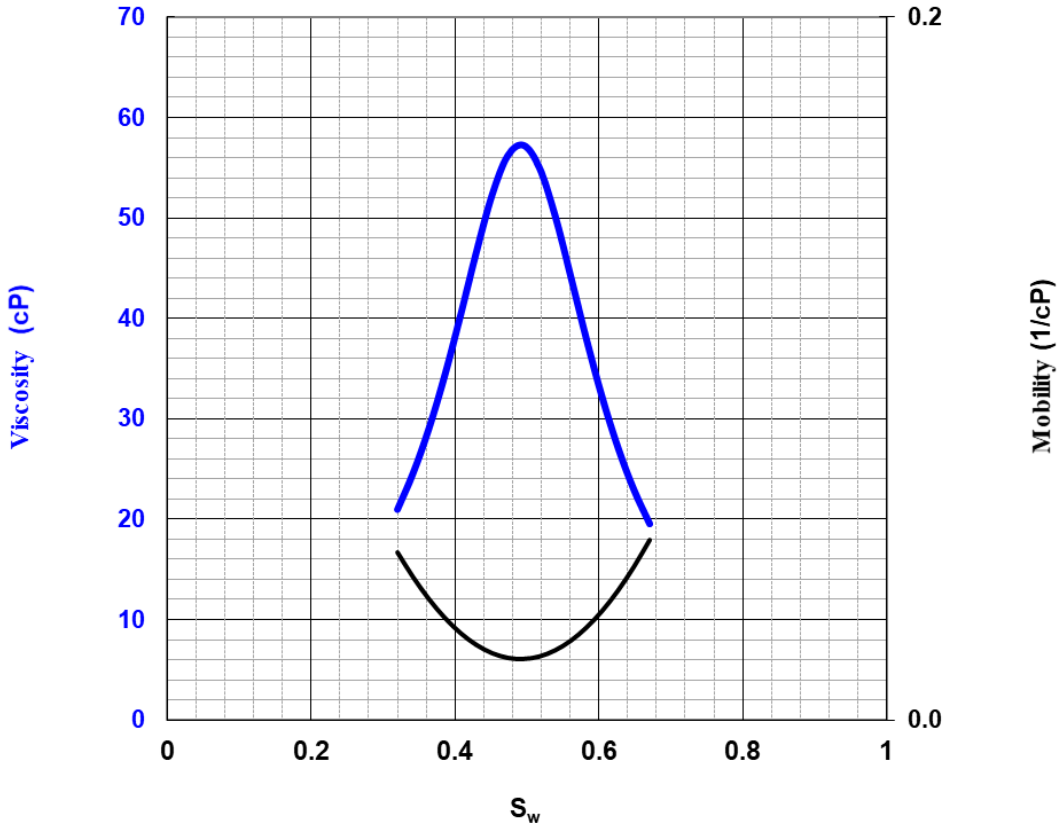

Figure 4.3. 55 Total Relative Mobility Curve for Experiment C-4

Table 4.3. 47 Total Relative Mobility Curve Parameters for Experiment C-4

k_{rw}^{o}	0.037	
k_{ro}^{o}	1.00	
n_w	2.5	
n_o	2.5	
S_{wr}	0.32	
S_{or}	0.33	
m_w	0.72	cP
m_o	21	cP

The equivalent shear rate in the core was estimated to be 13.40 s^{-1} when n is 0.6 and C is 3. The constant C was kept high here because of the failure of experiment C-1. Higher C constant caused higher equivalent shear rate calculation which is an also additional safety precaution to obtain a robust displacement. Viscosity of chemical solutions were tested with different concentrations of polymer FP3330S, and with 5250ppm, the required viscosity was obtained at the target shear rate.

Chemical Flood

The SP slug and the polymer drive were prepared by following the procedure described in Chapter III. Slugs were injected at 1ft/D (0.05ml/min) .The effluents were collected with 5ml in each tube. At the end of the flood, the effluents were analyzed for the surfactant retention, pH, viscosity and salinity.

Table 4.3. 48 Surfactant slug and polymer drive properties for Experiment C-4

	Surfactant Slug	**Polymer Drive 1**	**Polymer Drive 2**
PV Injected	0.5	2.5	1
Polymer	FP 3330S	FP 3330S	FP 3330S
Polymer Concentration (ppm)	5250	5250	5000
Frontal Velocity (ft/D)	1	1	1
Salinity (ppm TDS)	80	3.7	2.5
pH	7.73	7.55	7.35
Viscosity at 10 s^{-1} & 40°C	65	69	71

Chemical Flood Results

The chemical flood was continued for an additional 0.5PV after 2.5PV of chemical solution injection, due to the observed continuing emulsion production. Before the injection was stopped, the collected effluents were analyzed after centrifuging them for 10mins at 2000rpm and room temperature, and the amount of oil collected was determined as ~85%ROIP with a S_{orc} of 0.047. However, at the end of the 3PV of chemical injection, the last effluent samples were still not at the polymer drive viscosity and salinity. To be able to produce all the surfactants and reach the polymer drive conditions, 2PV of an additional polymer drive at lower salinity was injected. The target here was to determine if the produced amount of surfactant after 2.5PV was detectable, and to observe if additional oil production was possible.

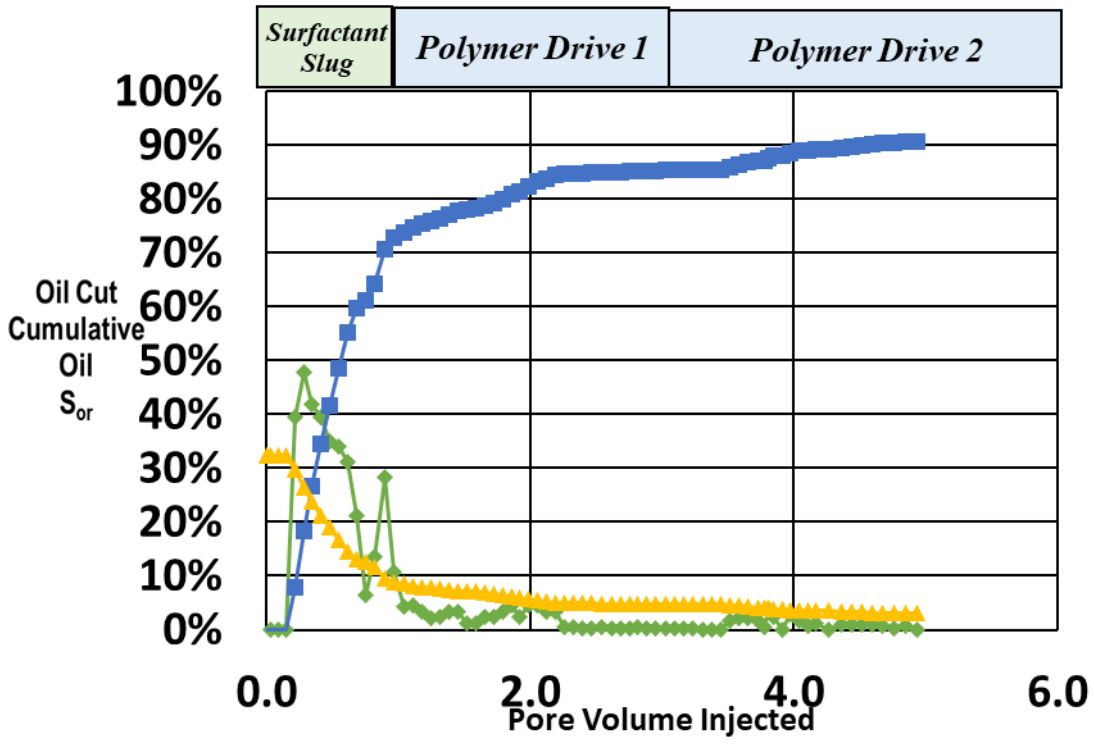

Figure 4.3. 56 Oil Recovery for Experiment C-4

The effluent surfactant concentration was measured by HPLC and the surfactant retention was determined to be 0.11mg/g-rock (75wt% of the injected surfactant was recovered). The surfactant break thorough was observed at 0.5PV and reached the peak at 1.1PV. The surfactant production continued for 5PV of injection due to the heterogeneity of the core. 55wt% of surfactants produced until 3PV of injection (Figure 4.3.60).

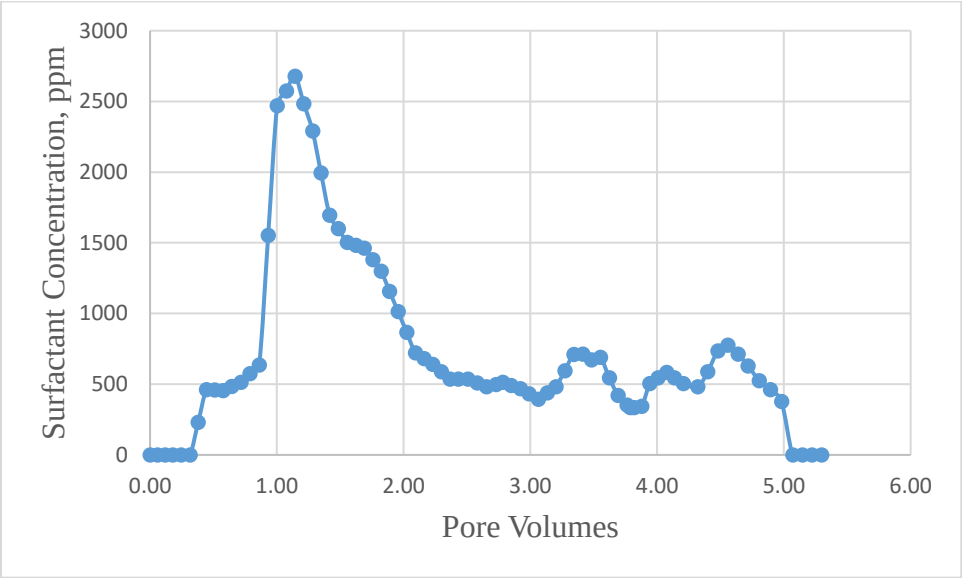

Figure 4.3. 57 Effluent Surfactant Concentration for experiment C-4

The salinity propagation was determined using a refractometer. The effluent salinity broke-through decreasing at 0.5PV of injection and increased to 75,000ppm as surfactant slug injected and after ~1PV of injection, started decreasing. The effluent salinity reached to the first polymer drive salinity after 1.3PV of chemical injection and continued decreasing as the polymer drive-2 was injected and effluents reached PD-2 conditions after 1.5PV of injection.

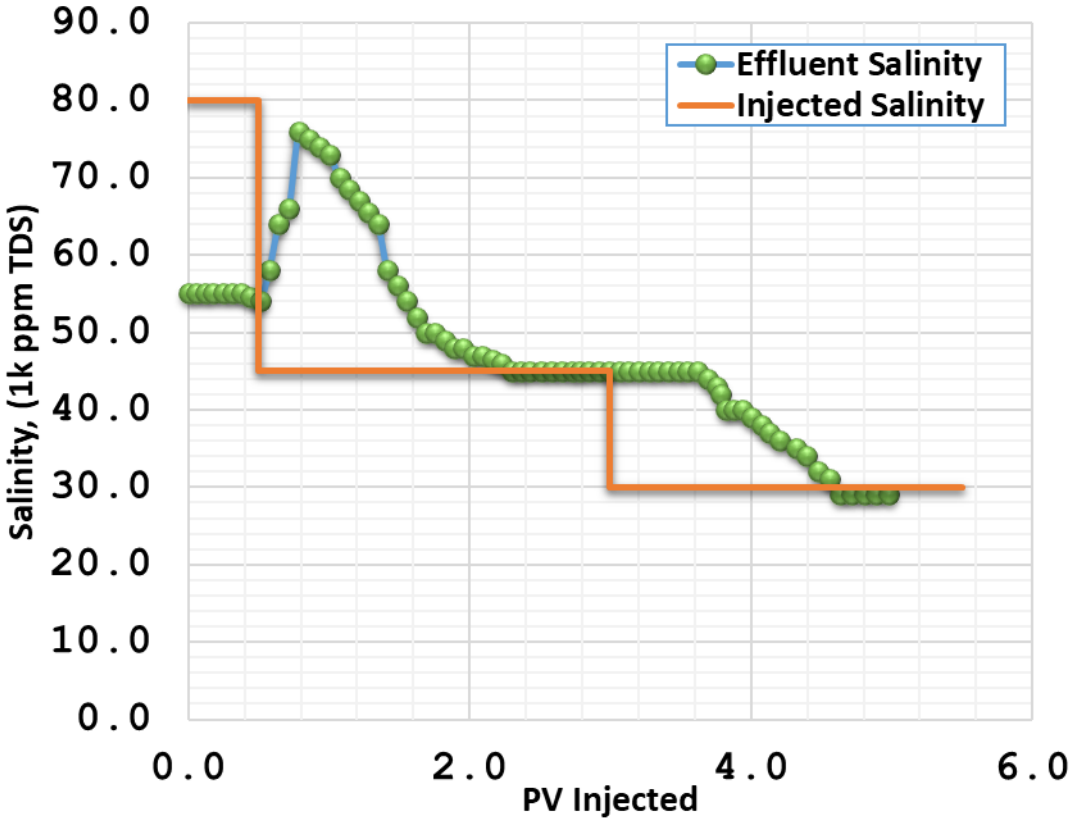

Figure 4.3. 58 Chemical Flood Effluent Salinity for Experiment C-4

The effluent pH was measured and compared to the pH of injected solutions. The pH of injected chemical solutions were arranged to be neutral, prior to the flood. The pH of effluents were slightly higher than the injected pH; however, it was still within the neutral pH range.

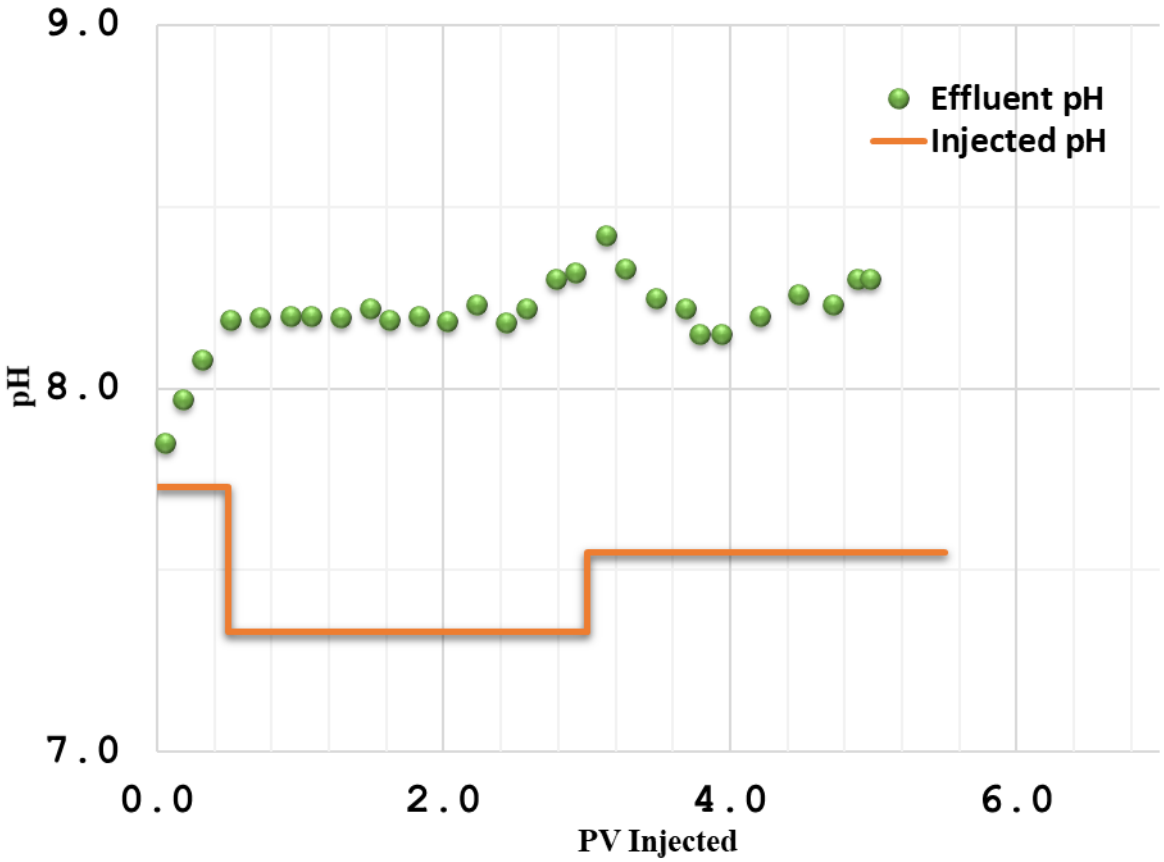

Figure 4.3. 59 Chemical Flood Effluent pH for Experiment C-4

The viscosity of effluents began increasing at 0.4PV of injection, and within the error range, reached the PD2 viscosity after 4PV of injection. This showed that viscosity retarded throughout the core and mobility did not controlled efficiently.

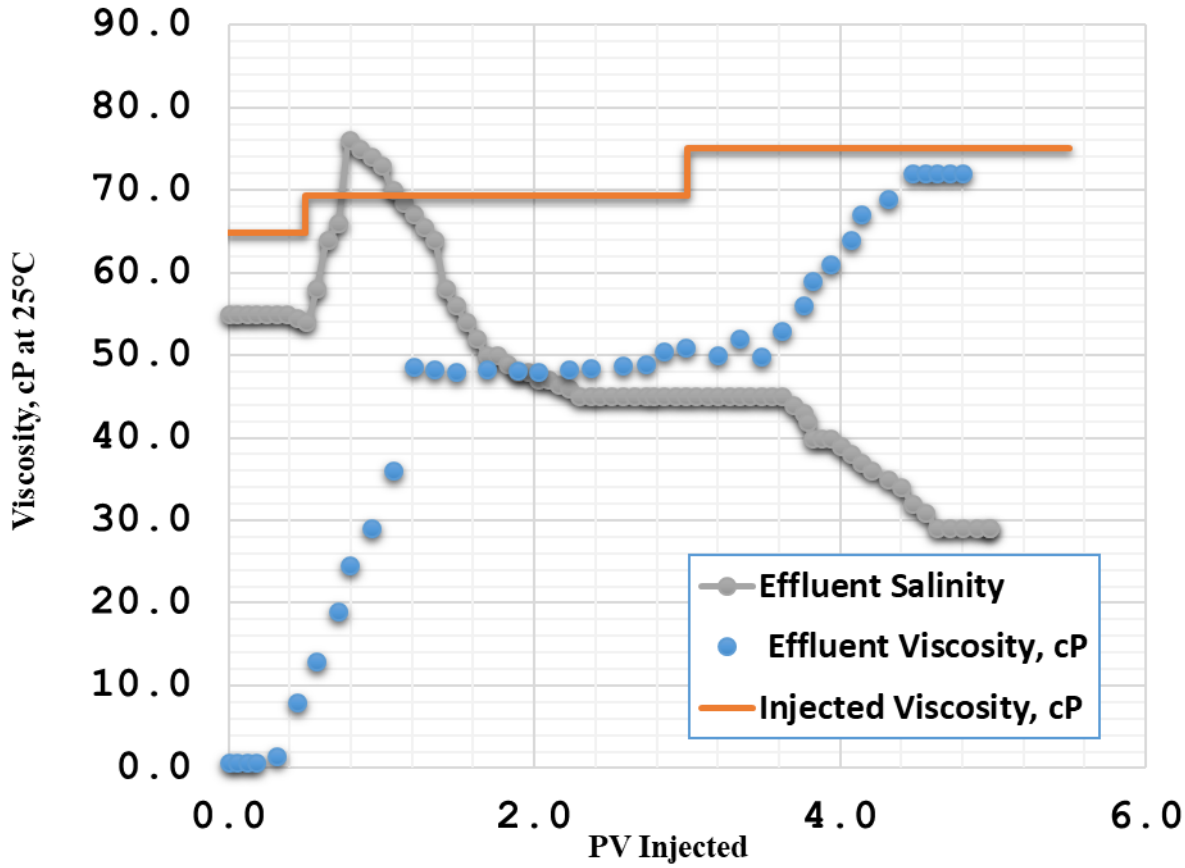

Figure 4.3. 60 Chemical Flood Effluent viscosity for Experiment C-4

Based on the pressure drop data, there was no plugging observed and the pressure drop reached steady state after 1PV of chemical injection. The pressure drop at the beginning increased as both the high viscosity of chemical slug injection and the oil displacement through the core. After 3PV of injection, PD-2 was started, and the fluctuation in pressure drops was caused by stopping the injection for a short time and connecting the PD-2, which was not a part of design at the beginning of the flood. The reason of the increase in the pressure drop after injection of PD-2 was accounted for slightly higher viscosity of PD-2 than the surfactant slug and PD-1. Besides that, after injecting PD-2, oil production was observed and produced amount of oil increased to 91% of residual oil with S_{or} 0.03.

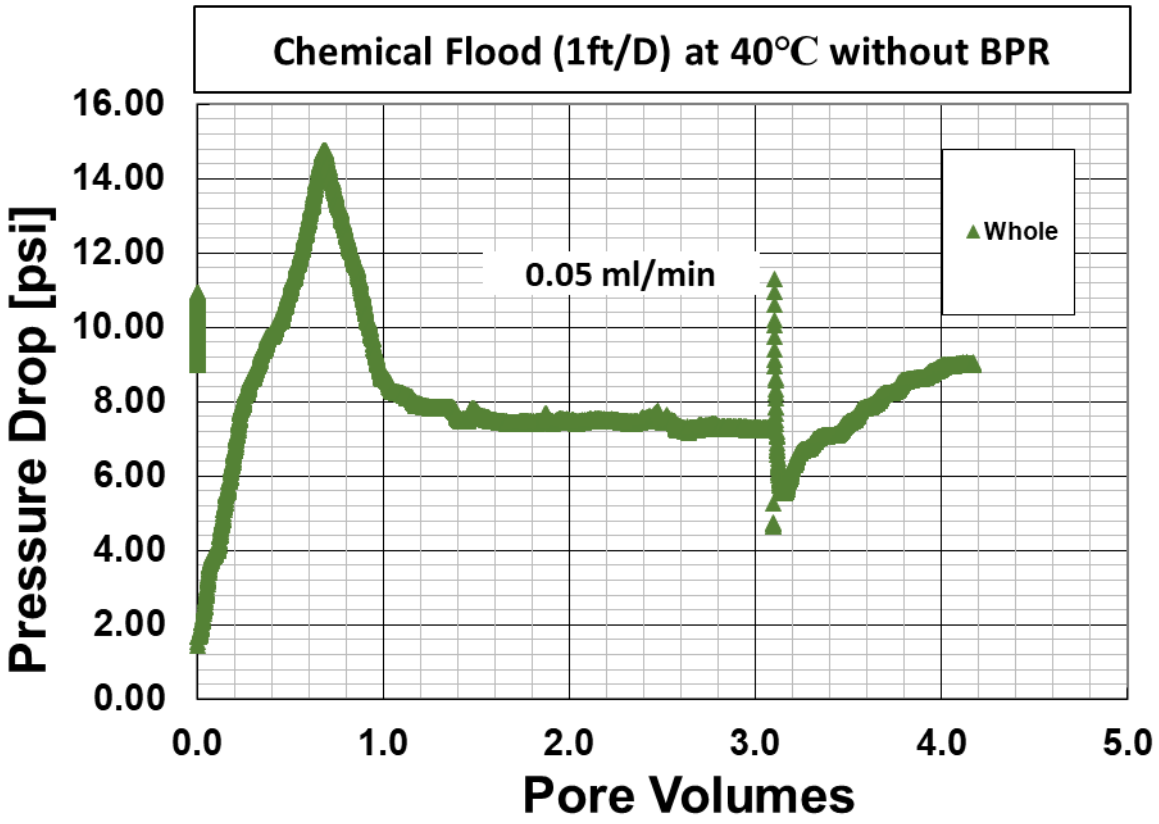

Figure 4.3. 61 Pressure Drops for Experiment C-4

Discussion of Results C-4

At the end of this experiment, total oil recovery was 91wt% of the residual oil with 3wt% of irreducible oil saturation. The chemical flood continued for 4.3PV with 0.5PV of surfactant slug injection. Even though, the viscosity propagated ineffectively throughout the core, most of the oil was produced until 1.5PV of chemical injection. At 1.5PV of injection, oil production was 82% of residual oil and at the end of 2.5PV of injection, the recovery reached to 85% with 4.7% of irreducible oil saturation. The oil recovered after 2.5PV of injection and the long tail of emulsion production were attributed to the narrow negative salinity gradient. Even though, in this experiment, PD-1 was designed with a lower salinity than S-9, which was designed with the same formulation including the same amount of NaPA, it was still not

enough. With a PD with salinity of 2.5wt% NaCl, this problem could have been solved, but that would also decrease the time for Type III behavior inside the core, and that would cause less oil production. Additional impact for that retardation could be the core heterogeneity, even though this was not a problem for most of the Berea outcrop sandstones, in this experiment it can be clearly observed by the early break-through of viscosity, pH and salinity. Considering both plausible reasons, oil production retardation could have been prevented with a higher viscosity and lower salinity of PD. Despite that poor viscosity and salinity propagation throughout the core, this chemical flood was considered as an efficient recovery experiment due to the high oil recovery and low surfactant retention.

4.4.5. Oil Recovery Experiment RC (C-5)

The purpose of this experiment was to measure the oil recovery and surfactant retention using the SP formulation F5 in sandstone reservoir core.

The composite core comprised of three core plugs that were obtained from the different parts of the reservoir. The core length was ~21cm in total and completed to ~1ft length with an additional plastic piece. After the core's dimensions and mass were measured the core was placed inside the core holder by aligning the plastic part to be at the top of the core holder (outlet side). During the experiment pressure drops were observed only for the first 3 sections with the last section being the combination of both the plastic part and the top section of the core. After all preparations were completed, the core was initially saturated with 2% KCl at 40°C.

Table 4.3. 49 Core Properties for Experiment RC

RC		
Core Properties		
Core Name	NOP	
Rock Type	Reservoir Sandstone	
Diameter	3.80	cm
Length	21.03	cm
Mass	538.8	g
Bulk vol.	236.58	cm3
Porosity	0.28	
Area	11.25	cm^2
PV	65.22	ml
Length (Section 1)	7.62	cm
Length (section 2)	7.68	cm
Length (section 3)	7.62	cm
Temperature	40	°C

Tracer Test and Brine Permeability

2wt% KCl was injected at different rates to determine the brine permeability at 40°C until the flow reached steady state. Afterwards, 5.3wt% KCl tracer brine was injected to determine the pore volume of the core. The tracer brine broke-through at 0.5PV of injection, and it took almost 2PV for the influent brine to completely displace the in-situ brine. This shows that the core was a very heterogeneous core with a pore volume of 65ml. The average brine permeability at 40°C was calculated as 41.6mD for the core. For the sectional permeability see Table 4.3.46.

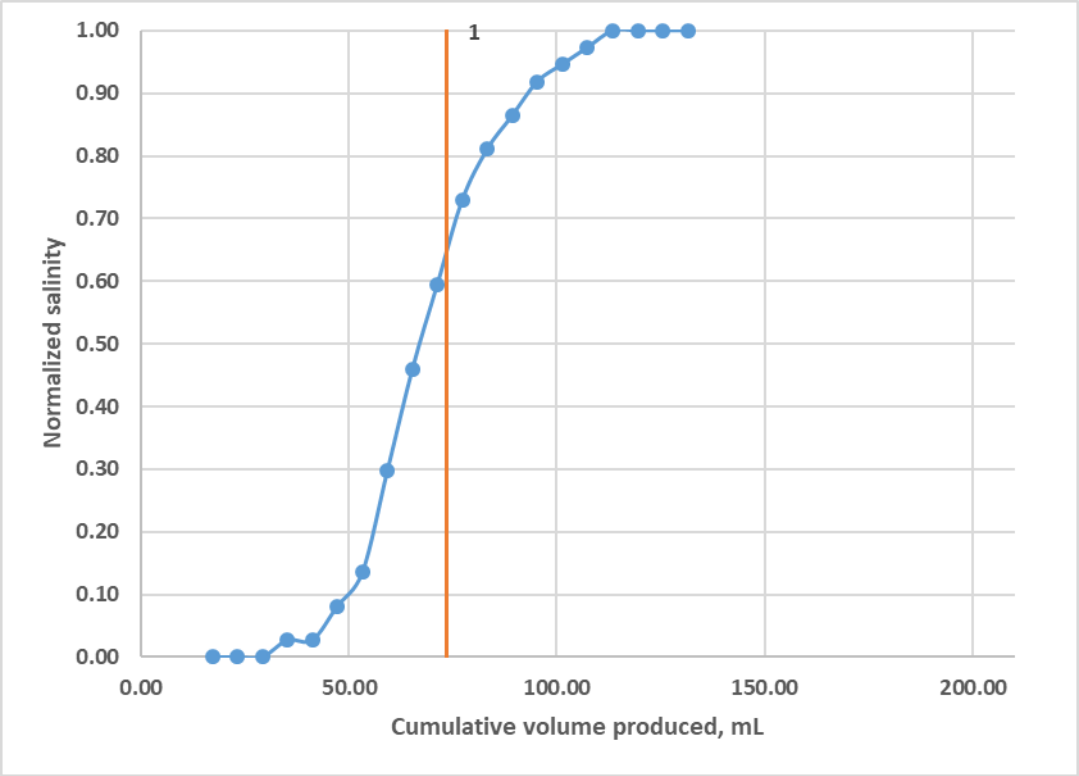

Figure 4.3. 62 Normalized Salinity Tracer for Experiment RC

Oil Flood

The core was oil flooded at 40℃. The oil was filled into a stainless steel column and displaced by argon gas at 120psi. The BPR was set to ~15psi, allowing for a 105psi pressure differential. Injection of the oil was continued until the oil cut was zero. When water saturation reached to the residual value, the oil injection was continued to determine the oil pressure drop at steady state conditions and determine the end point oil relative permeability k_{ro}^{o}, which is 1.0. Using volume balance, S_{oi} was estimated to be 0.57. Due to the high pressure drops through sections, exceeding the sectional pressure transmitters' detection limit, sectional pressure drops could not observed.

Water Flood

Due to the narrow Type III region of the formulation, the core was just pre-flushed with the optimum salinity (5.3wt% NaCl). Injection of water flood brine was continued at 2ft/D (0.1ml/min) until the oil cut was less than 1% and the pressure drops reached steady state. The pressure drops at steady state were used to estimate the end point water relative permeability k_{rw}^{o} as 0.09. S_{orw} was calculated to be 0.13.

Table 4.3. 50 Summary of Brine Flood, Oil Flood and Water Flood permeability and Relative Permeability for Experiment RC

	Average Brine Permeability @40°C	**Average Oil Permeability @40°C**	**k_{ro}^{o}**	**Average Water Permeability @40°C**	**k_{rw}^{o}**
Whole	42	73.64	1	4	0.09
Section1	19	-	-	2	0.09
Section2	250	-	-	32	0.13
Section3	38	-	-	53	1.37

Table 4.3. 51 Summary of Oil Flood and Water flood for Experiment RC

Oil Flood		**Water Flood**	
k_{ro}^{o}	1	**k_{rw}^{o}**	0.08
S_{oi}	0.57	**S_{orw}**	0.13

Mobility Control

At the end of the water flood, the required minimum viscosity for a stable displacement was designed by using the total mobility curve. The inverse of the minimum mobility was estimated and set as the required minimum viscosity for chemical slugs. Due to the low average permeability of the reservoir core, for the safety factor of 1.5 was used instead of 1.2; thus the

chemical flood viscosity was designed to be more than 63cp. See Table 4 for the parameters used in this calculation.

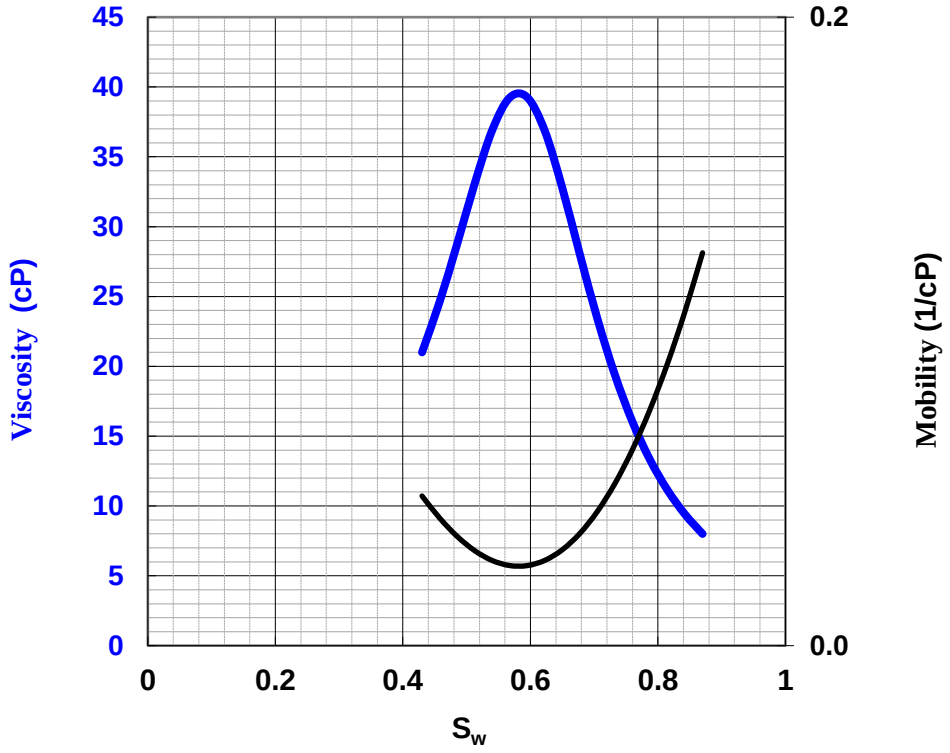

Figure 4.3. 63 Total Relative Mobility Curve for Experiment RC

Table 4.3. 52 Total Relative Mobility Curve Parameters for Experiment RC

k_{rw}^{o}	0.080	
k_{ro}^{o}	1	
n_w	2.5	
n_o	2.5	
S_{wr}	0.43	
S_{or}	0.13	
μ_w	0.72	cP
μ_o	21	cP

The equivalent shear rate in the core was estimated to be $20.52s^{-1}$ where n is 6 and C was 2. Viscosity of SP slug was tested with different concentration of FP3330S after shearing the 1wt% of polymer FP3330S for 6mins. Polymer concentration of 6000 ppm was estimated to be the necessary concentration to satisfy the required viscosity for the coreflood experiment at the target shear rate.

Chemical Flood

Surfactant slug was prepared at optimum salinity 5.3wt% NaCl while the first polymer drive was prepared at 4wt% NaCl in order to keep the Type III behavior longer as experiment C-3, which has been done under same conditions with Berea outcrop. Since experiment C-3 was an effective chemical flood because of the long optimum salinity period, in this experiment the same effect was targeted by keeping the PD-1 salinity high. On the other hand, in order to prevent the long tail of emulsion production and produce all displaceable surfactant earlier, an additional PD was designed to be injected after 1PV injection of PD1 at lower salinity (2.5wt% NaCl). Slugs were prepared and filtered through filter papers in the micron size of 0.4, 0.2, 0.1 and 0.4 respectively. Surfactant slug was filtered successfully through 0.1μm filter paper while PD1 and PD2 did not go through and plugged after 20ml of filtration with loosing almost 85wt% of its original viscosity because of their lower salinity, and higher viscosity. Therefore, PD1 and PD2 did not filtered through 0.1μm filter papers, but to ensure that the polymer drive solutions can go through 20mD of core section without any plugging, the PD1 filtered twice through 0.2μm filter paper and it was observed that it lost the 35wt% of its original viscosity with second time of filtration through 0.2μm. Thus, PD2 was filtered via 0.2μm filter paper for only once. Subsequently, all chemical solutions filtered through 0.4μm filters just to ensure that filtration ratio of <1.2 was obtained for each solution. After argon bubbling and degassing, the injection of chemicals was started at ~0.65ft/D (0.03ml/min) at 40℃. The effluents were

collected with the fraction of 5ml. At the end of the flood, the effluents were analyzed for the surfactant retention, and the effluent pH, viscosity and salinity.

Table 4.3. 53 Surfactant Slug and Polymer Drive Properties for Experiment RC

	Surfactant Slug	**PD-1**	**PD-2**
PV Injected	0.5	1	2
Polymer	FP 3330S	FP 3330S	FP 3330S
Polymer Concentration (ppm)	6000	6000	5500
Frontal Velocity (ft/D)	1	1	1
Salinity (ppm TDS)	72	50	31
pH	6.96	8.32	8
Viscosity at 21 s^{-1} & 40°C	55	40	57

Chemical Flood Results

At the end of the experiment, the effluents were analyzed visually for oil recovery after centrifuging them for 10mins at 2000rpm at room temperature. Amount of oil collected was determined to be ~83wt% with S_{orc} 0.022.

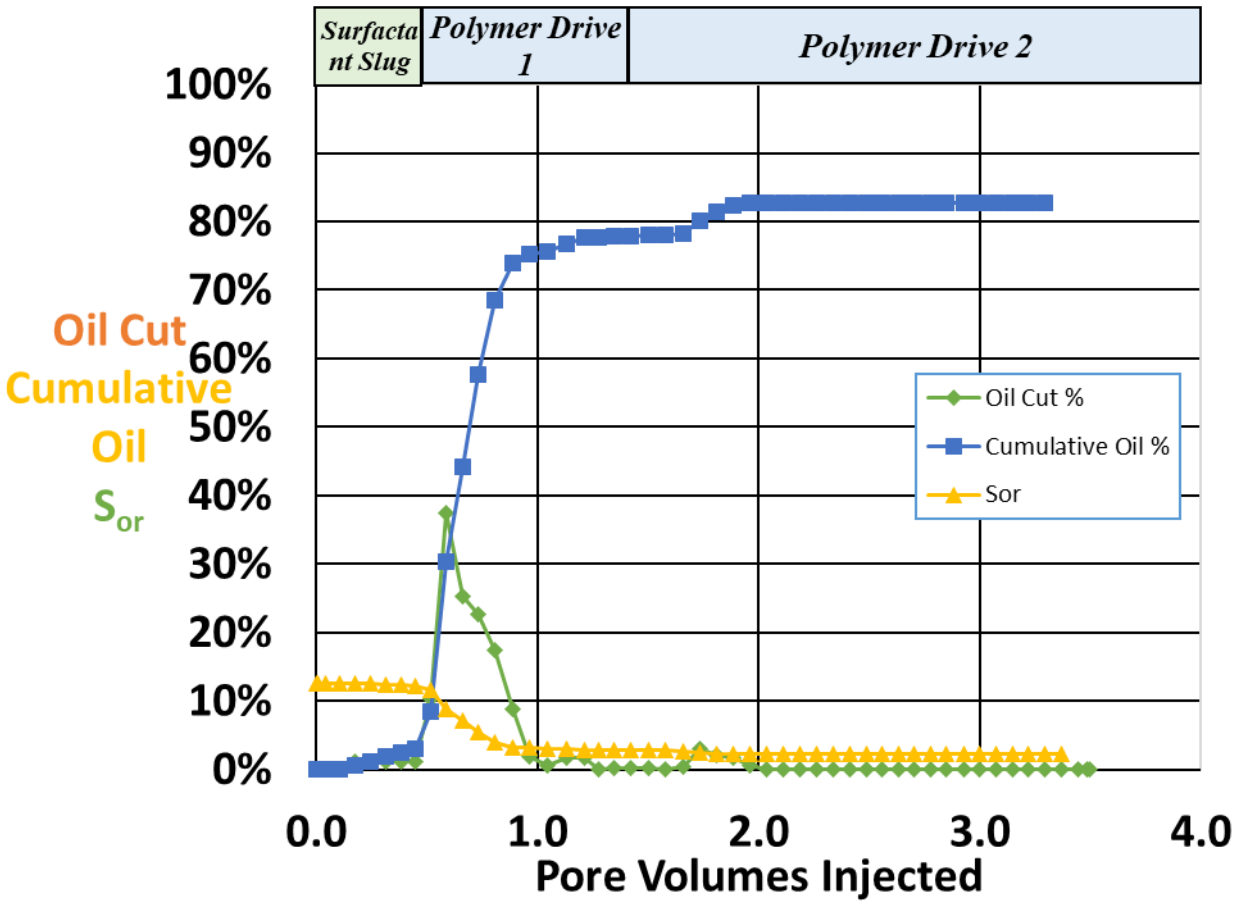

Figure 4.3. 64 Oil Recovery for Experiment RC

The effluent surfactant concentration was measured by HPLC and the surfactant retention was determined to be 0.27mg/g-rock. The surfactant break-thorough was observed at 0.5PV and reached the peak value at 1.8PV and 2.3PV, and continued producing up to 3.5PV because of continuous emulsion production towards the end of the experiment. Due to the unstable displacement, being caused by lower viscosity of PD1 than surfactant slug (SS), surfactant production was more gradual. By injecting higher viscosity of PD-2 resulted in a damage control, sweeping the surfactant and displacing the trapped surfactant from the rock matrix more effectively.

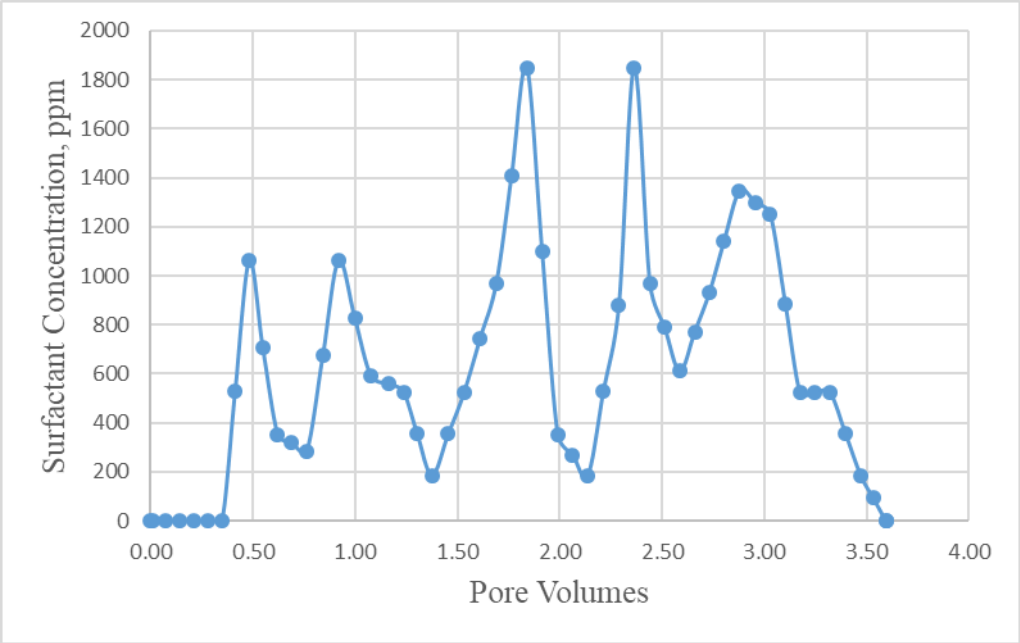

Figure 4.3. 65 Effluent Surfactant Concentration for Experiment RC

The salinity propagation was determined using a refractometer. The effluent salinity broke-through after 1PV of injection and decreased as the polymer drive at lower salinity injected. Effluents reached Type I condition (the polymer drive salinity) after 2.5 PV of chemical injection.

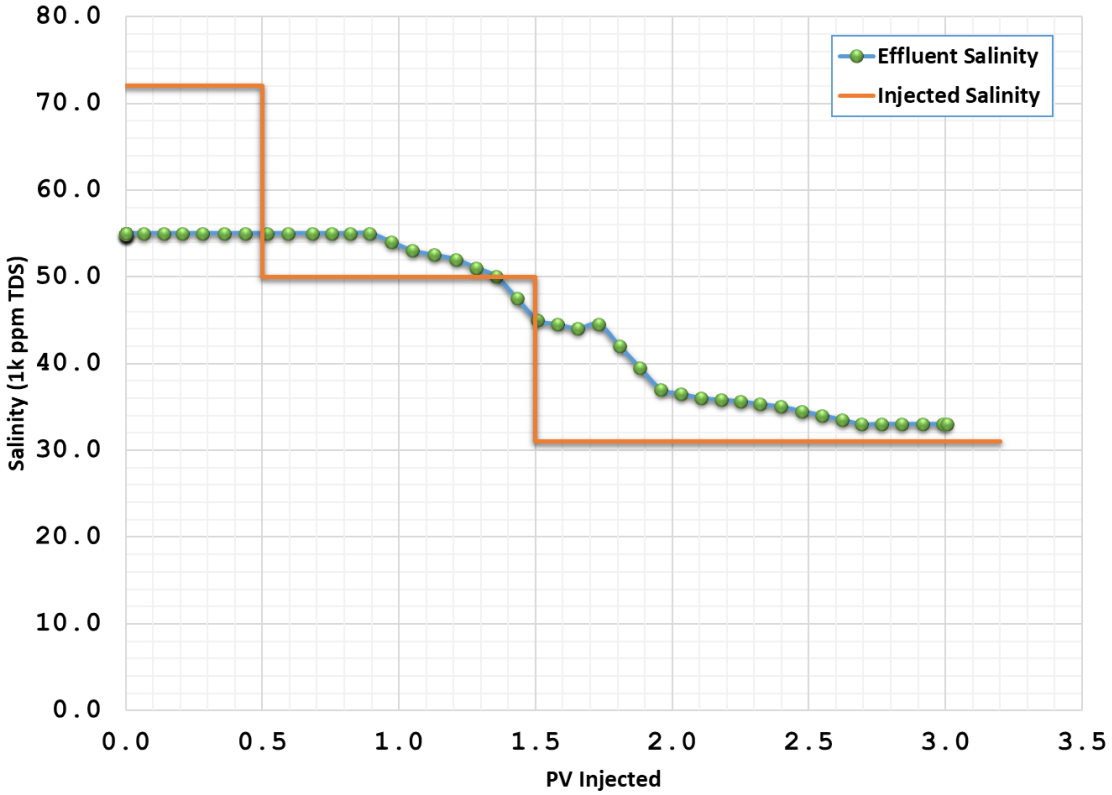

Figure 4.3. 66 Chemical Flood Effluent Salinity for Experiment RC

The effluent pH was measured and compared to the pH of injected solutions. The pH of injected chemical solutions were almost same as injected fluids and stayed neutral all along the chemical flood.

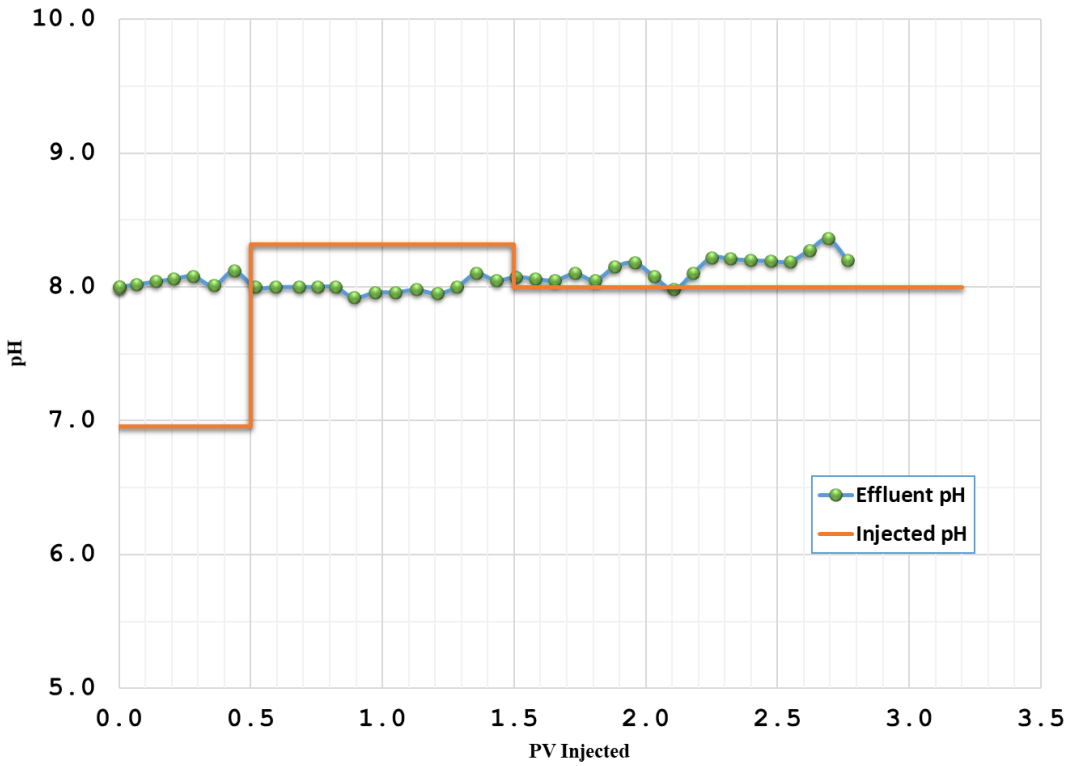

Figure 4.3. 67 Chemical Flood Effluent pH for Experiment RC

Injected viscosity was lower than the targeted viscosity (63cp) due to the loss of viscosity during filtration. However, still slugs were meeting the requirement of minimum viscosity of 42cp without any safety factor. Viscosity degradation was not observed in the core;

however, because of low viscosity of PD1, viscosity propagation was poor and effluents reached the polymer drive conditions at 3PV of injection

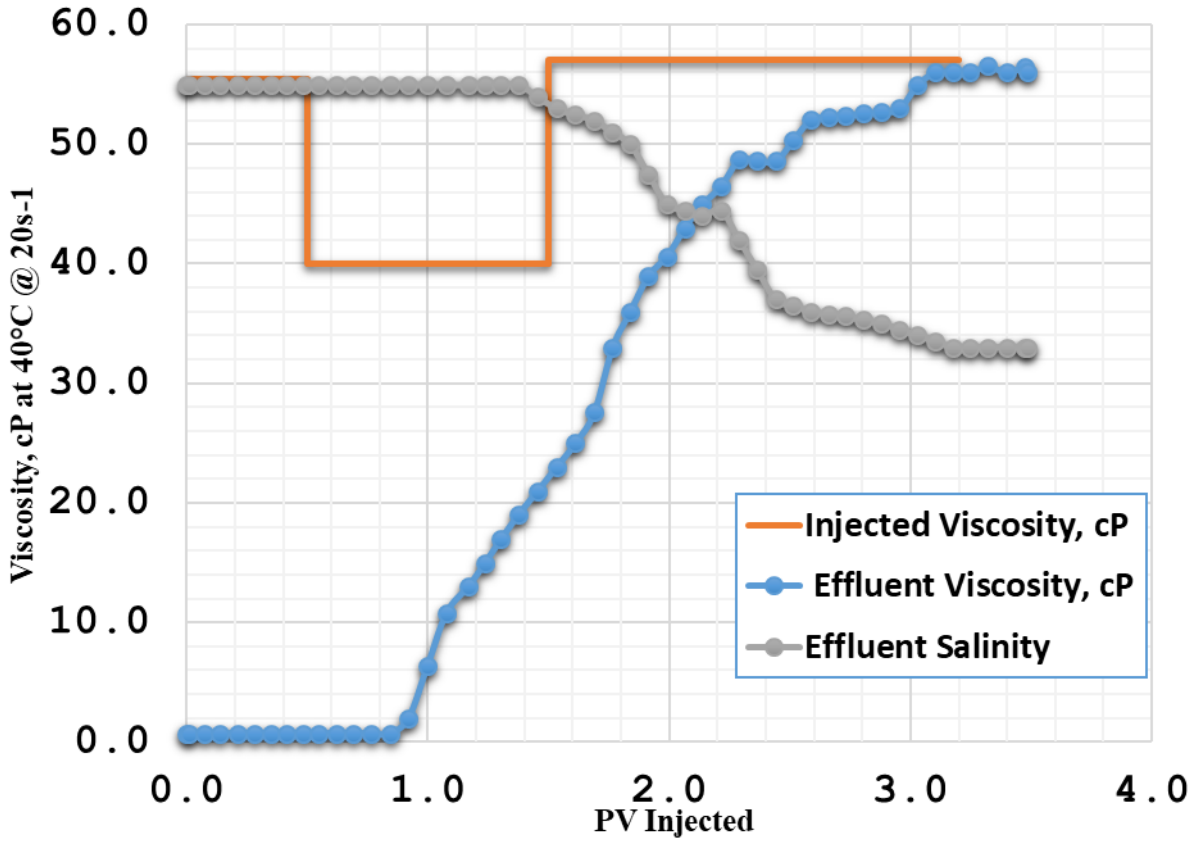

Figure 4.3. 68 Chemical Flood Effluent viscosity and salinity for Experiment RC

No plugging were observed along the core from the steady state pressure drops. During the chemical flood, the pressure drop reached steady state after 2PV of the chemical injection. The pressure drop at the beginning increased due to the high viscosity of the chemical slug injection and the oil displacement through the core. The sectional pressure drops also increased respectively as high viscosity chemical solutions displaced the water flood brine and displaced the oil bank. Figure 9 shows the sectional pressure drop data.

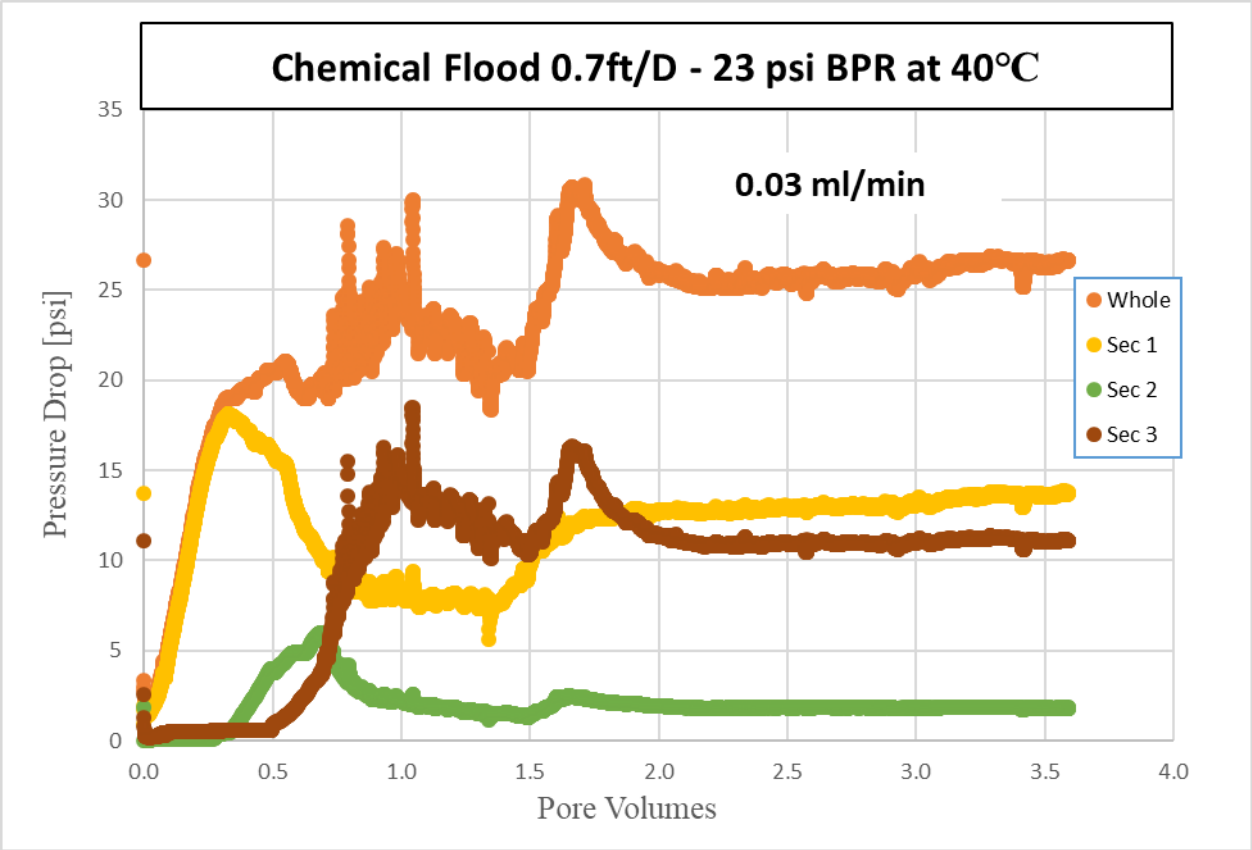

Figure 4.3. 69 Pressure Drops for Experiment RC

Discussion of Results

Despite the high viscosity requirement for a very low permeability, challenging reservoir core, transportation of chemical solutions were efficiently achieved. However, low viscosity of PD1 caused some instability in polymer transportation. The second peak observed in whole pressure drop was attributed to that instability, which was adjusted by the injection of a higher viscosity of PD2. As expected, as soon as PD2 was injected, the effect of the high viscosity was observed through higher pressure drop in section 1. However, from the sectional pressure drops it was also observed that section 2 and section 3 pressure drops were also increasing as PD2 started being injected. Since, it is not plausible for PD2 to reach section 2

and 3 that suddenly, the reason of that increasing pressure drop was questionable. Thus, it was hypothesized that the increase in the pressure drops for section 2 and 3 was caused by displacing the SS which was fingered by lower viscosity of PD1. Very likely, the surfactant slug was fingered by PD1 as it was injected with considerable amount of viscosity difference between two solutions. However, this damage was successfully controlled by the injection of PD2.

Regarding the oil production, the amount of the oil left behind after the water flood was 13wt% of OOIP and with the chemical flood it was decreased to 2.2wt% of OOIP with 83wt% of the residual oil being produced. The oil production was completed before 2PV of chemical injection, so the flood was considered as a successful chemical flood. On the other hand, the surfactant retention (0.26-0.28mg/g-rock) was found to be relatively high, however, for a real reservoir rock with very low permeability of two sections (section 1 ~20mD, Section 3 ~38mD) and in the absence of alkali, the retention of surfactant was found to be low.

In overall, despite the fact that polymer transport could have been designed better and transported more efficiently, and with all unknowns including the pore throat size of the core and the transportability of the low permeability sections, the experiment was successful. The experiment was considered as a successful tertiary chemical flood with high oil recovery and acceptable amount of surfactant retention. See Table 4.3.54 for the summary of oil recovery experiments.

Table 4.3. 54 Summary of oil recovery experiments

CF Experiments	Core Permeability, mD	Formulation used	Oil Recovery, %	Sorc	Surfactant Retention, mg/g-rock
C-1	168	F-1	48	0.14	0.31
C-2	264	F-2	63	0.18	0.1
C-3	208	F-5	92	0.025	0.2
C-4	154	F-5+1%NaPA	91	0.03	0.11
C-5 (RC)	42	F-5	83	0.022	0.27

Chapter 5: Summary and Conclusions

Summary

Surfactant formulations were developed (in the absence of alkalis) via phase behavior tests. A systematic series of experiments were conducted to determine the adsorption and retention of the surfactant formulations with and without oil.

First, formulations were examined through the static adsorption tests. Static adsorption tests results showed that formulations with novel surfactants (F1 & F4) gave higher adsorption than conventional surfactants (F2 & F3). Formulation F5 (conventional formulation) shows the highest adsorption of all formulations. Formulations were tested at their optimum salinities in order to compare them with single phase dynamic and coreflood experiments. Since, salinity has a considerable impact on static adsorption, the comparison between formulations here may not be applicable. Overall, the adsorption values are consistent to formulations' salinity (higher salinity, higher adsorption). However, for formulation F5 the adsorption value is relatively higher than others, which is attributed to the uncertainties of the crushed rock samples. Even though, crushed Berea was properly mixed to uniform the distribution of the clay particles inside, still the representability of 2 grams of crushed rock is questionable. Therefore, to be able to determine the adsorption/retention properties of formulations comprehensively, single phase dynamic and coreflood experiments were conducted. On the other hand, in the presence of NaPA, up to 40% lower adsorption was observed for each formulations. Thus, the impact of NaPA on surfactant adsorption was also further examined through corefloods with and without oil.

Single phase dynamic experiments were conducted in the absence of oil, with and without NAPA. In the experiments without NaPA, overall the surfactant retention was about

0.22mg/g-rock for the novel surfactants while it was lower (~0.18mg/g-rock) for the conventional surfactant mixtures. For Single Phase Flood (SPF) experiments, the polymer concentrations were kept at a very low value to allow surfactants to adsorb onto the Berea sandstone during the flood (as higher concentration of polymer would sweep more efficiently and produce most of the surfactants). At the end of SPF dynamic experiments, a new set of experiments with NaPA was designed to observe its effect on surfactant retention. Formulation F1 (the novel surfactant system with oil O-1), F2 (the conventional surfactant system with oil O-1) and F5 (the conventional surfactant with oil O-2) were chosen for that test. Even though, the usage of NaPA did not cause much changes in formulation F1 (experiment SN-1), it caused about 40% lower surfactant retention with formulation F2 (experiment SN-2) and 90% lower surfactant retention with formulation F5 (experiment SN-3). A possible reason for the obtained high retention for formulation F1 (experiment SN-1) can be the high clay content of the core. Despite the given XRD data, the amount of clay in each core is not the same.

To determine the surfactant retention in the presence of the oil, corefloods were performed with and without NaPA for formulation F1, F2 and F5. Coreflood C-1 (with formulation F1) resulted in a poor oil recovery and so that higher surfactant retention (0.3mg/g-rock). This high retention was attributed to the poor oil recovery with Sorc=0.14. Most plausibly, surfactants were trapped in the remaining oil. On the contrary, coreflood C-2 and C-3 resulted in lower retention than the SPF experiments for the same formulations. The surfactant retention was determined to be 0.1mg/g-rock and 0.18mg/g-rock for experiment C-2 and C-3, respectively. The reason for lower surfactant retention for these corefloods can be explained with less surface area of Berea that is in contact with surfactants in the presence of oil. Additionally, high oil recovery causes lower surfactant retention because of the amount of surfactants trapped inside the oil was lower. Besides these reasons, a higher viscosity of

polymer (FP3330S) was used in the core flood experiments C-2 and C-3; due to the stable and robust displacement though the core, most of the surfactants were produced.

Additionally, the effect of NaPA was tested with corefloods in the presence of oil. For that purpose, Formulation F5 with oil O-2 was chosen, due to high oil recovery of the same formulation in experiment C-3. 1% of NaPA was (MW 4500Da) was added to the formulation and experiment was conducted at the same conditions of C-3. The experiment resulted in high oil recovery (Sorc=0.03) and lower surfactant retention of 0.114mg/g-rock.

Furthermore, after successful experiments C-3 and C-4, formulation F5 with oil O-2 was examined in a very low permeability reservoir sandstone. The objective of this experiment was to determine the surfactant retention and oil production properties of formulation F5 in a real reservoir core. The experiment resulted in a high oil recovery (Sorc=0.02) and 0.26mg/g-rock of surfactant retention, which is in an acceptable range for a very low permeability sandstone.

Conclusions

To put it in a nut shell, after all experiments, it was concluded that formulation development is the most important part of all of these experiments. Formulations with high solubilization ratio resulted in higher oil production and lower surfactant retention in coreflood experiments. Conventional surfactants (TDA 13 PO SO_4 & TDA 7PO SO_4) with very similar structure, gave almost the same adsorption in static adsorption tests and in SPF experiments. However, their optimum salinity was different due to their slightly different hydrophobicity. As a more hydrophobic surfactant TDA 13 PO SO_4 has a lower optimum salinity. Also, phase behavior of both surfactant were different. Even though, both of them showed ultra-low IFT, TDA 13 PO SO_4 had a wider Type III range and even lower IFT. With a similar structure but slightly different hydrophobicity TDA 7PO SO_4 and 2EH 7PO SO_4 showed different behaviors

in phase behaviors tests, and resulted in different retention due to their hydrophobicity; while both novel surfactants, CH_3O 21PO 10OE SO_4 and 2EH 7PO SO_4 were showing almost the same retention properties and phase behaviors.

On the other hand, some types of oil behave differently in the rock medium than in borosilicate pipettes. Even though formulations showed ultra-low IFT with oil O-1, the production was very poor. So, after formulation development, it is very essential to test the formulation, in a rock medium via corefloods to have a comprehensive understanding of the phase behavior for the developed formulations.

Tracer tests were a good representative of the heterogeneity of the core and it was concluded that for heterogeneous cores, the chemical flooding design should be done with higher safety factor of polymer viscosity. Also, the narrow negative salinity gradient caused retardation of oil production and delayed Type I salinity, leading to long time of emulsion production. In most of the cases, narrow salinity gradient increased the necessity of more chemicals to be injected to produce both more of the oil and surfactant. Chemical floods should be designed with a wide negative salinity gradient.

The usage of NaPA decreased the surfactant retention in static adsorptions for each formulation. For single phase flood experiments, it mostly decreased the retention of surfactants. However, in the presence of oil the effect of NaPA was not as significant as it was in single phase flood experiments. It is conjectured that due to the oil presence in the core, NaPA could not be adsorbed on to the rock grains.

Recommendations for Future Work

Although this research has examined the SP applications (no alkali), more research is still necessary. This work was performed under the simple conditions (such as no hardness, at low temperature and on Berea sandstones). Further experiments with hardness and in different rocks such as carbonates and other types of sandstones are needed. Berea is a simple rock mostly composed of silicate. In real reservoir applications, phase behavior, capillary effect and all other design parameters will be different. With the scope of this work, more experiments on SP applications, with hard brines at high temperatures and in different types of cores are recommended. Additionally, the usage of NaPA on surfactant retention should be investigated further. With the better understanding of the geochemical interactions that occur in the presence of NaPA, NaPA could be a potential replacement for alkalis. Especially with the need of SP applications in industry, more research should be done on SP formulation development and SP applications to obtain a comprehensive understanding of how SP applications can reduce the cost of chemical EOR both in carbonates and sandstones.

References

Abalkhail, N. A., Liyanage, P. J., Upamali, K. A., Pope, G. A., & Mohanty, K. K. (2019). ASP Flood Application for a High-Temperature, High-Salinity Carbonate Reservoir. *SPE Middle East Oil and Gas Show and Conference*. doi:10.2118/194948-ms

Adkins, S., Arachchilage, G. W., Solairaj, S., Lu, J., Weerasooriya, U., & Pope, G. A. (2012). Development of Thermally and Chemically Stable Large-Hydrophobe Alkoxy Carboxylate Surfactants. *SPE Improved Oil Recovery Symposium*. doi:10.2118/154256-ms

Arachchilage, G. W., Spilker, K. K., Tao, E. B., Alexis, D., Linnemeyer, H., Kim, D. H., . Dwarakanath, V. (2018). Evaluating the Effect of Temperature on Surfactant Phase Behavior and Aqueous Stability to Forecast Optimum Salinity at High Temperature. *SPE Improved Oil Recovery Conference*. doi:10.2118/190249-ms

Becher, P. (1990). Microemulsions and Related Systems: Formulation, Solvency, and Physical Properties (Surfactant Science Series, Vol. 30). M. Bourrel and R. S. Schechter. Marcel Dekker, Inc., New York and Basel, 1988. pp. nil 483. $99.75. *Journal of Dispersion Science and Technology*,*11*(4), 431-432. doi:10.1080/01932699008943264

Bourrel, M., & Schechter, R. S. (1988). *Microemulsions and related systems formulation, solvency, and physical properties* (Vol. 30, Surfactant Science Series). Paris: Éd. Technip. Taylor& Francis

Cannella, W., Huh, C., & Seright, R. (1988). Prediction of Xanthan Rheology in Porous Media. *Proceedings of SPE Annual Technical Conference and Exhibition*. doi:10.2523/18089-ms

Churcher, P., French, P., Shaw, J., & Schramm, L. (1991). Rock Properties of Berea Sandstone, Baker Dolomite, and Indiana Limestone. *SPE International Symposium on Oilfield Chemistry*. doi:10.2118/21044-ms

Dwarakanath, V., Chaturvedi, T., Jackson, A., Malik, T., Siregar, A. A., & Zhao, P. (2008). Using Co-solvents to Provide Gradients and Improve Oil Recovery During Chemical Flooding in a Light Oil Reservoir. *SPE Symposium on Improved Oil Recovery*. doi:10.2118/113965-ms

Flaaten, A. K. (2012). *An integrated approach to chemical EOR opportunity valuation: Technical, economic, and risk considerations for project development scenarios and final decision*(Unpublished master's thesis).

Flaaten, A., Nguyen, Q. P., Pope, G. A., & Zhang, J. (2009). A Systematic Laboratory Approach to Low-Cost, High-Performance Chemical Flooding. *SPE Reservoir Evaluation & Engineering,12*(05), 713-723. doi:10.2118/113469-pa

Ghosh, P., Sharma, H., & Mohanty, K. K. (2018). Development of Surfactant-Polymer SP Processes for High Temperature and High Salinity Carbonate Reservoirs. *SPE Annual Technical Conference and Exhibition*. doi:10.2118/191733-ms

Ghosh, P., Sharma, H., & Mohanty, K. K. (2019). ASP flooding in tight carbonate rocks. *Fuel,241*, 653-668. doi:10.1016/j.fuel.2018.12.041

Green, Don W., and G. Paul Willhite. (2018) Enhanced Oil Recovery. Richardson, Texas: 2nd ed., Society of Petroleum Engineers.

Grigg, R., & Bai, B. (2005). Sorption of Surfactant Used in CO2 Flooding onto Five Minerals and Three Porous Media. *SPE International Symposium on Oilfield Chemistry*. doi:10.2118/93100-ms

Han, M., Alsofi, A., Fuseni, A., Zhou, X., & Hassan, S. (2013). Development of Chemical EOR Formulations for a High Temperature and High Salinity Carbonate Reservoir. *International Petroleum Technology Conference*. doi:10.2523/iptc-17084-ms

Hirasaki, G. J., Miller, C. A., & Puerto, M. (2008). Recent Advances in Surfactant EOR. *SPE Annual Technical Conference and Exhibition*. doi:10.2118/115386-ms

Huh, C. (1979). Interfacial tensions and solubilizing ability of a microemulsion phase that coexists with oil and brine. *Journal of Colloid and Interface Science,71*(2), 408-426. doi:10.1016/0021-9797(79)90249-2

Jang, S. H., Liyanage, P. J., Tagavifar, M., Chang, L., Upamali, K. A., Lansakara-P, D., . . . Pope, G. A. (2016). A Systematic Method for Reducing Surfactant Retention to Extremely Low Levels. *SPE Improved Oil Recovery Conference*. doi:10.2118/179685-ms

Koh, H., Lee, V. B., & Pope, G. A. (2016). Experimental Investigation of the Effect of Polymers on Residual Oil Saturation. *SPE Improved Oil Recovery Conference*. doi:10.2118/179683-ms

Kossack, C., & H.l., B. (1976). The Sensitivity of Micellar Flooding to Reservoir Heterogeneities. *Proceedings of SPE Improved Oil Recovery Symposium*. doi:10.2523/5808-ms

Levitt, D., Jackson, A., Heinson, C., Britton, L. N., Malik, T., Dwarakanath, V., & Pope, G. A. (2006). Identification and Evaluation of High-Performance EOR Surfactants. *SPE/DOE Symposium on Improved Oil Recovery*. doi:10.2118/100089-ms

Levitt, D., Jackson, A., Heinson, C., Britton, L. N., Malik, T., Dwarakanath, V., & Pope, G. A. (2009). Identification and Evaluation of High-Performance EOR Surfactants. *SPE Reservoir Evaluation & Engineering,12*(02), 243-253. doi:10.2118/100089-pa

Lu, J., Britton, C., Solairaj, S., Liyanage, P. J., Kim, D. H., Adkins, and Pope, G. A. (2014, December 1). Novel Large-Hydrophobe Alkoxy Carboxylate Surfactants for Enhanced Oil Recovery.*SPE Journal,* **19**(6):1024-1034. doi:10.2118/154261-PA

Lu, J., Liyanage, P. J., Solairaj, S., Adkins, S., Arachchilage, G. P., Kim, D. H., . . . Pope, G. A. (2013). Recent Technology Developments in Surfactants and Polymers for Enhanced Oil Recovery. *International Petroleum Technology Conference*. doi:10.2523/iptc-16425-ms

Lv, W., Bazin, B., Ma, D., Liu, Q., Han, D., & Wu, K. (2011). Static and dynamic adsorption of anionic and amphoteric surfactants with and without the presence of alkali. *Journal of Petroleum Science and Engineering,77*(2), 209-218. doi:10.1016/j.petrol.2011.03.006

Miller, C. A., Ghosh, O., & Benton, W. J. (1986). Behavior of dilute lamellar liquid-crystalline phases. *Colloids and Surfaces,19*(2-3), 197-223. doi:10.1016/0166-6622(86)80336-5

N, R., Reed, R., & Stenmark, D. (1976). Multiphase Microemulsion Systems. *Society of Petroleum Engineers Journal,16*(03), 147-160. doi:10.2118/5565-pa

Nelson, R., & Pope, G. (1978). Phase Relationships in Chemical Flooding. *Society of Petroleum Engineers Journal,18*(05), 325-338. doi:10.2118/6773-pa

Nelson, R., Lawson, J., Thigpen, D., & Stegemeier, G. (1984). Cosurfactant-Enhanced Alkaline Flooding. *Proceedings of SPE Enhanced Oil Recovery Symposium*. doi:10.2523/12672-ms

Panthi, K., Clemens, T., & Mohanty, K. K. (2016). Development of an ASP formulation for a sandstone reservoir with divalent cations. *Journal of Petroleum Science and Engineering,145*, 382-391. doi:10.1016/j.petrol.2016.05.034

Pope, G., Wang, B., & Tsaur, K. (1979). A Sensitivity Study of Micellar/Polymer Flooding. *Society of Petroleum Engineers Journal,19*(06), 357-368. doi:10.2118/7079-pa

Sahni, V., Dean, R. M., Britton, C., Kim, D. H., Weerasooriya, U., & Pope, G. A. (2010). The Role of Co-Solvents and Co-Surfactants in Making Chemical Floods Robust. *SPE Improved Oil Recovery Symposium*. doi:10.2118/130007-ms

Shamsijazeyi, H., Hirasaki, G., & Verduzco, R. (2013). Sacrificial Agent for Reducing Adsorption of Anionic Surfactants. *SPE International Symposium on Oilfield Chemistry*. doi:10.2118/164061-ms

Shamsijazeyi, H., Verduzco, R., & Hirasaki, G. J. (2014). Reducing adsorption of anionic surfactant for enhanced oil recovery: Part I. Competitive adsorption mechanism. *Colloids and Surfaces A: Physicochemical and Engineering Aspects,453*, 162-167. doi:10.1016/j.colsurfa.2013.10.042

Sharma, H., Dufour, S., Weerasooriya, U., Pope, G. A., & Mohanty, K. (2014). ASP Process for Anhydrite-Containing Oil Reservoirs. *SPE Improved Oil Recovery Symposium*. doi:10.2118/169065-ms

Sharma, H., Lu, J., Weerasooriya, U. P., Pope, G. A., & Mohanty, K. K. (2016). Adsorption in Chemical Floods with Ammonia as the Alkali. *SPE Improved Oil Recovery Conference*. doi:10.2118/179682-ms

Sharma, H., Panthi, K., Ghosh, P., Weerasooriya, U., & Mohanty, K. (2018). Novel Surfactants without Hydrocarbon Chains for Chemical EOR. *SPE Improved Oil Recovery Conference*. doi:10.2118/190232-ms

Solairaj, S., Britton, C., Kim, D. H., Weerasooriya, U., & Pope, G. A. (2012). Measurement and Analysis of Surfactant Retention. *SPE Improved Oil Recovery Symposium*. doi:10.2118/154247-ms

Somasundaran, P., & Krishnakumar, S. (1997). Adsorption of surfactants and polymers at the solid-liquid interface. *Colloids and Surfaces A: Physicochemical and Engineering Aspects,123-124*, 491-513. doi:10.1016/s0927-7757(96)03829-0

Sorbie, K. S. (1991). Polymer stability. *Polymer-Improved Oil Recovery*,83-125. doi:10.1007/978-94-011-3044-8_4

Stegemeier, G. (1977). Mechanisms Of Entrapment And Mobilization Of Oil In Porous Media. *Improved Oil Recovery by Surfactant and Polymer Flooding*,55-91. doi:10.1016/b978-0-12-641750-0.50007-4

Tagavifar, M., Herath, S., Weerasooriya, U. P., Sepehrnoori, K., & Pope, G. (2016). Measurement of Microemulsion Viscosity and Its Implications for Chemical EOR. *SPE Improved Oil Recovery Conference*. doi:10.2118/179672-ms

Tagavifar, M., Herath, S., Weerasooriya, U. P., Sepehrnoori, K., & Pope, G. (2017). Measurement of Microemulsion Viscosity and Its Implications for Chemical Enhanced Oil Recovery. *SPE Journal*. **23** (01): 66-83. SPE-179672-PA https://doi.org/10.2118/179672-PA

Upamali, K. A., Liyanage, P. J., Cai, J., Lu, J., Jang, S. H., Weerasooriya, U. P., & Pope, G. A. (2016). New Surfactants and Co-Solvents Increase Oil Recovery and Reduce Cost. *SPE Improved Oil Recovery Conference*. doi:10.2118/179702-ms

Veedu, F. K., Thomas, D., Wang, P., Eskandaridalvand, K., Hornbrook, J., Pope, G., . . . Tiwari, S. (2015). EOR Feasibility Study through an Integrated Laboratory Evaluation and Reservoir Simulation for a Large Carbonate Field in Kuwait. *SPE Reservoir Simulation Symposium*. doi:10.2118/173255-ms

Wang, D., Liu, C., Wu, W., & Wang, G. (2008). Development of an Ultralow Interfacial Tension Surfactant in Systems With No-Alkali for Chemical Flooding. *SPE Symposium on Improved Oil Recovery*. doi:10.2118/109017-ms

Wang, D., Maubert, M., Pope, G. A., Liyanage, P. J., Jang, S. H., Upamali, K. A., . . . Morel, D. (2019). Reduction of Surfactant Retention in Limestones Using Sodium Hydroxide. *SPE Journal*,*24*(01), 092-115. doi:10.2118/194009-pa

Winsor, P. (1954). Solvent Properties of Amphiphilic Compounds. London: Butterworths

Winsor, P. A. (1948). Hydrotropy, solubilisation and related emulsification processes. *Transactions of the Faraday Society*,*44*, 451. doi:10.1039/tf9484400451

Yan, L., Li, Y., Cui, Z., Song, B., Pei, X., & Jiang, J. (2017). Performances of Guerbet Alcohol Ethoxylates for Surfactant–Polymer Flooding Free of Alkali. *Energy & Fuels*,*31*(9), 9319-9327. doi:10.1021/acs.energyfuels.7b01843

Yang, H. T., Britton, C., Liyanage, P. J., Solairaj, S., Kim, D. H., Nguyen, Q. P., Pope, G. A. (2010). Low-Cost, High-Performance Chemicals for Enhanced Oil Recovery. *SPE Improved Oil Recovery Symposium*. doi:10.2118/129978-ms

Zhao, P., Jackson, A., Britton, C., Kim, D. H., Britton, L. N., Levitt, D., & Pope, G. A. (2008). Development of High-Performance Surfactants for Difficult Oils. *SPE Symposium on Improved Oil Recovery*. doi:10.2118/113432-ms